ADAPTIVE ARRAY PROCESSING OF HF SIGNALS PROPAGATED OVER A 2600 KM PATH

Lloyd J. Griffiths, et al

Colorado University

Prepared for:

Defense Advanced Research Projects Agency

1 January 1973

RADC-TR-73-75
Technical Report
January 1973

ADAPTIVE ARRAY PROCESSING OF HF SIGNALS PROPAGATED OVER A 2600 KM PATH

University of Colorado

Sponsored by
Defense Advanced Research Projects Agency
ARPA Order No. 1423

Approved for public release;
distribution unlimited.

The views and conclusions contained in this document are those of the authors and should not be interpreted as necessarily representing the official policies, either expressed or implied, of the Defense Advanced Research Projects Agency or the U. S. Government.

Rome Air Development Center
Air Force Systems Command
Griffiss Air Force Base, New York

NOTICE

When Government drawings, specifications, or other data are used for any purpose other than in connection with a definitely related Government procurement operation, the United States Government thereby incurs no responsibility nor any obligation whatsoever; and the fact that the government may have formulated, furnished, or in any way supplied the said drawings, specifications, or other data, is not to be regarded by implication or otherwise as in any manner licensing the holder or any other person or corporation, or conveying any rights or permission to manufacture, use, or sell any patented invention that may in any way be related thereto.

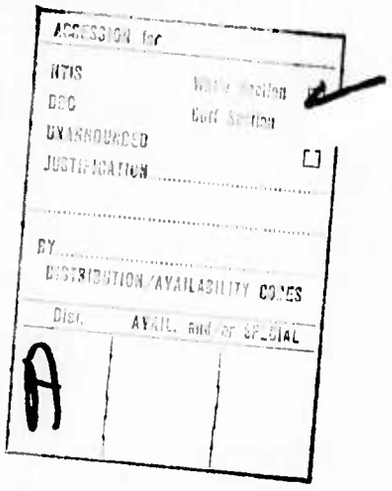

Copies of this report should not be returned unless return is required by security considerations, contractual obligations, or notice on a specific document.

NOTICE

When Government drawings, specifications, or other data are used for any purpose other than in connection with a definitely related Government procurement operation, the United States Government thereby incurs no responsibility nor any obligation whatsoever; and the fact that the government may have formulated, furnished, or in any way supplied the said drawings, specifications, or other data, is not to be regarded by implication or otherwise as in any manner licensing the holder or any other person or corporation, or conveying any rights or permission to manufacture, use, or sell any patented invention that may in any way be related thereto.

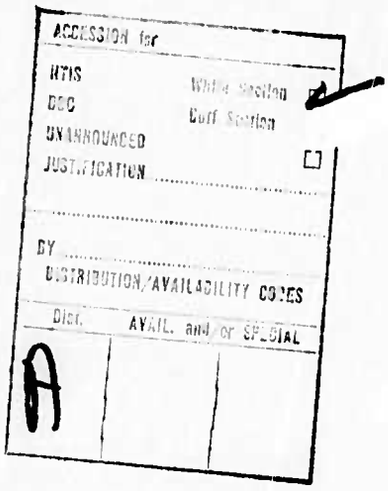

Copies of this report should not be returned unless return is required by security considerations, contractual obligations, or notice on a specific document.

UNCLASSIFIED
Security Classification

DOCUMENT CONTROL DATA - R & D
(Security classification of title, body of abstract and indexing annotation must be entered when the overall report is classified)

1. ORIGINATING ACTIVITY *(Corporate author)*
The Regents of the
University of Colorado
Boulder, Colorado 80302

2a. REPORT SECURITY CLASSIFICATION
UNCLASSIFIED

2b. GROUP

3. REPORT TITLE
Adaptive Array Processing of HF Signals Propagated Over a 2600 KM Path

4. DESCRIPTIVE NOTES *(Type of report and inclusive dates)*
FINAL REPORT covering activity during the period Jan. 1, 1972 - Dec. 31, 1972

5. AUTHOR(S) *(First name, middle initial, last name)*
Lloyd J. Griffiths
Michael J. Larimore

6. REPORT DATE	7a. TOTAL NO. OF PAGES	7b. NO. OF REFS
January 1, 1973	122	28

8a. CONTRACT OR GRANT NO.	9a. ORIGINATOR'S REPORT NUMBER(S)
F 30602-72-C-0386	
b. PROJECT NO. 14235101	
c. Program Code Number 2E20	9b. OTHER REPORT NO(S) *(Any other numbers that may be assigned this report)*
d. ARPA Order Number 1423	RADC-TR 73-75

10. DISTRIBUTION STATEMENT
Approved for Public release; distribution unlimited.

11. SUPPLEMENTARY NOTES	12. SPONSORING MILITARY ACTIVITY
Monitored by: Leonard Strauss 315-330-3055 RADC GAFB, NY 13441	Defense Advanced Research Projects Agency Washington, D. C. 20301

13. ABSTRACT

The purpose of this study was to investigate the potential advantages which may accrue to HF antenna array systems by employing adaptive beamforming techniques. Data for the study were obtained using a CW transmitter located in Bearden, Arkansas and an eight element, narrow band (31.25 Hz) receiving array in Los Banos, California. The Bearden signal was presumed to be an undesired interference. The individual array element signals were combined using tapped-delay-line filters for purposes of rejecting the Bearden signal while simultaneously forming a beam in the direction of a weak desired signal. It was shown that adaptive adjustment of the delay line weights provided better than 25 db improvement over conventional beamforming methods. The adaptive time constant was measured as 27,000 adaptations for each 3 db improvement, corresponding to a real time rate of less than 100 msec for special purpose digital hardware.

DD FORM 1 NOV 65 1473

UNCLASSIFIED
Security Classification

14. KEY WORDS	LINK A		LINK B		LINK C	
	ROLE	WT	ROLE	WT	ROLE	WT
Adaptive Processing						
HF Arrays						
Adaptive Beamforming						
Interference Rejection						
Adaptive Feedback Filtering						
Two-Dimensional Signal Processing						
Doppler-Azimuth Displays						
Optimum Array Processing						
Tapped-Delay-Line Filtering						
Minimum Mean-Square Error Criterion						
Two-Dimensional Beam Patterns						

ADAPTIVE ARRAY PROCESSING OF HF SIGNALS PROPAGATED OVER A 2600 KM PATH

Lloyd J. Griffiths
Michael J. Larimore

Contractor: University of Colorado
Contract Number: F30602-72-C-0386
Effective Date of Contract: 1 January 1972
Contract Expiration Date: 31 December 1973
Amount of Contract: $17,580.00
Program Code Number: 2E20

Principal Investigator: Prof. L. J. Griffiths
Phone: 303 443-2211 Ext. 7653

Project Engineer: Frederick Wilson
Phone: 315 330-3085

Contract Engineer: Leonard Strauss
Phone: 315 330-3055

This research was supported by the Defense Advanced Research Projects Agency of the Department of Defense and was monitored by Leonard Strauss RADC (OCSE), GAFB, NY 13441 under Cont F30602-72-C-0386.

PUBLICATION REVIEW

This technical report has been reviewed and is approved

Joseph J. Simons
For Frederick K. Wilson
RADC Project Engineer

Leonard Strauss
Contract Engineer

ABSTRACT

This report summarizes the results of an investigation which was carried out during the period January 1, 1972 to December 31, 1972. The purpose of this study was to investigate the potential advantage which may accrue to HF array systems by employing adaptive beamforming techniques. Data for the investigation were obtained using a 2600 km. path between a CW transmitter located at Bearden, Arkansas and a receiving array at Los Banos, California. These data were originally recorded for purposes of measuring the azimuthal resolution of the ionosphere.

The data consisted of digitized recordings taken sequentially from eight individual whip antennas in a linear array. Elemental spacing was 360 m. providing a total aperature of about 2.5 km. A receiver bandwidth of 31.25 Hz was used for each of the eight elements.

For the purposes of this research, the Bearden signal was presumed to be an undesired interference. The array element outputs were combined through tapped-delay-line filters for purposes of rejecting this interference while simultaneously forming a beam in the direction of a weak, desired signal. It was shown that by adaptively adjusting the delay-line weights, the Bearden signal could be reduced by more than 25 db over conventional time delay and sum beamforming. The 3 db adaptive time constant was measured to be about 27,000 adaptations, corresponding to a real time rate of less than 100 msec for high-speed, special-purpose digital processors.

CONTENTS

		Page
I	SUMMARY	1
II	INTRODUCTION	4
	A. Purpose	4
	B. Motivation	4
	C. Background	6
	D. Approach Taken in Present Study	9
III	EXPERIMENTAL FACILITIES AND DATA BASE	15
	A. Equipment	15
	B. Data Format	17
	C. Preliminary Data Processing and Spurious Signal Rejection	17
	D. Selection of Desired Weak Signals	26
IV	ADAPTIVE SIGNAL PROCESSING THEORY	37
	A. Model Formulation	37
	B. The Adaptive Algorithm	43
V	RESULTS	47
	A. Optimum Processor Calculations	47
	B. Conventional Processor Calculations	50
	C. Performance Comparisons for Desired Signal d_1	56
	D. Performance Comparisons for Desired Signal d_2	68
	E. Adaptive Algorithm Implementation	70
VI	CONCLUSIONS	80
VII	SUGGESTIONS FOR FUTURE RESEARCH	83

CONTENTS

	Page
APPENDIX. THE DESIGN OF ADAPTIVE TAPPED-DELAY LINE PROCESSORS WHICH EMPLOY FEEDBACK	85
A. Deconvolution and Inverse Filtering	87
B. Topelitz Matrices	89
C. Stability of Inverse Filters	90
D. Inverse Filters in Recursive Filter Design . .	93
E. Design Approaches and Examples.	95
F. Discussion and Conclusions	107
REFERENCES	108

TABLES

		Page
1.	Summary of Spurious Signal Reduction in db	26
2.	Amplitude Weights for Conventional Processor	50
3.	SNR Performance Comparison	57
4.	Average Processor Gain	88
5.	Adaptive Time Constant Measurements	76
6.	Eigenvalues of R_{XX} Matrix For 4^{th} Data Block	78
7.	Theoretical Bounds on Adaptation Rates for 4th Data Block	79
A1	Inverse Approximations	92
A2	Mean-Square Error Calculations	100

ILLUSTRATIONS

		Page
Fig. 1.	Sensor array tapped-delay line processor.	7
Fig. 2.	Conventional receiving array beamforming system .	10
Fig. 3.	Hybrid adaptive receiving array beamforming system	12
Fig. 4.	All digital adaptive receiving array beamforming system	13
Fig. 5.	Los Banos receiving array system	16
Fig. 6.	Two-dimensional transform processing procedure .	19
Fig. 7.	Two-dimensional transform display of calibration data block for 03-04-70 at 0617Z	21
Fig. 8.	Two-dimensional transform display of first data block for Bearden signal 03-04-70 at 0617 Z. (Transmitter frequency 5.267 MHz.)	21
Fig. 9.	Two-dimensional transform of Bearden signal data for sixth data block 03-04-70 at 0617Z (5.267 MHz)	22
Fig. 10.	Replot of Fig. 7 at times ten gain.	24
Fig. 11.	Replot of Fig. 8 at times ten gain	24
Fig. 12.	Data plot for Bearden signal 03-04-70 at 0617Z, first data block after spurious correction . .	25
Fig. 13.	Calibration transform plot of Fig. 7 with identification of spurious zones	27
Fig. 14.	Bearden data transform for block no. 1 at 2212Z, 03-02-70, and frequency 11.7 MHz showing identification of desired signals	28
Fig. 15.	Replot of Fig. 14 at times ten gain	29
Fig. 16.	Bearden data transform for block no. 3 at 2212Z, 03-04-70	31
Fig. 17.	Bearden data transform for block no. 5 at 2212Z, 03-02-70	32
Fig. 18.	Bearden data transform for block no. 7 at 2212Z, 03-02-70	33

Page

Fig. 19. Bearden data transform for block no. 9 at 2212Z, 03-02-70 34

Fig. 20. Bearden, Arkansas to Los Banos, California ionogram for 03-02-70 at 2132Z 35

Fig. 21. Narrow-band tapped-delay-line filter 38

Fig. 22 Eight-tap broad band delay-line processor . . . 40

Fig. 23 Non-adaptive time-delay and amplitude weighting beamforming system 51

Fig. 24. Antenna array pattern for conventional array processor with raised cosine weighting . . . 53

Fig. 25. Two-dimensional array pattern for conventional processor steered to receive desired signal d_1 54

Fig. 26. Two-dimensional array pattern for conventional processor steered to receive desired signal d_2 55

Fig. 27. Two-dimensional array pattern for optimal array processor with 16 weights on data block no. 1 59

Fig. 28. Two-dimensional array pattern for optimal array processor with 40 weights on data block no. 1 60

Fig. 29. Two-dimensional array pattern for optimal array processor with 80 weights on data block no. 1 60

Fig. 30. Two-dimensional array pattern for optimal array processor with 16 weights on data block no. 3 61

Fig. 31. Two-dimensional array pattern for optimal array processor with 40 weights on data block no. 3 62

Fig. 32. Two-dimensional array pattern for optimal array processor with 80 weights on data block no. 3 62

Fig. 33. Two-dimensional array pattern for optimal array processor with 40 weights on data block no. 5 63

Page

Fig. 34. Two-dimensional array pattern for optimal array processor with 40 weights on data block no. 7 63

Fig. 35. Two-dimensional array pattern for optimal array processor with 40 weights on data block no. 9 64

Fig. 36. Single frequency antenna array patterns for optimal filter shown in Fig. 28 65

Fig. 37. Performance of block 1 optimal filter on succeeding blocks 67

Fig. 38. Performance of block 3 and block 5 optimal filters 67

Fig. 39. Optimal filter with 40 weights designed for data block 1 and desired signal d_2 69

Fig. 40. Adaptive processor output SNR for four values of μ 71

Fig. 41. Adapted out SNR with trend line, $\mu = 200$ 73

Fig. 42. Adapted output SNR with trend line, $\mu = 400$ . . 73

Fig. 43. Adapted output SNR with trend line, $\mu = 1{,}000$. 74

Fig. 44. Adapted output SNR with trend line, $\mu = 2{,}000$. 75

Fig. 45. Tapped-delay line with feedback. 86

Fig. 46. Power Density Spectrum of Desired Signal 98

Fig. 47. Power density Spectrum of Undesired Noise . . . 99

Fig. 48. Amplitude response for optimal non-causal filter 101

Fig. 49. Amplitude response for optimal causal filter . . 102

Fig. 50. Amplitude response for twenty-weight optimal non-recursive filter 103

Fig. 51. Amplitude response for suboptimal processor $H_I(Z)$ given in Eq. (A3). 104

Fig. 52. Amplitude response for suboptimal recursive processor $H_{II}(Z)$ given in Eq. (A4). 105

Fig. 53. Amplitude response for suboptimal recursive processor $H_{III}(Z)$ given in Eq. (A5) 106

I. SUMMARY

This report contains the technical results obtained under RADC Contract No. F 30602-72-C-0386 during the period January 1, 1972 to December 31, 1972. The primary results are summarized briefly in this section. Detailed descriptions are presented in the sections following. The objective of this research program is to study and investigate the potential advantages which may accrue to HF antenna array systems by applying adaptive signal processing techniques similar to those currently used in sonar and seismic systems. Data for this study are obtained from phase-coherent, digitized recordings taken using high-frequency radio research facility at Los Banos, California. The recordings consisted of data samples from eight individual whip antennas in the array uniformly spaced at 360 meters. These data were supplied by the Ionospheric Dynamics Group at Stanford Research Institute, Menlo Park, California.

On March 15, 1972 two digital tape recordings were received from SRI. All data were taken over the Bearden, Arkansas, to Los Banos 2600 km path under conditions of high signal-to-noise ratio (25 db) at the individual whips. Although these data were originally taken to investigate the resolution of a large-aperture HF array, they were also amenable to adaptive processing studies in that the signals were recorded using eight phase-coherent receivers.

It was decided that in the scope of the present research program, the Bearden transmitter would be treated as an unwanted jamming signal. Adaptive processing was then used to extract

a weak signal which was incident on the array from a slightly different angle and at a different frequency than was the Bearden signal. Results of this processing were then compared with those of a conventional array processor (time delay steering with amplitude shading) designed to receive the same weak signal.

The reason for characterizing the Bearden signal as undesired interference was that in high signal-to-noise ratio environments, optimal array processing provides approximately the same output SNR as does conventional processing. Under conditions of low input SNR, however, the improvement can be as high as 40 db. Since the purpose of this research program was to investigate the potential advantages of adaptive processing, a low SNR environment was selected.

It was found that when a weak signal d_1 displaced in frequency by 25 Hz. and in angle by 0.51 degrees from the Bearden transmitter was selected as the desired signal, adaptive processing provided an improvement of 29 db over conventional beamforming. When a signal d_2 at the same frequency, but displaced in angle by 1.02 degrees, was used as the desired, the improvement was about 6 db. These results are summarized below:

COMPARISON OF PROCESSED OUTPUT SIGNAL-TO-NOISE RATIOS

PROCESSING METHOD	OUTPUT SNR d_1	d_2
individual whip	-51.6	-51.6
conventional processor	-43.3	-30.9
16 coefficient adaptive	-37.5	
40 coefficient adaptive	-19.4	-25.0
80 coefficient adaptive	-14.4	

The adaptation time constant for these studies was measured as 680 adaptations for the 40 weight processor. Existing special purpose digital hardware could achieve this time constant in less than 100 milliseconds.

A second result which has been obtained from these data is the design of a simple filtering procedure to remove equipment-generated spurious signals from the raw data. This procedure uses the calibration signal as a reference and has been shown to reduce spurious levels by 15 to 25 db.

A third area was also investigated. The adaptive tapped-delay lines used to form a beam output have previously been implemented as non-recursive filters -- that is, no feedback connections are employed. It is well known that feedback delay lines can achieve a wider range of transfer functions, for a given number of taps, than can non-feedback lines. Feedback has not been previously implemented into adaptive systems, however, because of the problem of maintaining filter stability. During the course of the present research, a procedure was devised for adaptive feedback systems which is guaranteed to produce a stable filter. This result is new and represents a significant step in adaptive technology. Results are presented illustrating this procedure for the case of a single input, single output filter.

II. INTRODUCTION

A. PURPOSE

The purpose of the research described in this report was to investigate the potential advantages which may accrue to an HF antenna array system which employs adaptive beamforming techniques. The direction taken in this study was to compare adaptive array signal processing methods similar to those presently used in several sonar, seismic, and microwave systems with conventional array processing methods currently employed in HF systems. Conventional methods generally involve the use of time-delay steering amplitude shading, such as Tchebeychev, at each array element. While the present study was limited to a comparison of single beam systems, the results obtained are also applicable to multiple beam comparisons.

B. MOTIVATION

Recent years have demonstrated an ever-increasing number of users of the HF spectrum, and a resulting increase in the interference levels experience by any one user. Such interference appears as unwanted noise in the users' receiver and therefore degrades his signal-to-noise ratio. From the viewpoint of a communications channel this degradation is reflected directly in terms of reduced reliability of data transmission which, in turn, necessitates a reduced information rate to recover reliability.

In order to improve the performance of HF systems operating in a greatly increased interference environment, users have

resorted to three basic techniques:

1. increased transmitter power.
2. complex modulation and signal design.
3. increased antenna directivity

The first of these is clearly the least desirable since an attempt to increase signal-to-noise ratio in one system raises the interference level in all other systems. The second technique has become increasingly important in recent years. It involves the use of time and frequency dispersed signals which employ pulse compression techniques at the receiver. An example of this approach is the use of sweep-frequency signals in ionospheric sounders.

The third technique listed above is the one most closely related to the present study. Previous investigators have reported on the use of large aperture transmit and receive antennas in HF systems. The work described in Sweeney[1], for example, showed that a 2.5 Km receiving aperture antenna can be effectively employed in the HF environment. The use of narrow beams is particularly attractive because in contrast with increased transmitter power, increased antenna directivity in one HF system will have the effect of reducing the interference level in many other systems.

The research program described in this report was undertaken to investigate a fourth and equally desirable technique for interference elimination -- namely, the use of automated beamforming to produce directivity nulls in the direction of interfering sources at the receive antenna.

C. BACKGROUND

The research effort described in this report has relied upon the extensive results obtained in the area of adaptive beamforming in the fields of sonar, seismology and microwave systems. A complete literature survey of these results has been completed and the reader is referred to Reference 2 for detailed information. The following paragraphs present a brief summary of the major results achieved to date.

Since the work of Mermoz[3] in the late 1950's, a significant number of results have been obtained relating to the problem of improving the quality of signals received by a spatial array of sensing elements. The early efforts in this development, including those of Mermoz were directed toward the processing of sonar signals. Shor[4], Stocklin[5], Vanderbulk[6], Anderson[7], and Brynn[8] all suggested procedures for containing the outputs of an array of sensor through a system of tapped-delay-line filters similar to that shown in Figure 1. This system represented a marked departure from conventional array processing which consists of delaying the sensor outputs in order to steer the array in a prespecified direction and then summing the delayed outputs.

Tapped-delay-line processors are easily constructed and provide a wide variety of spatial and temporal processing flexibility. For example, by correct choice of the filter coefficients, the processor can null out several directional interferences while simultaneously presenting a preformed beam in the direction of the desired signal. Considerable

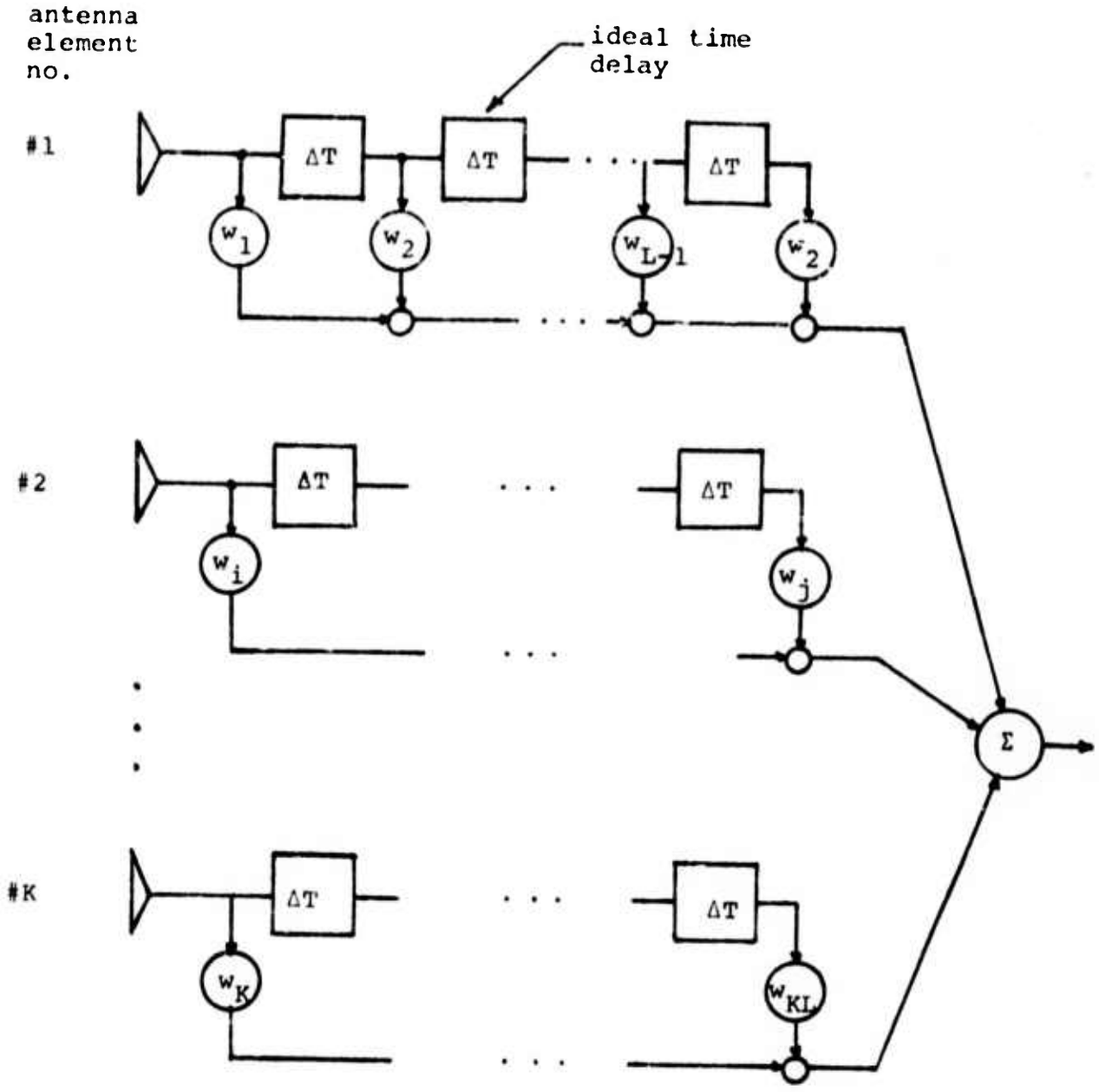

FIG. 1. Sensor array tapped-delay line processor.

effort has been devoted to the development of optimality criteria for setting the coefficient values and a comparison of the resulting performance. These include minimum mean-square error Burg[9], maximum likelihood estimation Kelley[10], and maximum signal-to-noise ratio Shor[4]. It has been shown that all criteria, however, offer substantial processing gain in comparison with conventional delay and sum techniques.

One problem encountered in optimum array signal processing was the requirement for knowledge of the noise correlation statistics in order to calculate the filter coefficient values. This difficulty has been circumvented, however, through the development of adaptive array processing methods by Widrow[11], Chang and Tuteur[12], Compton[13], and Griffiths[14]. In effect, adaptive processing provides a method for continual updating of the filter coefficients using a simple feedback rule. Adaptive processors may be implemented using either analog or digital hardware and offer the additional advantage of being able to track slowly varying noise sources.

An additional area which has provided research results in array studies is in the processing of seismic signals. Seismic processing techniques have been developed at the MIT Lincoln Laboratory under the Large Aperture Seismic Array program (Capon, et al[15]) and by several researchers concerned with oil exploration (Burg[9], Robinson[6], Claebout[17], and Treitel[18]). Results in this latter area are particularly significant in that seismic "noise" is generated by the signal source energy reflecting and reverberating from undesired

boundaries. Noise of this type is identical to the clutter returns observed in the operation of electromagnetic radar systems.

In summary, during the past ten years a large number of signal processing techniques have been developed for use in sensor arrays. These methods provide increased spatial resolution and improved output signal-to-noise ratio through clutter and interference rejection. The purpose of the present research program was to demonstrate that such methods are directly applicable to HF systems and to measure the extent of their improvement.

D. APPROACH TAKEN IN PRESENT STUDY

A conventional receiver array beamforming system which forms a single output beam uses time delay steering as shown in Fig. 2. The delays are arranged such that when a planar wavefront is incident on the array from the direction of interest, it appears in phase at the delay outputs. Amplitude weights (Tchelsychev, raised cosine, etc.) are added to provide lower average sidelobe level. The beam output is formed by summing the delayed and weighted element signals. This output is demodulated using a single-channel receiver and is then processed to provide signal parameter information.

Existing HF systems have employed digital post-receiver processing in which an analog to digital converter (ADC) is placed at the receiver output. Such a system offers great flexibility in signal processing and generating display formats.

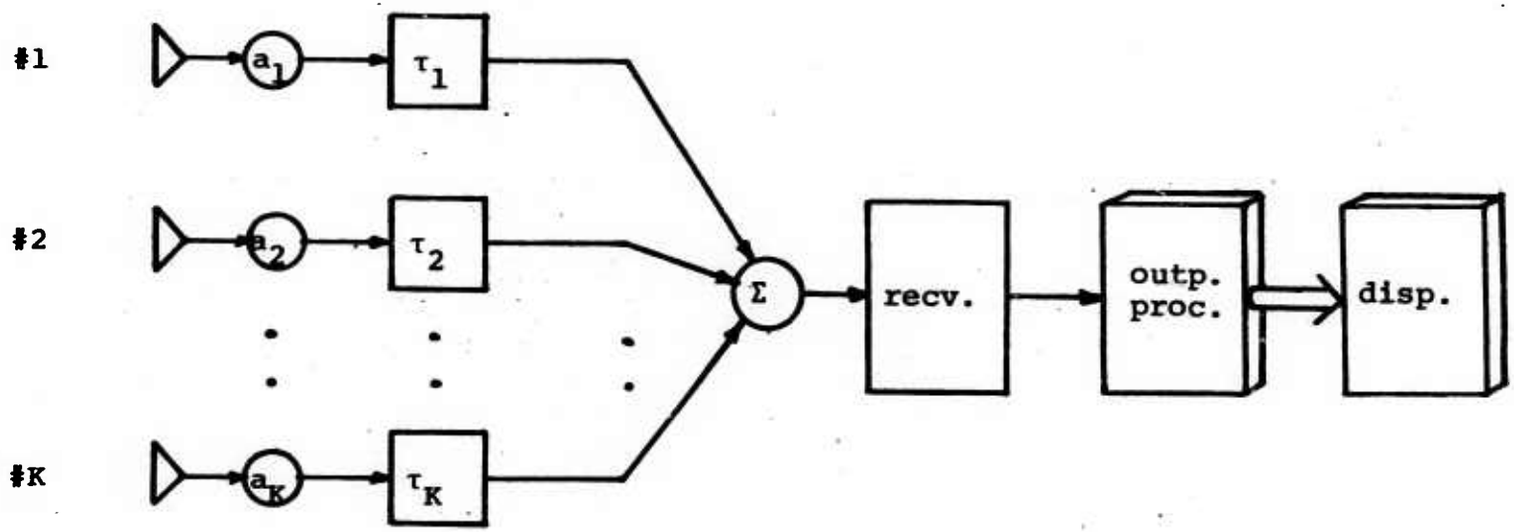

FIG. 2. Conventional receiving array beamforming system

The digital portions of this processor are indicated in Fig. 2 using shaded blocks and large signal flow arrows.

The array processing configuration of interest in this research is shown in Fig. 3. Each antenna element is processed using a tapped-delay-line filter of the type shown in Fig. 1. The coefficients in the delay lines are adjusted periodically using an algorithm which is computed in the adaptive processor. The combination of tapped-delay lines and adaptive algorithm may be viewed as a time-varying filter in space and frequency. In effect, correct choice of the coefficients will ensure the formation of maximum array sensitivity in the direction of interest and the formation of minimum sensitivity -- i.e. pattern nulls -- in the direction of interfering noise sources. The specification of desired look direction and frequency structure of the desired signal is made using reference inputs as shown in Fig. 3. It should be noted that the connection between the output display and adaptive processor shown in this figure is included for purposes of generality. The algorithms reported herein use only the received, demodulated signal and the signals at the adaptive weights.

The digital processing blocks shown as shaded are used to indicate one structure which may be used to implement a real-time adaptive HF array processing system. The delay lines, summing operation and receiver in this system are all analog devices. An alternative, all digital approach is shown in Fig. 4. In this system, a phase-coherent receiver is used to demodulate each element output which is in turn digitized and

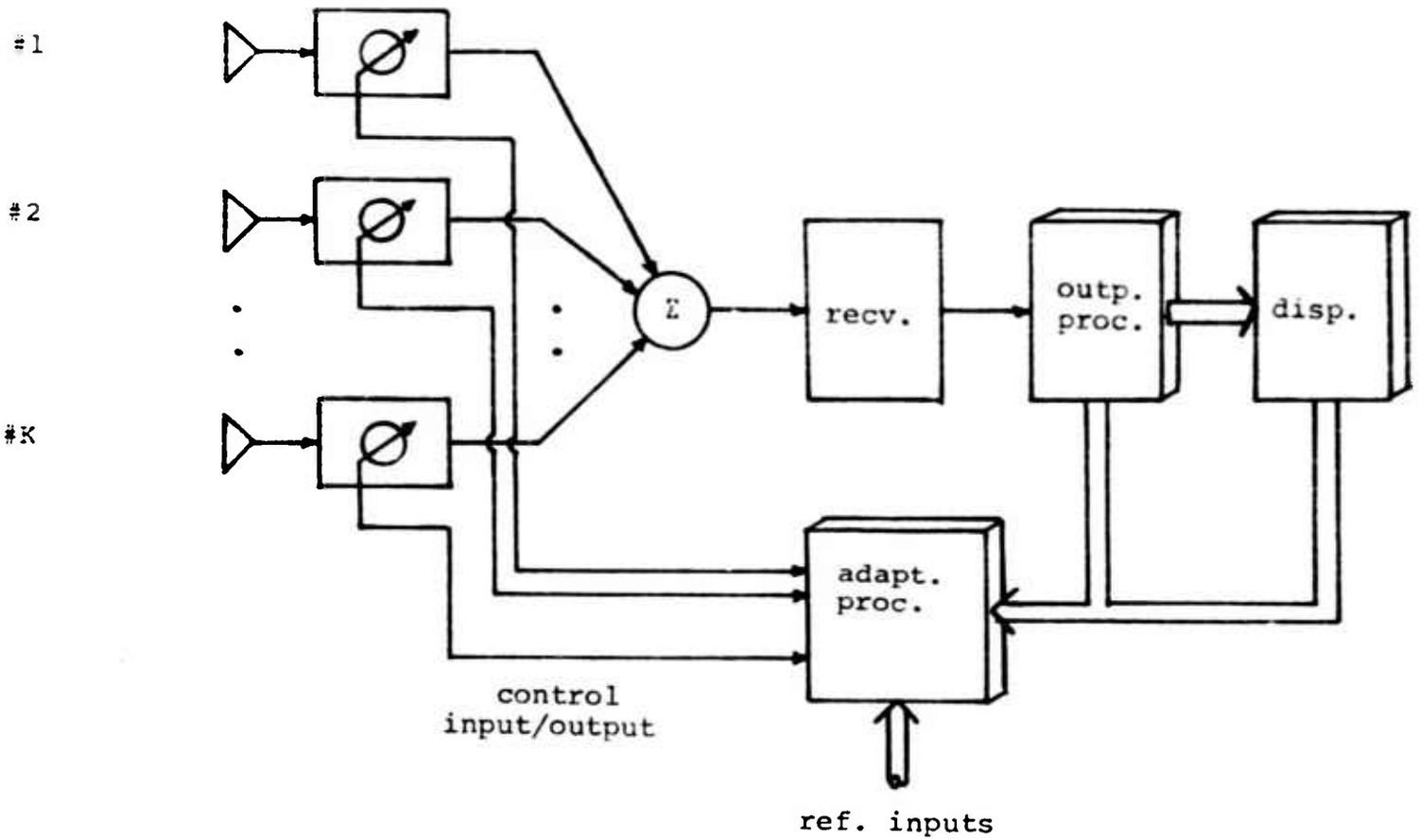

FIG. 3. Hybrid adaptive receiving array beamforming system

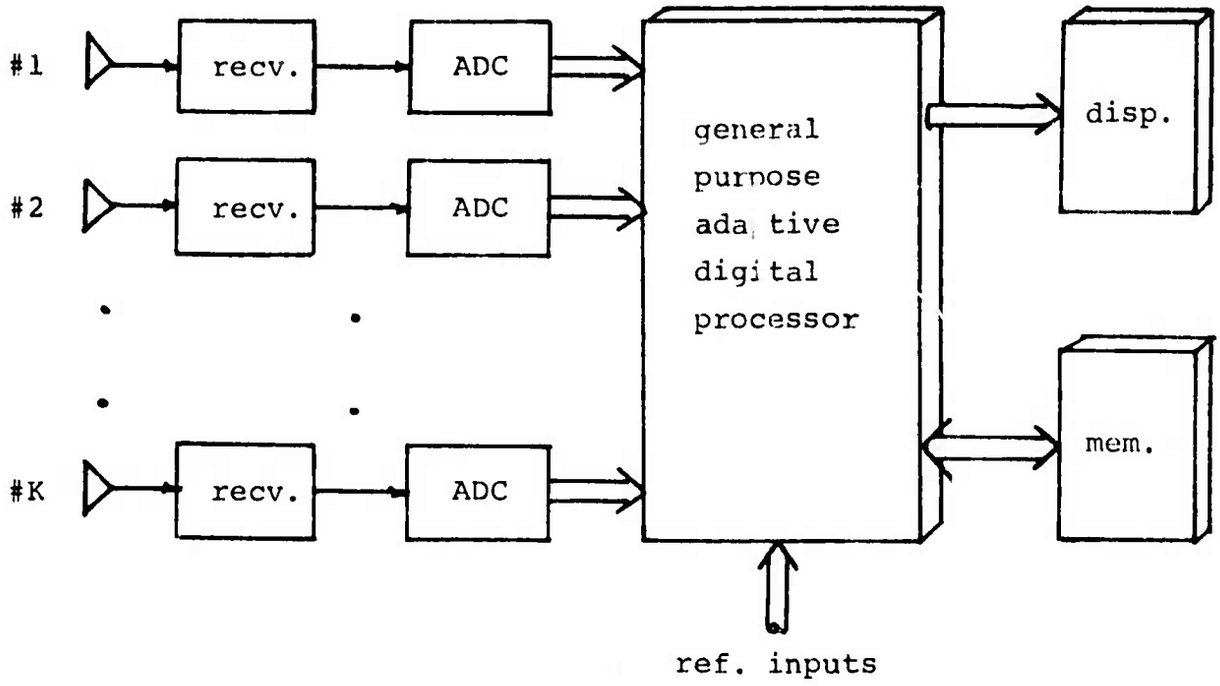

FIG. 4. All digital adaptive receiving array beamforming system

processed using a general purpose computer. While this system is considerably more flexible than that shown in Fig. 3, it requires a digital processing speed N times greater than that shown in Fig. 2, for an array of N elements. In choosing between these alternatives, parameters such as signal bandwidth, number of simultaneous beams, and number of antenna elements must all be taken into account. This subject is beyond the scope of the present research and the reader is referred to Ref. 19 for a more detailed discussion. Although the data used in this research program were obtained by recording digitized element output signals, the results obtained and conclusions drawn are applicable to either the hybrid or all-digital system.

III. EXPERIMENTAL FACILITIES AND DATA BASE

A. EQUIPMENT

The data processed in this report were taken using CW HF signals propagated over a 2600 Km east-west path between Bearden, Arkansas and Los Banos, California. The equipment used to collect these data is part of the wide-aperture high-frequency radio research facility (WARF) operated by the Ionospheric Dynamics Group at Stanford Research Institute, Menlo Park, California. A complete description of this facility may be found in Reference 20. The transmitter, located in Bearden, had a power output of 1 kw and was tuneable over the 3-30 MHz HF frequency band. The transmitting antenna consisted of a horizontal log periodic antenna mounted on a 100 ft. tower. In addition, an FMCW transmitter was also available in Bearden for purposes of obtaining high resolution oblique ionograms over the path.

The Los Banos receiving array consisted of eight vertical whip antennas linearly spaced at a horizontal separation of 360 meters, thus providing a total array aperture of 2.5 km. The array element output signals were demodulated using eight identical receivers driven by a common local oscillator (Fig. 5). A multiplexed ADC was used to sample the receiver outputs sequentially and store the resulting digital signals on magnetic tape. An interactive mini computer provided automatic data collection as well as operator documentation of the experimental parameters. Operating personnel for the tests were provided by

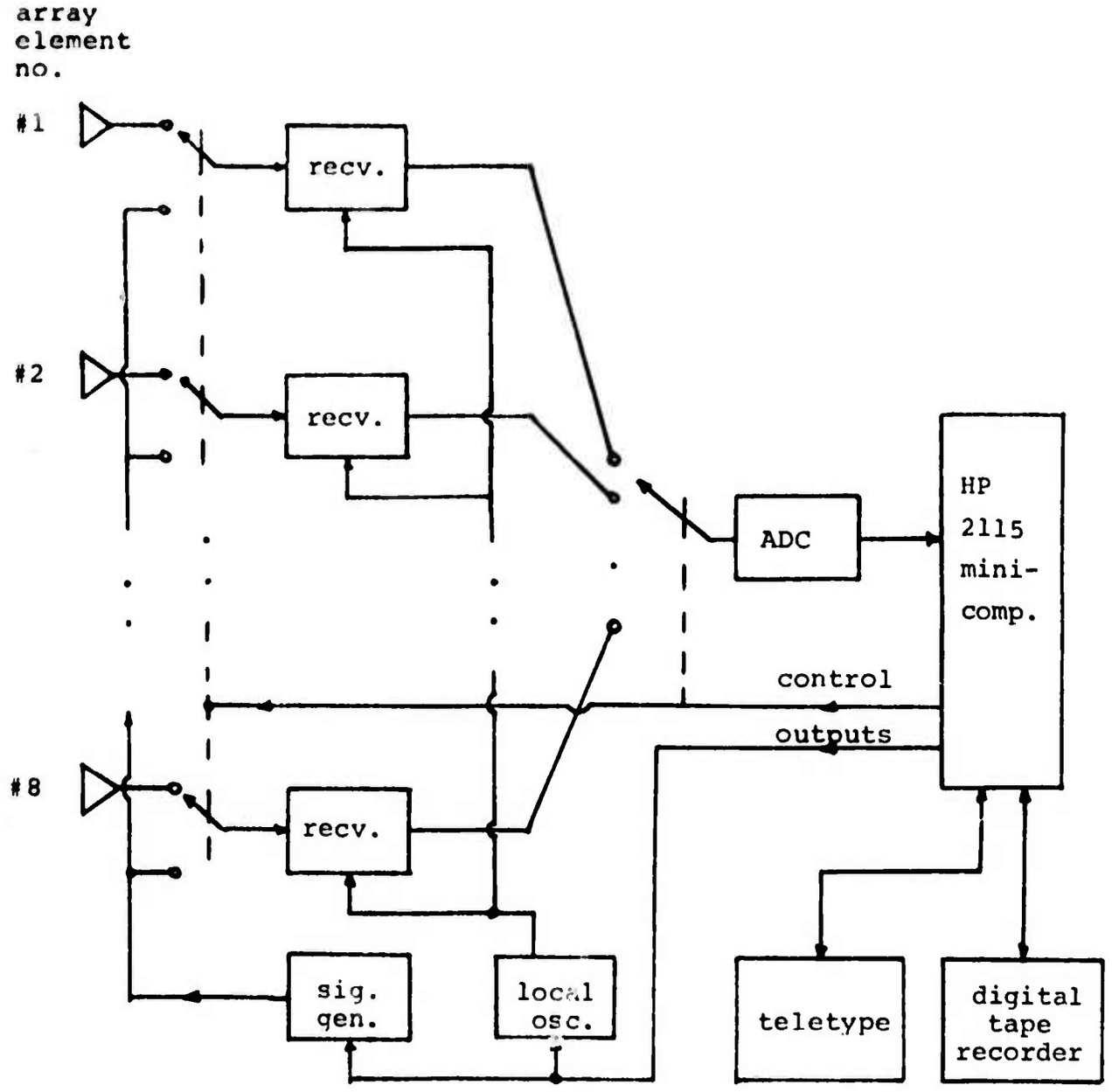

FIG. 5. Los Banos receiving array system

Stanford Research Institute.

B. DATA FORMAT

The data processed in this research were recorded using an ADC sampling rate of 500 samples per second. Due to the multiplexed sampling procedure employed, this provided an effective per element sampling rate of 62.5 samples per second. A total of 4096 samples (512) samples per channel) were recorded per data block representing eight seconds of received data. Each experiment consisted of recording a total of eleven such blocks, separated by one minute intervals. The first data block recorded was a calibration block in which the vertical whips were disconnected and a fixed frequency local signal generator was connected in phase to all eight receiver inputs as shown in Fig. 5. This calibration allowed a measurement of the amplitude and phase variations introduced by the receivers. During the succeeding ten data blocks, the elements were reconnected and the Bearden transmitter frequency was held constant. Experiments were carried out under a wide variety of ionospheric conditions and Bearden transmitter frequencies. Oblique ionograms were recorded at regular intervals during the tests so that propagation modes could be identified.

C. PRELIMINARY DATA PROCESSING AND SPURIOUS SIGNAL REJECTION

The data used for the analysis described in this report were originally collected by SRI personnel for an experiment to determine the spatial characteristics of ionospherically reflected

signals[1]. For this reason, the Bearden transmitting signal frequency was carefully selected to avoid interference from other spectrum users. Typical per element received signal-to-noise ratios for these tests were the order of 25 db to 35 db. It is well known[3,5,6,8,11] that under conditions of high signal-to-noise ratio, the optimum array processor consists of time delay steering and summing the element outputs -- i.e. conventional array processing. Although this statement is correct only if the noise field is isotropic, the output SNR for the conventional processing is for all practical purposes identical to that for optimum processing whenever the per element SNR exceeds about 15 db, regardless of the spatial structure of the noise field. For this reason, it was decided that during the present investigations, the Bearden signal would be considered to be an undesired interfering signal or jammer, and optimum adaptive array processing techniques would be used to extract a weak signal, presumed to be incident on the array from some other direction of arrival. The effectiveness of this processing was then measured by comparing its performance with that of a conventional beamsteering system phased to receive the same weak signal.

Preliminary data processing was employed in an attempt to locate a weak signal in the recorded data. The processing method, which was identical to that described in Ref. 1, consisted of performing a two dimensional transform of the original data. Figure 6 summarizes this procedure. The original data was arranged in a matrix in which the rows contain the time

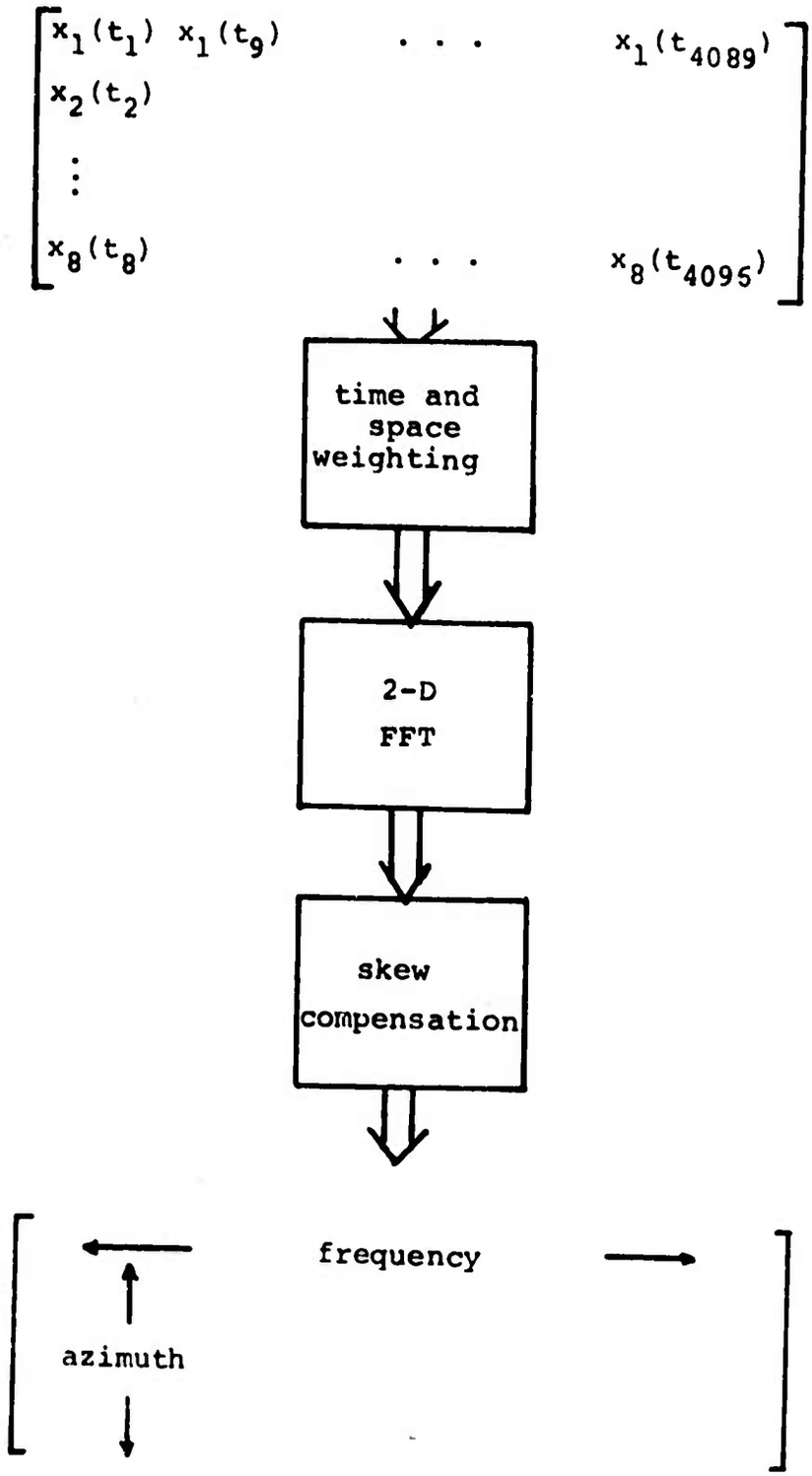

FIG. 6. Two-dimensional transform processing procedure

samples from the eight receivers. Note that the multiplex system provides successive time samples at all eight elements prior to returning to the first element (i.e. simultaneous time samples at the elements are not available). A raised cosine weighting was applied in both space and time to improve sidelobe levels in the final display. By transforming each row and, in turn, each column of this matrix, a frequency-azimuth matrix is obtained in which each row is the received frequency spectrum for a particular azimuth. Eight resolvable azimuths may be obtained using this procedure and the azimuthal spacing is given by $\lambda/(260\times8)$ radians for a received signal wavelength of λ meters.

The operation labelled skew compensation includes a linear phase term to account for the sequential element sampling and a gain phase correction to eliminate local receiver differences. This latter correction causes the calibration block data to appear as an ideal signal in the final display, as shown in Fig. 7. Similar displays for the first and tenth data blocks immediately following this calibration are shown in Figures 8 and 9. All plots clearly demonstrate the high signal-to-noise ration of the recorded data. (Note that the amplitude scales are linear.)

In an attempt to locate weak signals in these data, output plots were computed at gains of 5, 10, 50 and 100 with clipping applied to the largest signals. After processing several blocks of data in this manner, a repeatable pattern of low amplitude energy was observed at several points in the two-dimensional

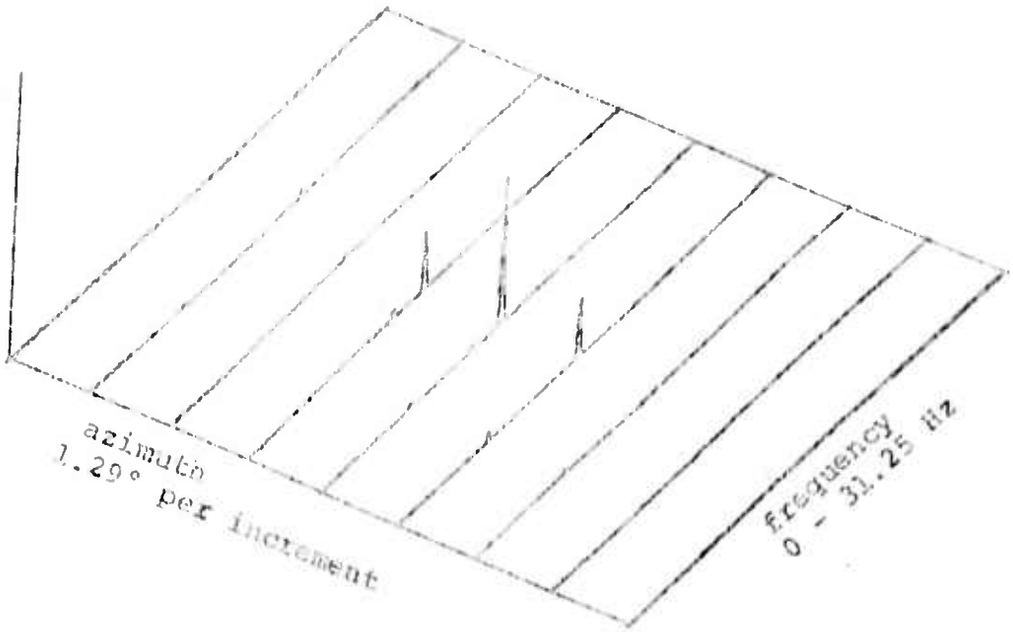

FIG. 7. Two-dimensional transform display of calibration data block for 03-04-70 at 0617 Z.

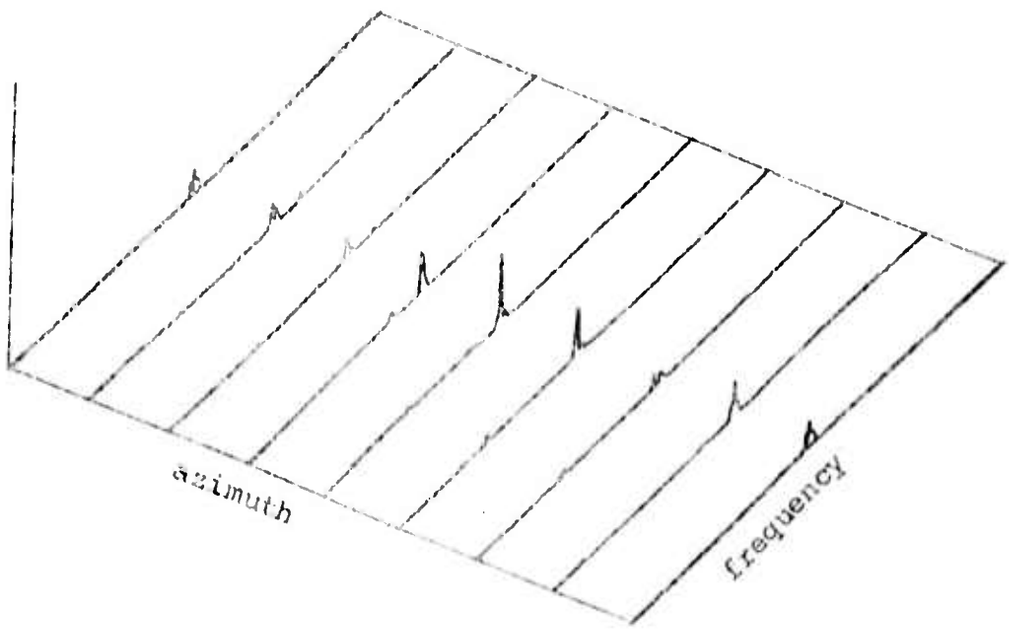

FIG. 8. Two-dimensional transform display of first data block for Bearden signal 03-04-70 at 0617 Z. (Transmitter frequency 5.267 MHz.)

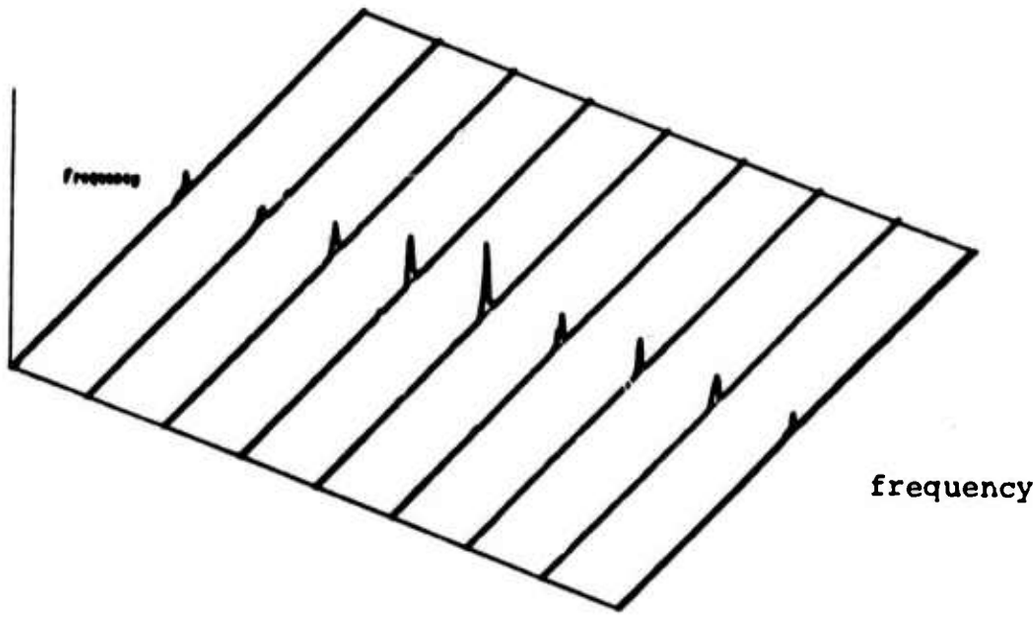

FIG. 9. Two-dimensional transform of Bearden signal data for sixth data block 03-04-70 at 0617Z (5.267 MHz)

transform domain. The fact that this pattern was also observed in the calibration block indicated that the energy was due to spurious signals present in the receiving equipment. Examples of these signals as found in the data are shown in Figure 10 and 11 which are Figure 7 and 8 reploted at a gain of 10.

An effective procedure was found for eliminating these spurious signals. First, the portion of the transformed calibration block which contains the true calibration signal energy is set to zero. This is a simple procedure because the calibration frequency is known exactly and, as can be seen from Figure 7, it occupies a relatively small portion of the transform domain. The remaining energy, which consists of quantization noise and spurious signals, is then subtracted, point for point, from the transforms of the data blocks containing received signals. Since each point of a two-dimensional transform is a complex number, attention must be given to both magnitude and phase in the subtraction process. It is reasonable to assume that the magnitude of spurious signals will remain relatively constant from one data block to the next. The phase, however, will be highly variable depending upon the absolute time at which samples are taken. Therefore, to effectively eliminate the spurious signal pattern in the data, it is sufficient to subtract only the amplitude of the modified calibration transform and to leave the phase transform unaltered.

The effectiveness of this subtraction procedure is shown by comparing Figure 12, which has been processed to eliminate

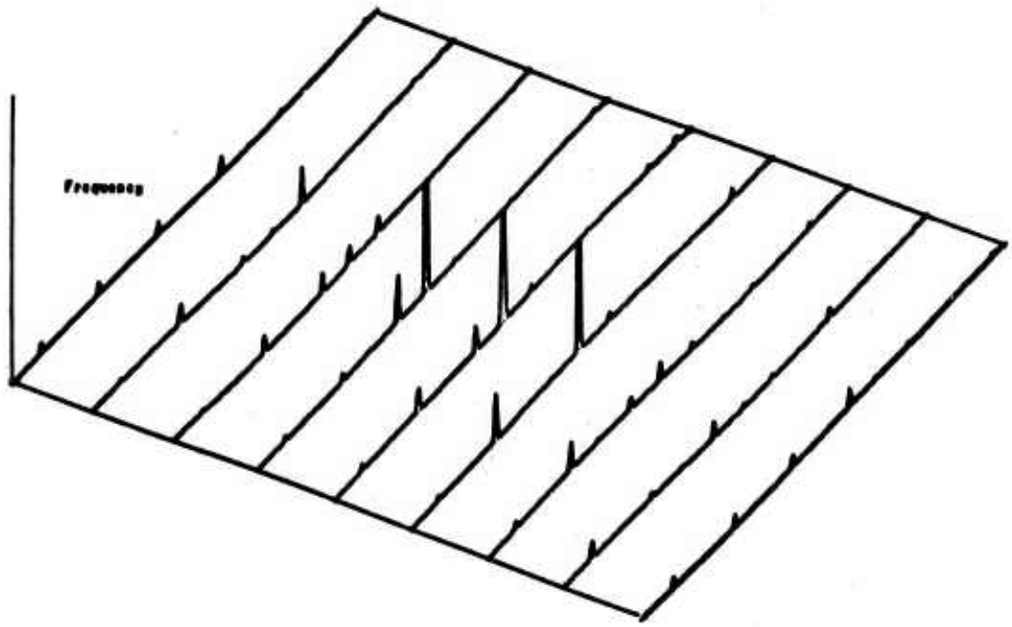

FIG. 10. Replot of Fig. 7 at times ten gain

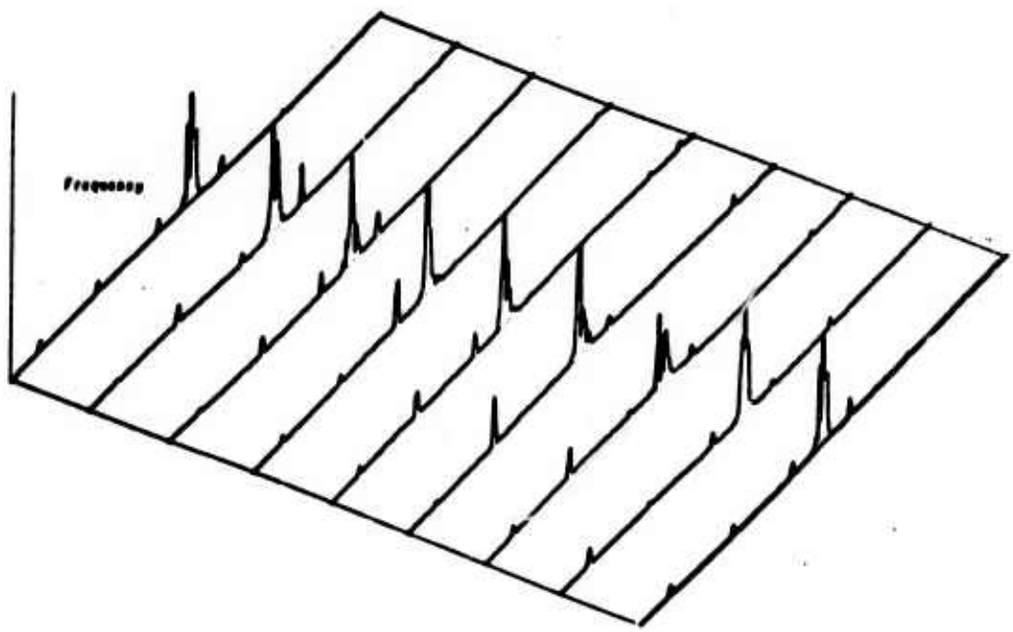

FIG. 11. Replot of Fig. 8 at times ten gain

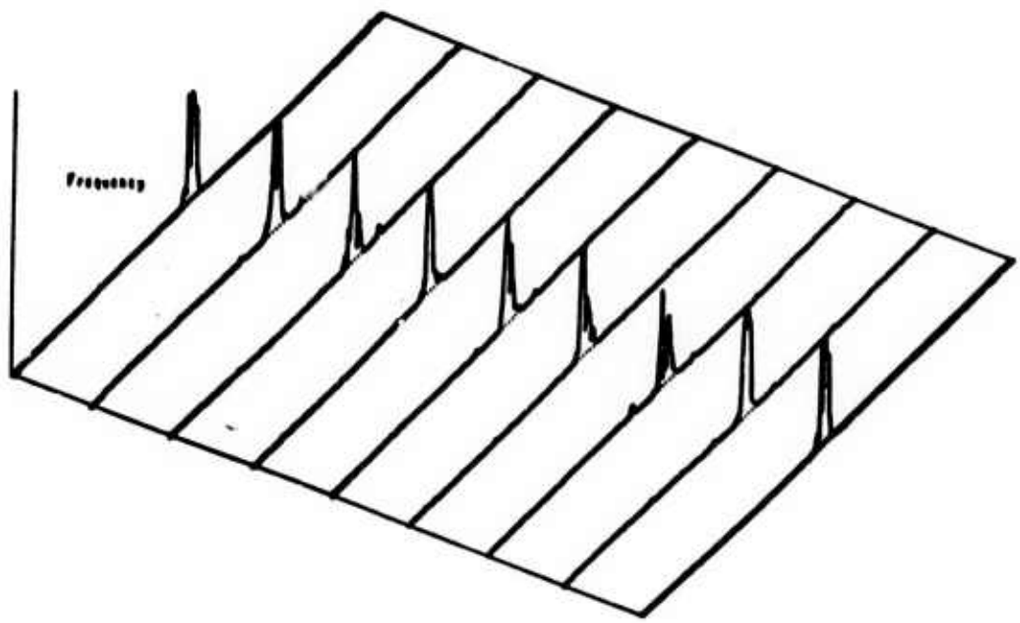

FIG. 12. Data plot for Bearden signal 03-04-70 at 0617Z, first data block after spurious correction.

spurious signals with Figure 11, which has not. After processing records in this manner, gain factors of up to 100 were successfully applied to locate weak signals. A quantitative measure was also obtained by identifying 6 regions of particularly high spurious level in the original data, as shown in Figure 13. The reduction in spurious level for each of these regions as a function of data block number is summarized in Table I

TABLE 1 SUMMARY OF SPURIOUS SIGNAL REDUCTION IN DB

SPURIOUS SIGNALS*	DATA BLOCK 1	DATA BLOCK 2	DATA BLOCK 3	DATA BLOCK 4	DATA BLOCK 5
1	-25.0db	-19.9	-21.5	-24.1	-16.5
2	-30.9	-11.3	-15.1	-16.0	-16.7
3	-19.3	-12.2	-15.0	-14.4	-17.8
4	- 6.0	- 6.6	- 5.6	-11.6	- 7.9
5	-22.2	- 8.8	- 9.5	-10.9	-16.0
6	-14.6	- 6.1	- 7.3	- 7.3	-13.2

*As indicated on Figure 13.

D. SELECTION OF DESIRED WEAK SIGNALS

The methods described in the previous section were used to preprocess several experimental data runs in an attempt to locate a weak signal in the background noise. In each case, spurious-free transform plots similar to that shown in Figure 12 were manually scanned. The data selected for further processing were recorded at 2200 GMT on March 3, 1970 at an operating frequency of 11.70 MHz. Figure 14 and 15 show the transforms

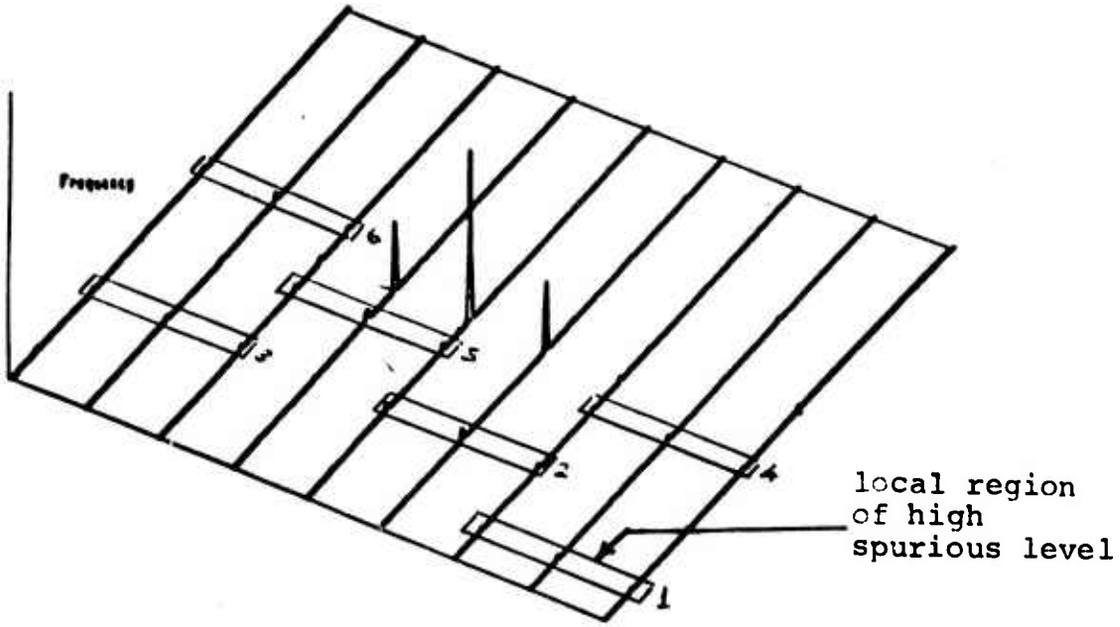

FIG. 13. Calibration transform plot of Fig. 7 with identification of spurious zones

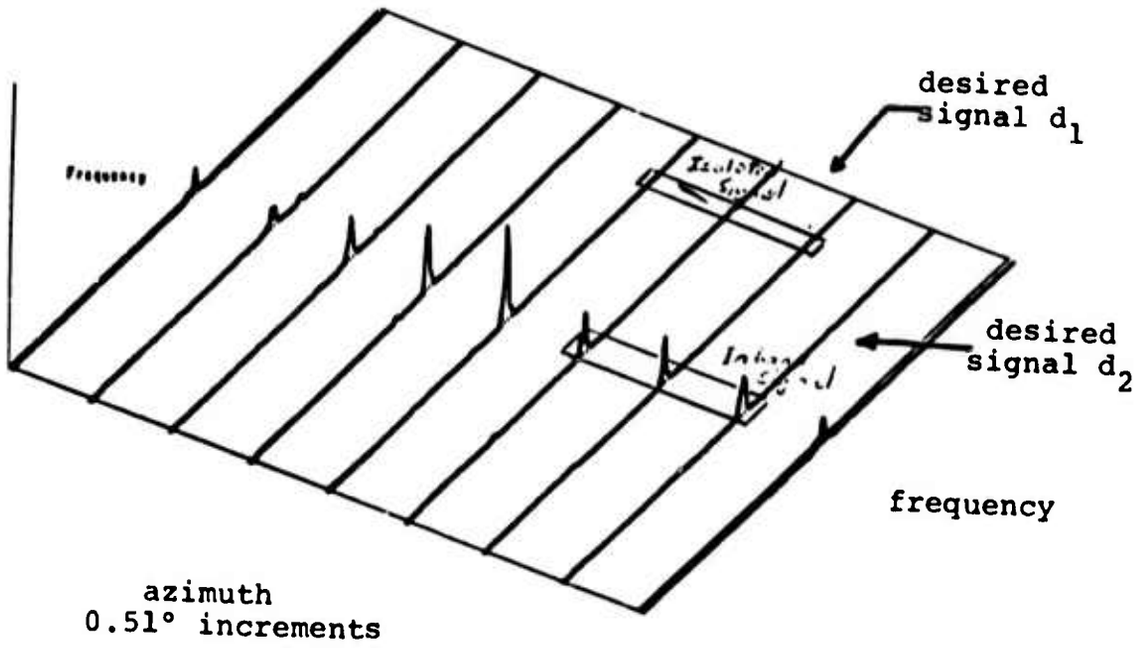

FIG. 14. Bearden data transform for block no. 1 at 2212Z, 03-02-70, and frequency 11.7 MHz showing identification of desired signals.

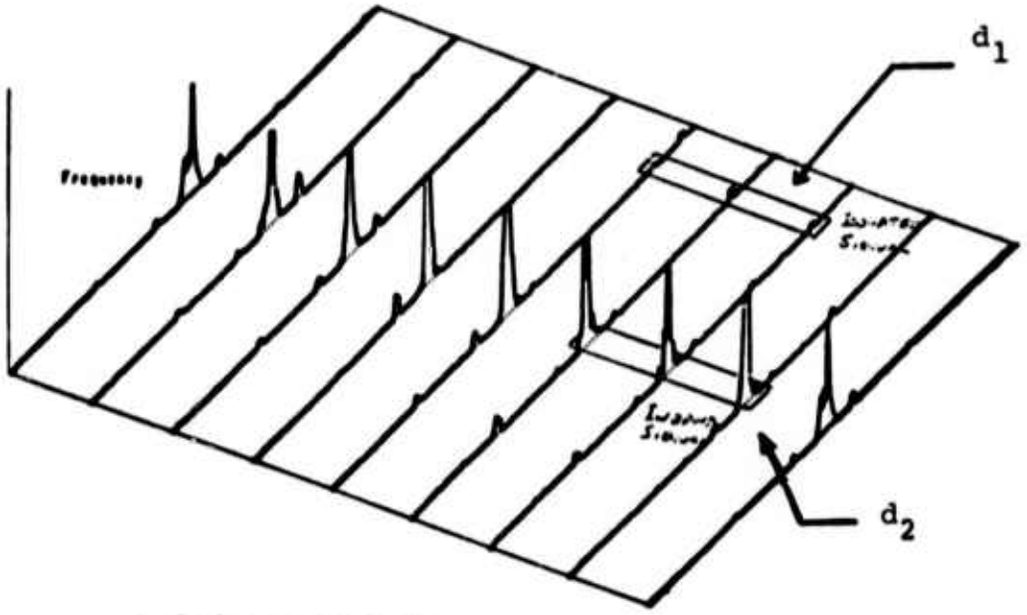

0.51° increments

FIG. 15. Replot of Fig. 14 at times ten gain.

for the first data block at unity and times five gain. A total of ten successive data blocks, taken at one minute intervals, were available, in addition to the initial calibration record. The transforms for blocks 3, 5, 7 and 9 are shown in Figures 16 - 19. All blocks indicated the presence of a weak out of band signal, denoted by d_1 in Figure 14 and 15, which appeared to have fading-like amplitude variations between successive blocks.

This signal was selected as the first desired signal for the adaptive array processor. It is located at a frequency offset of about 25 Hz and is displaced in azimuth 0.51 degrees from the Bearden transmitter. A second, in band, signal was assumed to be present in the region denoted by d_2 in Figures 14 and 15. Due to the presence of large in-band noise in this region, however, no direct evidence of the existence of energy not attributable to the Bearden transmitter was ever obtained. The assumed azimuthal deviation of this signal from the nominal Bearden azimuth was 1.02 degrees.

The azimuthal spread of the Bearden signal shown in Figures 14 - 19 is a consequence of the large number of ionospheric modes propagating during the experiment. An oblique ionogram which was recorded at 2130Z, immediately prior to the tests, is shown in Figure 20. At least four distinct modes are visible at the transmitter frequency (see arrow). Ionograms taken during the time periods one hour preceding and following 2130Z indicate that the ionosphere was stable for the duration of the ten data blocks of interest.

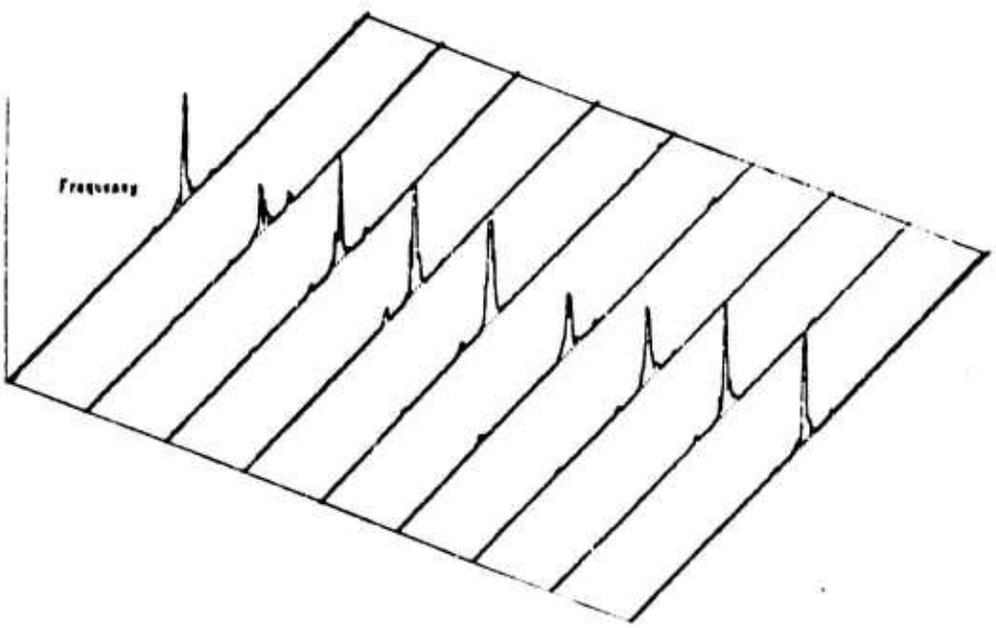

FIG. 16. Bearden data transform for block no. 3 at 2212Z, 03-04-70.

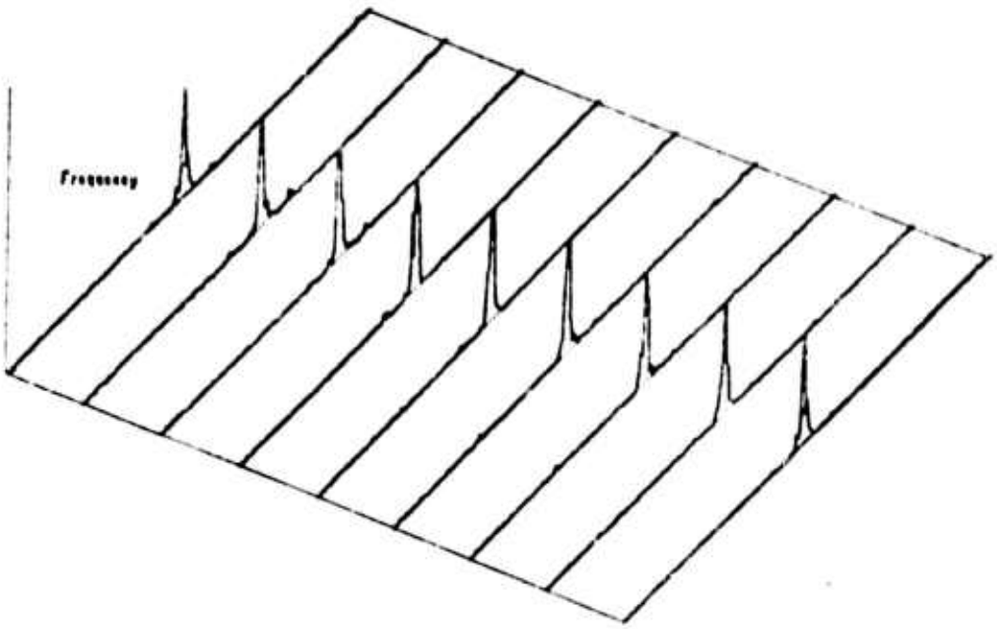

FIG. 17. Bearden data transform for block no. 5 at 2212Z, 03-02-70.

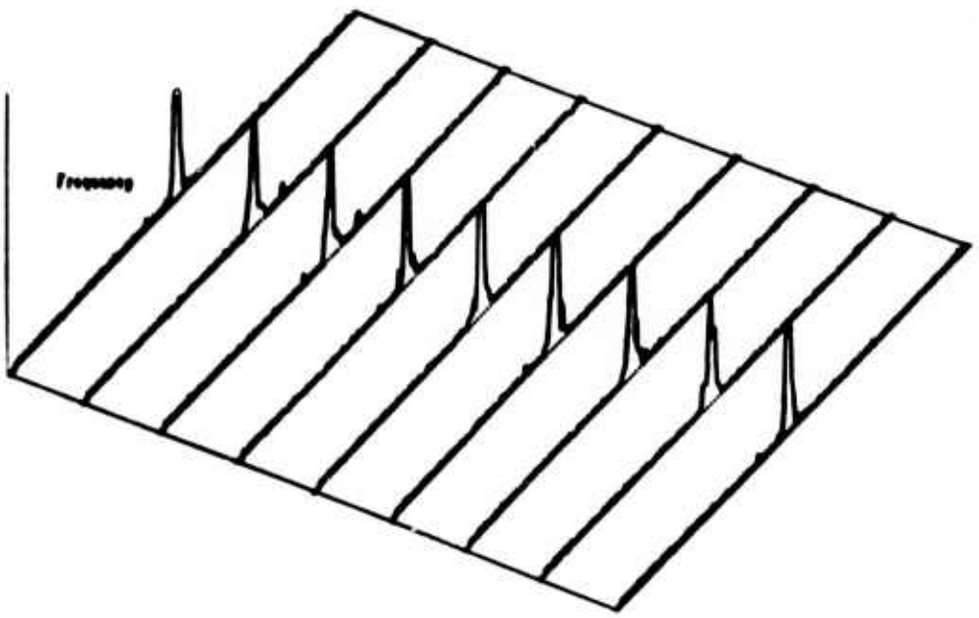

FIG. 18. Bearden data transform for block no. 7 at 2212Z, 03-02-70.

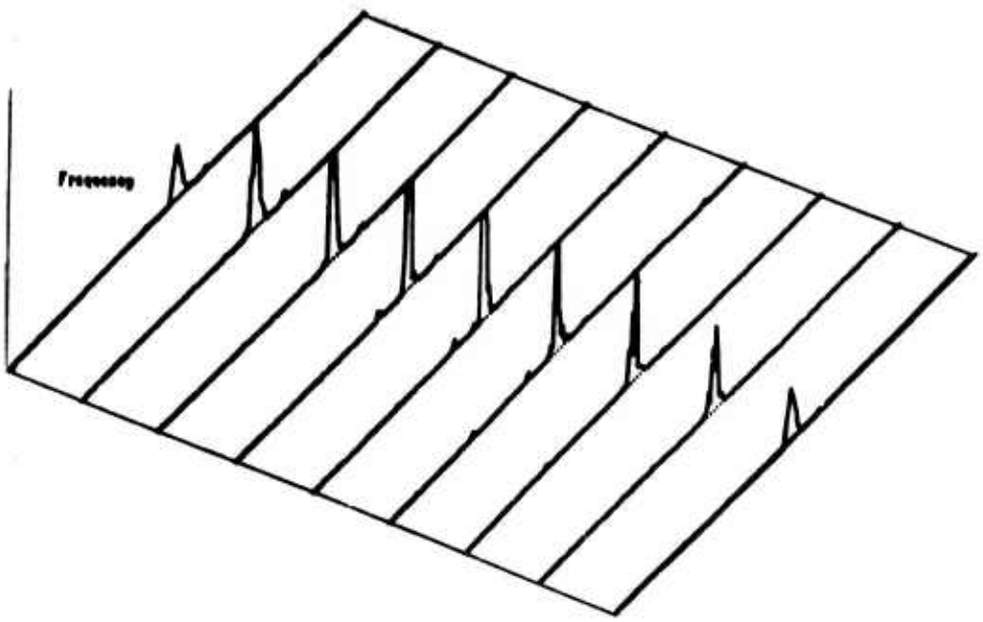

FIG. 19. Bearden data transform for block no. 9 at 2212Z, 03-02-70.

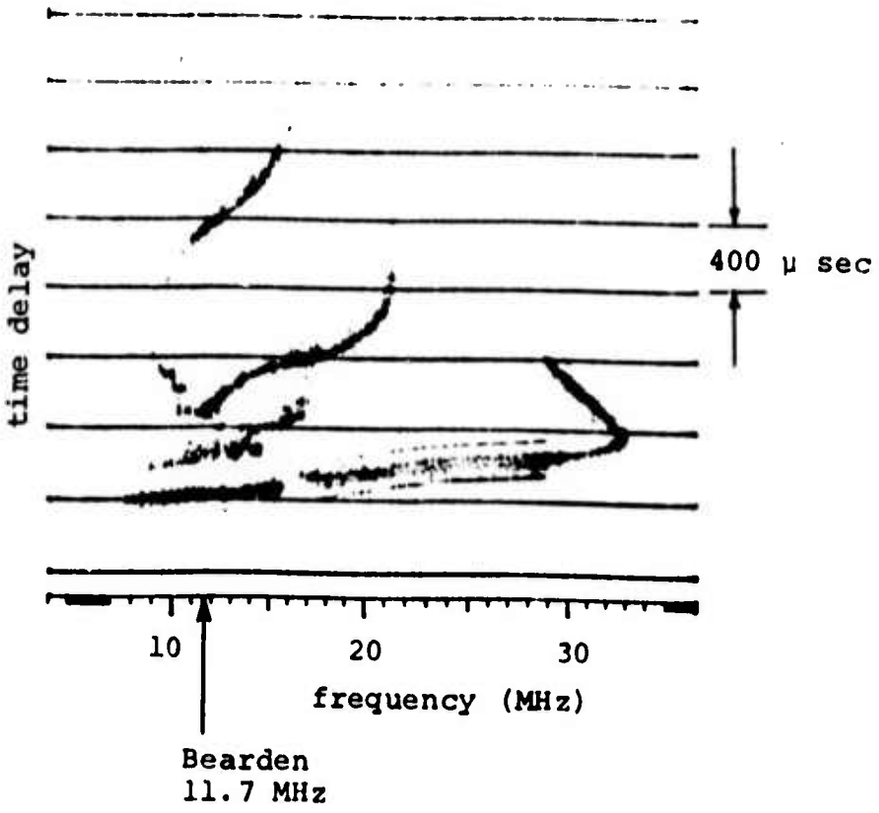

FIG. 20. Bearden, Arkansas to Los Banos, California ionogram for 03-02-70 at 2132Z.

It is to be noted that the rather extensive data processing procedure used in this research to identify the desired signals d_1 and d_2 shown in Figure 14 and 15 is not normally included as part of an adaptive HF processing system. It was used in the present study in order to make most efficient use of a data set which was recorded for other purposes. That is, the use of two dimensional transforms facilitated the identification of weak signals located in a strong interference background. In an operational adaptive system, the direction and frequency structure of these signals are presumed to be known a priori and this information is encoded directly into the adaptive algorithm, as described in the following section. The noise field structure, however, is assumed to be completely unknown a priori. The motivation for the present research is based on the assumption that real time HF array processors do not employ two-dimensional processing techniques due to the extremely large number of calculations required in such a system.

IV. ADAPTIVE SIGNAL PROCESSING THEORY

The theory of adaptive signal processing has been well developed in the last ten years and applications have been proposed for many diverse areas. The purpose of this section is to summarize the theory pertaining to the particular adaptive algorithm used during the course of the present research program. This algorithm was first proposed by Griffiths[14].

A. MODEL FORMULATION

The antenna array of interest is assumed to contain K receiving elements at known spatial locations. A tapped-delay-line processor (Fig. 1) is used to process the element outputs. Each line consists of L-1 time delays of Δ seconds each and L multiplying weights.

The tapped-delay line at each antenna element is a variable filter in which the frequency shaping characteristics of the filter are controlled by the tap settings. To illustrate the behavior of this filter, consider the case of a single delay and two weights, as shown in Fig. 21a. Given an input phasor $e^{j\omega_o t}$, where ω_o is a frequency such that the delay is one quarter wavelength -- i.e. $\Delta = \pi/2\omega_o$, then the output phasor is $w_1 e^{j\omega_o t} + w_2 e^{j(\omega_o t+\pi/2)}$ (Fig. 21b). Assuming that the weights can take on both positive and negative values, the gain and phase response of the filter $w_1 + jw_2$ can assume any complex value.

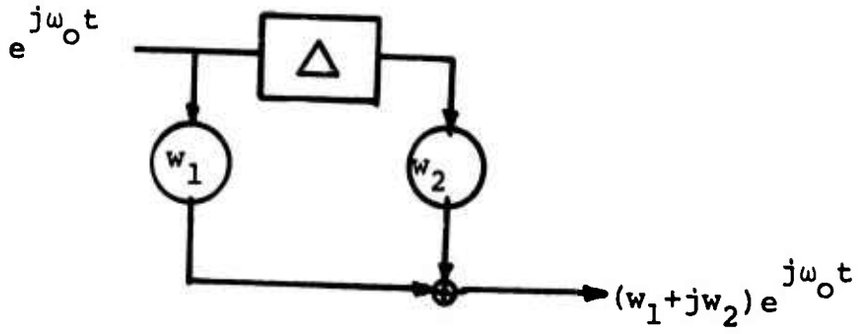

a) Block diagram

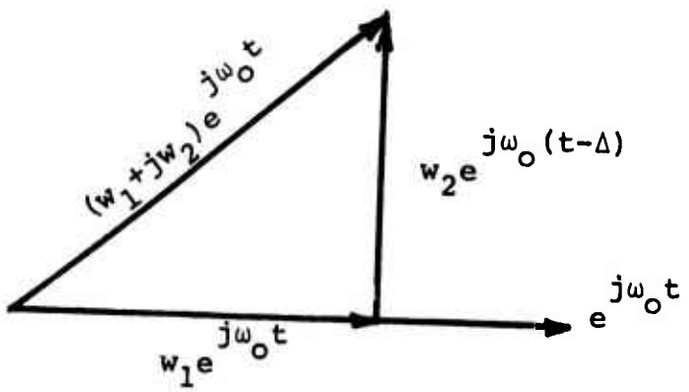

b) Phasor diagram

FIG. 21. Narrow-band tapped-delay-line filter.

A multiple tap delay line (Fig. 22a) can be described in similar terms. Weights spaced by Δ seconds are used to set the response at frequency $f_1 = 1/4\Delta$. Those at a spacing of 2Δ seconds control the gain and phase at one half this frequency, $f_2 = 1/8\Delta$. Thus, the frequency response of a delay line with L weights can be specified at $L-1$ independent, equally spaced points between $f_1 = 1/4\Delta$ and $f_{L-1} = 1/4(L-1)\Delta$ as illustrated in Fig. 22b. It should be noted that this discussion is presented to illustrate the frequency flexibility of a tapped delay line processor and that in an adaptive processor the tap values are selected on the basis of time domain signals rather than using a frequency spectrum specification (see Section B below). This discussion does, however, indicate the amount of delay needed for an array processor which uses tapped-delay line processors. Assuming that signals are received over a bandwidth of B Hz, a minimum delay of $\Delta = 1/2B$ seconds is required to achieve unambiguous frequency control over this bandwidth. If the line contains L taps or, equivalently, a total delay of $(L-1)/2B$ seconds, the minimum frequency resolution will be B/L Hz. For example, an HF system operating at a 100 kHz bandwidth which uses a five tap delay line would be capable of frequency discrimination within 20 kHz bandwidths and would require individual delays of 5 μsec. The total delay line length would be 20μsec.

The array output signal for the processor shown in Fig. 1 is formed from the summation of all delayed and weighted signals. Denoting the set of KL weights in this processor by a vector $\underline{W}$

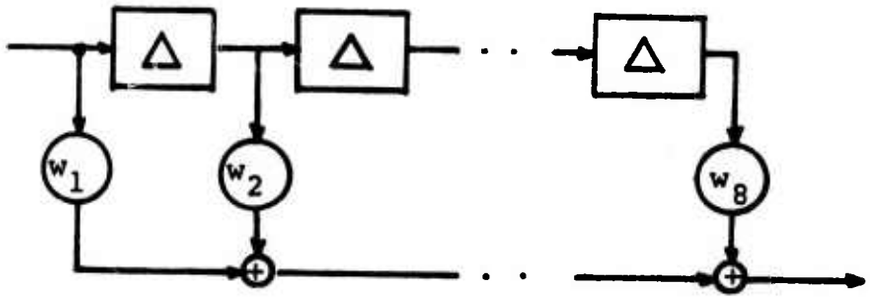

a) Block diagram

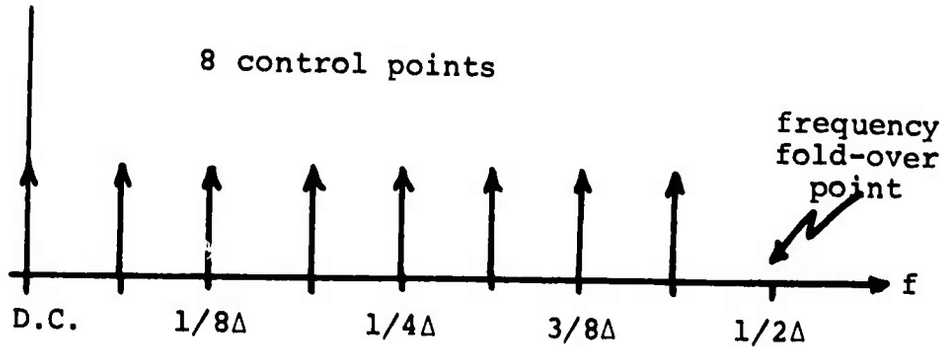

b) Equivalent frequency control points

FIG. 22. Eight-tap broad band delay-line processor

$$\underline{W} = \begin{pmatrix} w_1 \\ w_2 \\ \vdots \\ w_{KL} \end{pmatrix} \tag{1}$$

and the set of KL signals present at each weight at time t by the vector $\underline{X}(t)$

$$\underline{X}(t) = \begin{pmatrix} x_1(t) \\ x_2(t) \\ \vdots \\ x_{KL}(t) \end{pmatrix} \tag{2}$$

then the array output signal $y(t)$ can be expressed as an inner product, i.e.

$$y(t) = \underline{W}^T\underline{X}(t) = \sum_{i=1}^{KL} w_i x_i(t). \tag{3}$$

This notation may be easily modified to include the effects of adaptation in which the value of each weight w_i changes at each adaptive step. Let $\underline{W}(k)$ express the value of the weights after k adaptations, then

$$\underline{W}(k) = \begin{pmatrix} w_1(k) \\ w_2(k) \\ \vdots \\ w_{KL}(k) \end{pmatrix} \tag{4}$$

and the output signal at time t becomes

$$y(t) = \underline{W}^T(k)\underline{X}(t) \tag{5}$$

It is presumed that the k^{th} adaptation occurs at time t_k.

The array processor studied in this research is that which minimizes the mean-square error between a desired signal waveform $d(t)$ and the array output signal $y(t)$. The desired waveform was assumed to be planar and to propagate across the array from a known direction of arrival θ_d. Each antenna element is also assumed to receive noise signals consisting of both directional interference and non-directional background sky noise. Although the precise nature of these noises -- i.e. direction of arrival and spectrum -- is unknown, they are all assumed to be uncorrelated with the desired signal.

The set of coefficients $\underline{W}^*$ which minimizes the mean-square error between $y(t)$ and $d(t)$ is the Wiener filter which has been discussed by many authors[6,8,9,16] It is given by the solution to the normal equations

$$\underline{W}^* = \underline{\underline{R}}_{XX}^{-1} \underline{P}_{X_d} \tag{6}$$

where $\underline{\underline{R}}_{XX}$ is the autocorrelation matrix of the signals observed at the weights and $\underline{P}_{X_d}$ is the cross-correlation vector between these signals and the desired signal. That is

$$R_{XX} = E[\underline{X}(t)\underline{X}^T(t)] \tag{7}$$

$$\underline{P}_{X_d} = E[d(t)\underline{X}(t)] \tag{8}$$

where $E[\cdot]$ denotes expectation, or time average, and superscript T denotes transpose.

In general, an array processor similar to that shown in

Fig. 1 with the tapped-delay line weights set to the values given in Eq. (6) will have a mainlobe in the direction θ_d of the desired signal and will also contain pattern nulls in the direction of strong interfering noise sources. Clearly, a processor of this type can achieve considerable improvement in output signal-to-noise ratio as compared with conventional time-delay and sum processing under conditions of low per element signal-to-noise ratio. Optimization criteria other than minimum mean-square error have been studied in the literature--e.g. see References 4, 13 and 15 -- and these processors also achieve desirable antenna array patterns. The reason for choosing a minimum-mean-square error criterion in the present research was that a simple adaptive algorithm is available which achieves this solution using a minimal number of computations. Similar algorithms for other performance criteria have not yet been developed.

B THE ADAPTIVE ALGORITHM

Due to a lack of knowledge regarding the noise structure, the optimum weight set $\underline{W}^*$ defined by Eq. (6) cannot be calculated directly. Procedures are available[15] for measuring the correlation statistics at the element outputs and using this information to compute the $\underline{R}_{XX}$ matrix and the resulting optimum weight set. One difficulty with this method, however, is that the measurement of correlation parameters and weight set computation is complex, requiring numerous numerical calculations. In addition, the weight set so obtained will be incorrect in

the presence of changing noise fields.

An alternative procedure for computing $\underline{W}^*$ is the adaptive algorithm first proposed by Griffiths[14]. In this method, the weight vector is recalculated at successive times $t_1, t_2, \ldots t_k, \ldots$ using the equation

$$\underline{W}(k) = \underline{W}(k-1) + \mu[\hat{\underline{P}}_{X_d} - y(t_k)\underline{X}(t_k)], \tag{9}$$

where: t_k = time at which k^{th} adaptation takes place

$\underline{W}(k-1)$ = set of filter coefficients used prior to t_k

$\underline{W}(k)$ = set of filter coefficients used after t_k

$y(t_k)$ = array output signal at time t_k

$\underline{X}(t_k)$ = vector of signals stored in the filter

μ = proportionality constant which controls the rate of convergence of the algorithm

$\hat{\underline{P}}_{X_d}$ = estimate of signal cross-correlation vector

A complete description of the derivation and convergence properties of this algorithm may be found in Reference 14. It can be shown that for a value of μ which satisfies

$$0 < \mu < 2/ \sum_{i=1}^{KL} E[x_i^2(t_k)], \tag{10}$$

where $\sum_{i=1}^{KL} E[x_i^2(t_k)]$ is the total signal power present in the array processor, then $\underline{W}(k)$ converges in the mean to $\underline{W}^*$ as k tends to infinity. That is, the limiting mean value of $\underline{W}(k)$ is equal to $\underline{W}^*$ and the standard deviation is a non-zero value which is proportional to the constant μ.

Several practical factors must be considered when Eq. (9) is implemented as an array processor. The choice of the optimum value for μ involves a tradeoff between the convergence rate and the steady-state adaptation output noise which is produced by the fact that the weights are constantly changing. A value near the upper limit in Eq. (10) will produce a rapid convergence rate and relatively large output adaptive noise. Values near zero, however, have the opposite effect -- i.e. long convergence times and negligible output noise. Given that μ must be large enough to permit the processor to track time variations in the received noise field, an effective value can be determined. As shown in Section V, the convergence properties are relatively insensitive to small changes in μ and values between .04 and .40 of the upper limit in (10) produced satisfactory results.

An additional factor which must be considered is the estimated cross-correlation vector $\hat{\underline{P}}_{Xd}$. Given that the desired signal $d(t)$ is assumed to be planar and incident on the array from a known direction θ_d, the value of this vector may be calculated from a knowledge of the power spectrum of $d(t)$. For the linear array geometry of interest in this research, $\underline{P}_{Xd}$ has a particularly simple form. If $\Delta\tau$ is the interelement delay for signals arriving from direction θ_d, the i^{th} component of this vector (which is the cross-correlation between the signal observed at the i^{th} filter coefficient and the desired array output signal) is given by

$$p_i = r_d(\tau_o - n\Delta\tau - m\Delta T) \quad . \tag{11}$$

In this equation, $r_d(\cdot)$ is the autocorrelation function of the desired signal which is computed as the inverse of the given power spectrum, n is the receiving element number and m is the number of delays preceding the coefficient of interest. The symbol τ_o is the reference delay of the desired signal which is generally set equal to the delay to the center tap in the delay line connected to a central element in the array. Thus, the desired array output signal is assumed to be $d(t-\tau_o)$ when $d(t)$ is the signal received by the element nearest the desired source. The performance of the array processor can be shown to be relatively insensitive to changes in τ_o [21] so long as a value near that corresponding to the mid-point delay of the processor is used.

V. RESULTS

This section summarizes results obtained from the off-line processing of ten successive data blocks taken over the Bearden-Los Banos path, as described in Section III. The data were processed to demonstrate the advantages of optimum array processing techniques in low signal-to-noise ratio environments. Two desired signals of known center frequency and direction of arrival were assumed to be present in the data -- see Figs. 14 and 15. The Bearden signal, which constituted the major faction of the received energy, was assumed to be an undesired interfering signal of unknown spectral and spatial content. Least mean-square error array processors were developed to extract each of the desired signals, in turn. The performance of these processors was then compared with conventional time shift and spatial weighting methods of receiveing the same desired signals.

A. OPTIMUM PROCESSOR CALCULATIONS

As described in Section IV above, the set of filter coefficients $\underline{W}^*$ which minimizes the mean-square-error performance criterion can be calculated from a knowledge of the autocorrelation matrix of the received signals and the estimated cross-correlation vector for the desired signal (see Eqs. (6), (7),(8)). The array performance achieved with this set of coefficients is equal to that achieved on the average by an adaptive processor and therefore represents a performance baseline which may be used to evaluate the effectiveness of minimum mean-square-error array processing.

The optimum filter coefficients $\underline{W}^*$ were calculated for each of the ten successive data blocks. Correlation statistics were computed by using time averages over the eight seconds of data (512 samples per receiving element) within each data block. Statistics of this type were measured for processors consisting of two, five, and ten filter coefficients per array element. Since these statistics depend only upon the properties of the received signals, they are not dependent upon the direction of arrival and frequency of the presumed desired signal. This latter information is contained in the structure of the estimated cross-correlation vector $\hat{\underline{P}}_{\underline{X}_d}$ defined in Eq. (8).

The desired signals used throughout this research were presumed to have a sinusoidal CW time structure and planar spatial wavefronts. It was assumed that the phase of these signals, as measured at the array element nearest the desired source, could be modelled as a random variable uniformly distributed over 0 to 2π radians. This assumption is consistent with experimental observations of ionospherically reflected, single mode CW signals. The autocorrelation function for CW signals with random phase is given by

$$r_d(\tau) = \frac{A^2}{2} \cos \omega_o \tau \qquad (12)$$

where A is the received signal amplitude and ω_o is the center frequency. The components of the cross-correlation vector $\hat{\underline{P}}_{\underline{X}_d}$ for an array processor with KL coefficients are then given by

$$\hat{\underline{P}}_{\underline{X}_d} = \frac{A^2}{2} \begin{pmatrix} \cos\ \omega_o(\tau_o-\tau_1) \\ \cos\ \omega_o(\tau_o-\tau_2) \\ \vdots \\ \cos\ \omega_o(\tau_o-\tau_{KL}) \end{pmatrix} . \qquad (13)$$

In this expression, τ_i is the time delay between the i^{th} filter coefficient and the element nearest the desired source and τ_o is the reference delay of the desired signal (see Eq. (11)). The method used to calculate this delay was

$$\tau_o = \frac{\tau_{min} + \tau_{max}}{2} \qquad (14)$$

where τ_{min} and τ_{max} are the minimum and maximum values of τ_i in Eq. (13).

The only parameter in Eq. (13) which cannot be calculated from a knowledge of the direction of arrival and frequency of the desired signal is the amplitude A. It is not reasonable to assume that this parameter is known a priori in most applications since knowledge of A implies that the received per element signal-to-noise ratio is also known. Inspection of Eq. (6), however, shows that only the gain of the optimum filter $\underline{W}^*$ changes with varying A. Because the processor output signal-to-noise ratio is independent of gain -- i.e. increased gain increases both the output signal power and the output noise power -- an arbitrary gain $A = \sqrt{2}$ can be used without affecting the detection performance of the processor.

B. CONVENTIONAL PROCESSOR CALCULATIONS

A second type of fixed, non-adaptive processor was computed and tested using the received data. This processor consisted of time delays and amplitude weighting as shown in Fig. 23. The time delays $\Delta\tau, 2\Delta\tau, \ldots 7\Delta\tau$ are chosen such that a planar signal arriving from the known direction θ_d appears in phase at the output of the delays. Delay values were calculated for each of the two desired signals d_1 and d_2 shown in Fig. 15. The amplitude weights $c_1, c_2, \ldots c_8$ were selected using a raised cosine in which a ten element array was assumed with the outer two elements receiving zero weight values. The weights for the remaining eight elements are given in Table 2.

TABLE 2

AMPLITUDE WEIGHTS FOR CONVENTIONAL PROCESSOR

Element No.	Weight
1	.17
2	.41
3	.75
4	.97
5	.97
6	.75
7	.41
8	.17

The antenna array pattern for the conventional processor steered toward signal d_1 is shown in Fig. 24. A linear amplitude scale has been used in this display and the separation between adjacent azimuthal tick marks is 0.510 degrees. Note

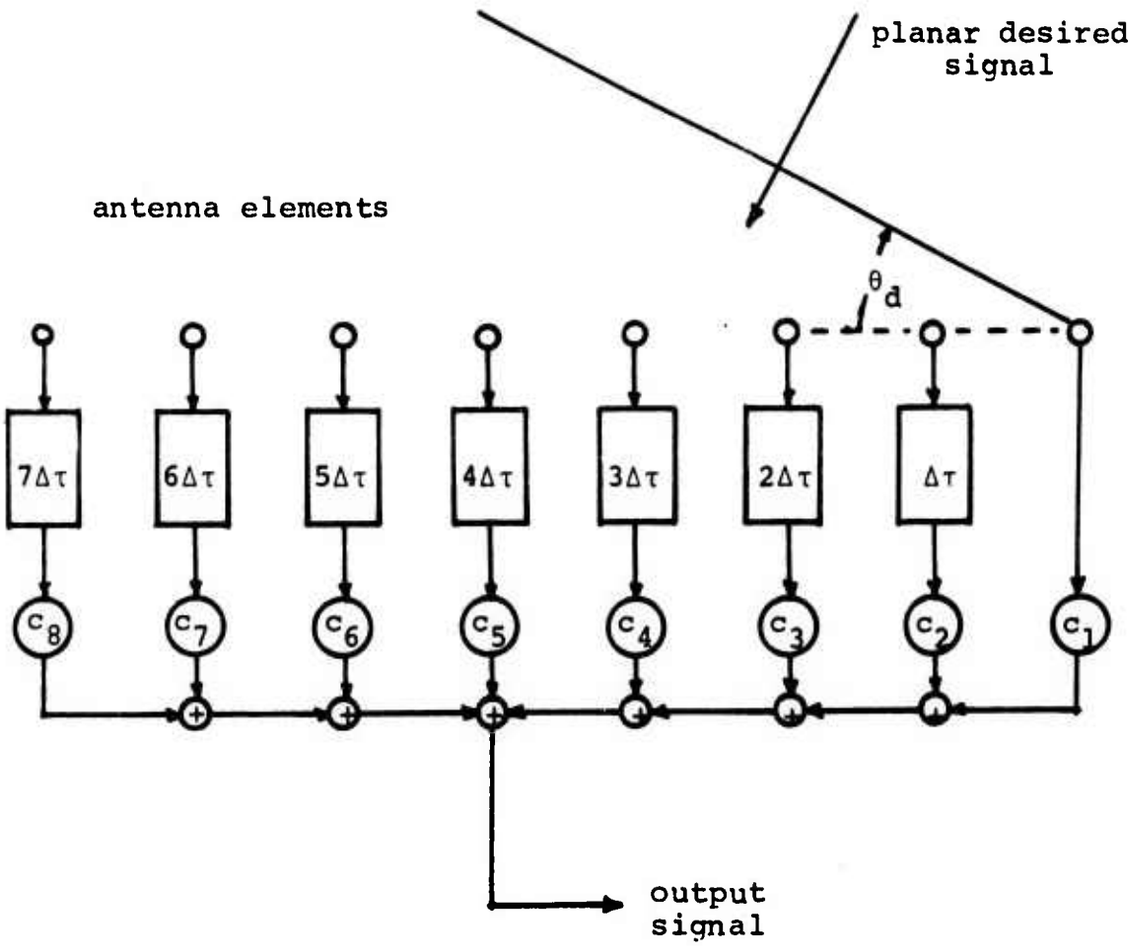

FIG. 23. Non-adaptive time-delay and amplitude weighting beamforming system

that only the mainlobe pattern has been plotted to simplify the display. Because of the wide spacing (360m) between the individual antenna elements, the complete pattern contains grating lobes at increments of 4.08 degrees for signals received at 11.70 MHz. The mainlobe pattern for the conventional processor steered toward the second desired signal d_2 is identical to that shown in Fig. 24, except that it is shifted one increment to the right.

Antenna patterns drawn for the conventional processors in this research are frequency independent over the bandwidth of the received signals. This is due to the fact that the processors are assumed to consist of ideal time delays and multiplying weights. In practice, narrow band conventional processors are constructed using 90° phase shift elements at the array center frequency, which will generally produce a frequency dependent array pattern. Due to the relatively low sampling rate of 62.5 Hz used in the present experiment, however, the received signals were bandlimited to 31.25 Hz and 90° phase shifters would effectively provide ideal time delay over this bandwidth. In summary, the conventional pattern for the signals recorded in this work is frequency independent for both time delay and phase shift steering.

An alternative method for displaying antenna array patterns is illustrated in Figs. 25 and 26 which show the conventional patterns for d_1 and d_2, respectively. This procedure presents the array response in the eight resolvable azimuthal directions as a function of frequency over the 31.25 Hz bandwidth. The ninth azimuthal line shown in these figures is a duplicate

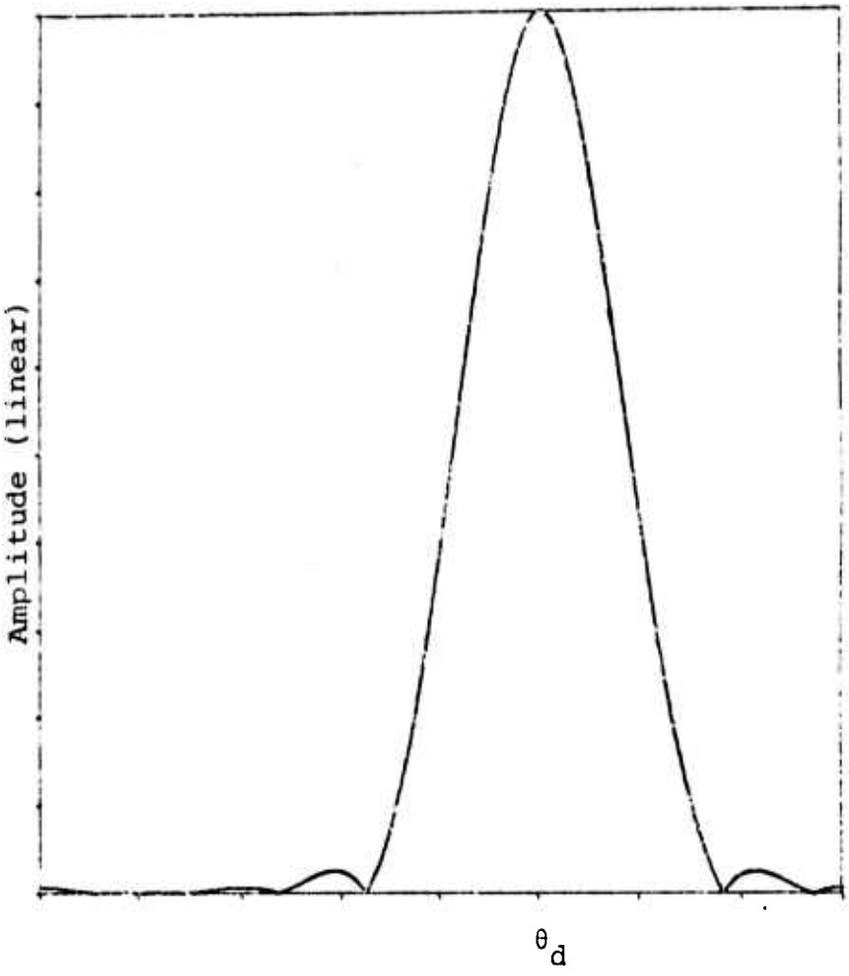

FIG. 24. Antenna array pattern for conventional array processor with raised cosine weighting.

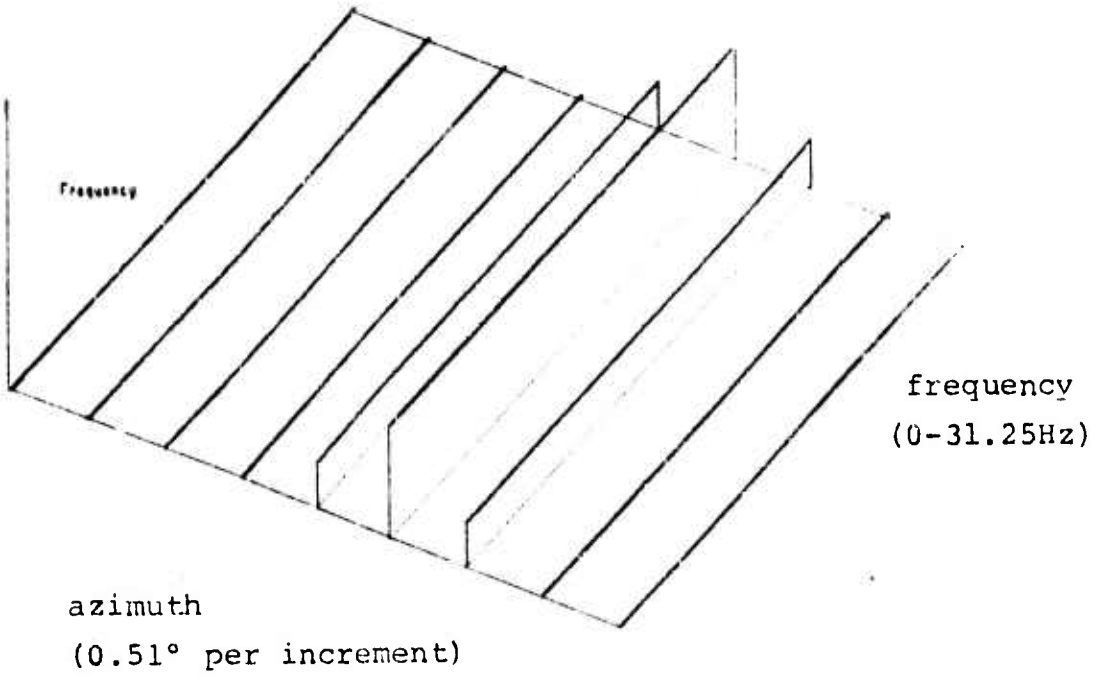

FIG. 25. Two-dimensional array pattern for conventional processor steered to receive desired signal d_1.

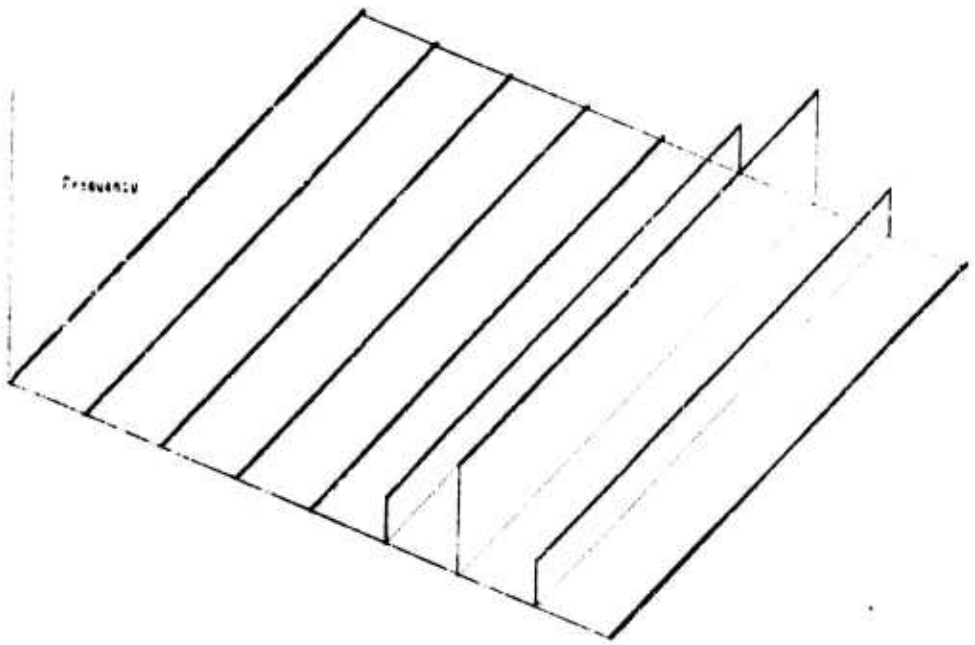

FIG. 26. Two-dimensional array pattern for conventional processor steered to receive desired signal d_2.

of the first line and is included for purposes of symmetry. Note that these figures demonstrate the frequency independence of the conventional processor.

C. PERFORMANCE COMPARISONS FOR DESIRED SIGNAL D_1.

The previous discussions have described two methods of computing fixed processors. The performance of these processors can be effectively compared by computing the resulting output signal-to-noise ratio for each processor. This calculation was carried out by first computing the total output signal power in terms of the known signal parameters and the processor coefficients. The sum of signal plus noise output power for the recorded data was then measured by implementing the processor and time averaging the square of the output signal. An equivalent, direct calculation can be made using the measured autocorrelation matrix.

A summary of the output signal-to-noise ratio performance for both optimal and conventional processors designed to receive signal d_1 is given in Table 3, as a function of the data block number. The individual element signal-to-noise ratios are also included for purposes of comparison. Optimal filters consisting of two weights per element (16 weights total), five weights per element (40 weights total), and ten weights per element (80 weights total) were computed for the first and third data blocks and the 40 weight processor was computed for all ten cases. The average array gain -- computed as the improvement above single element SNR -- for these processors is given in Table 4 below.

TABLE 3

SNR PERFORMANCE COMPARISON

DATA BLOCK NO.	PER ELEMENT SNR	CONVENTIONAL	16 WEIGHT OPTIMAL	40 WEIGHT OPTIMAL	80 WEIGHT OPTIMAL
1	-51.6	-43.3	-37.5	-19.4	-14.4
2	-39.8	-28.1	-	-6.1	-
3	-43.2	-24.3	-20.3	-7.5	-6.1
4	-41.7	-31.2	-	-8.8	-
5	-44.4	-35.9	-	-14.4	-
6	-64.6	-43.2	-	-25.6	-
7	-50.4	-39.3	-	-17.7	-
8	-52.8	-42.0	-	-18.3	-
9	-47.6	-37.2	-	-21.8	-
10	-40.4	-27.0	-	-12.2	-

TABLE 4

AVERAGE PROCESSOR GAIN

PROCESSOR TYPE	GAIN OVER SINGLE ELEMENT
conventional	12.5 db
16 weight optimal	17.4
40 weight optimal	32.5
80 weight optimal	41.6

Figures 28 through 36 illustrate the antenna array patterns achieved for the optimal processors. A comparison of the 16, 40, and 80 tap filters for block 1 is shown in Figs. 27-29 and for block 3 in Figs. 30-32. The performance of the 40 weight optimal filter on data blocks 5, 7, and 9 is given in Figs. 33-35. Finally, a conventionally displayed array pattern is shown in Fig. 36 for the 40 weight processor computed for block 1. The pattern is plotted at three frequencies: the Bearden transmitter frequency (minimum response), the d_1 desired frequency (maximum response) and an intermediate frequency. Note that all of the optimal patterns have a maximum in the direction of the desired signal, but that this maximum is frequency dependent and appears only at the frequency of the desired signal. Most patterns also show a spatially broad, deep null at the Bearden frequency.

It should be noted that block-to-block variations in the output SNR of the optimal filters shown in Table 3 is due to two factors: 1) The optimal filter calculation depends on the correlation statistics of the received data which may vary from

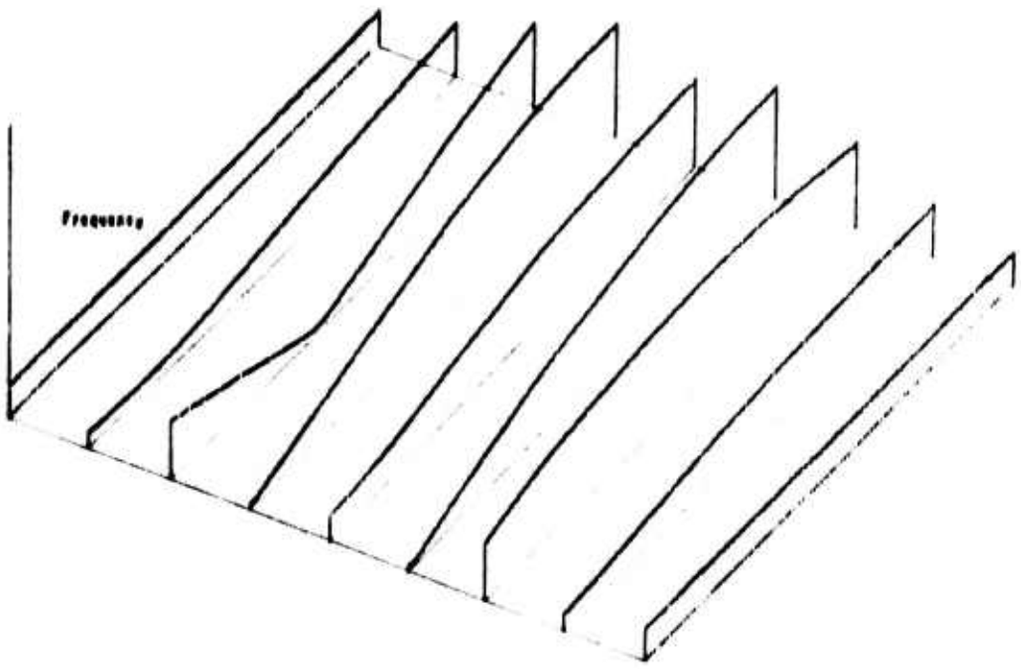

FIG. 27. Two-dimensional array pattern for optimal array processor with 16 weights on data block no. 1.

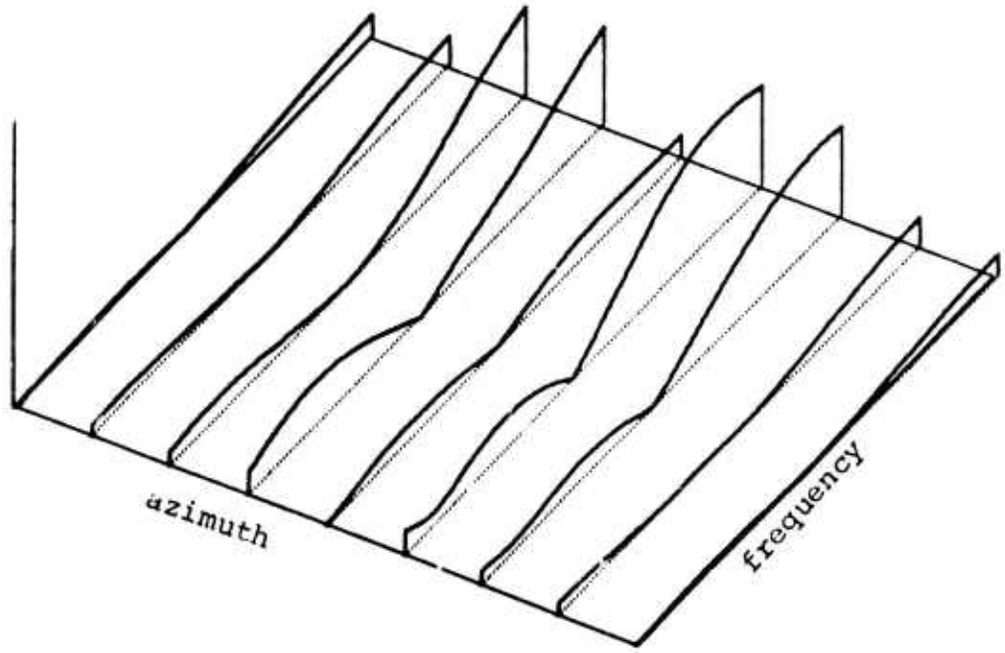

FIG. 28. Two-dimensional array pattern for optimal array processor with 40 weights on data block no. 1.

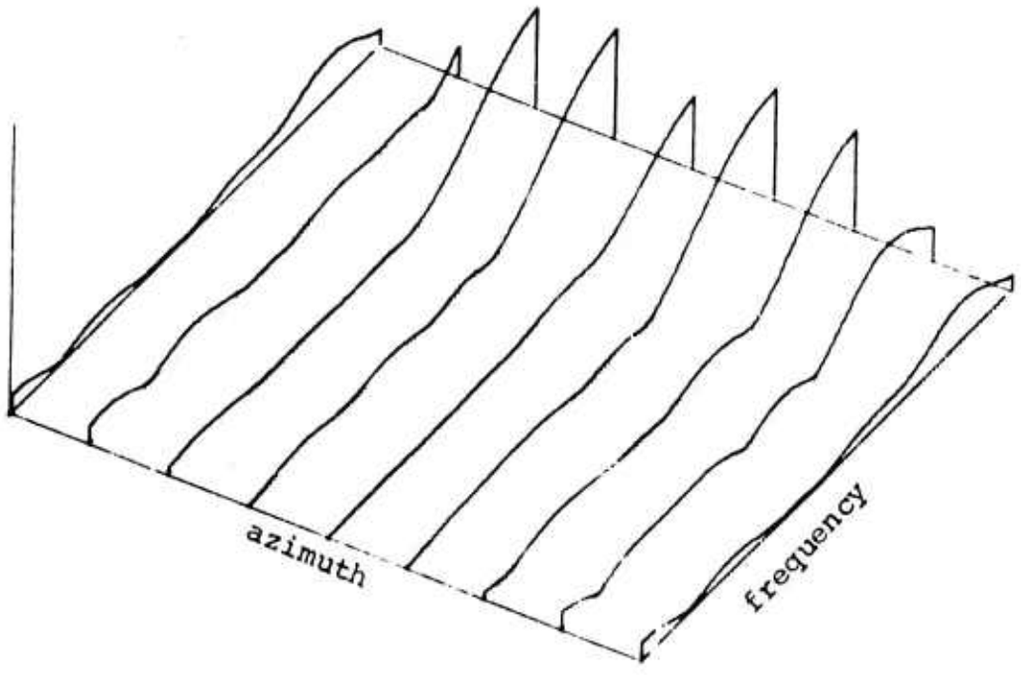

FIG. 29. Two-dimensional array pattern for optimal array processor with 80 weights on data block no. 1.

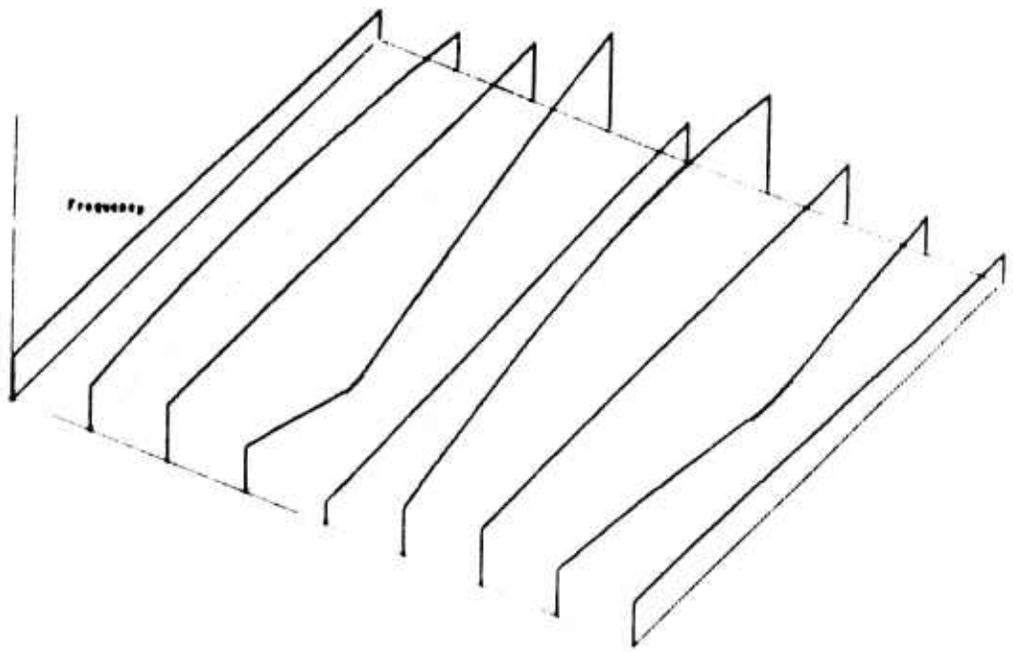

FIG. 30. Two-dimensional array pattern for optimal array processor with 16 weights on data block no. 3.

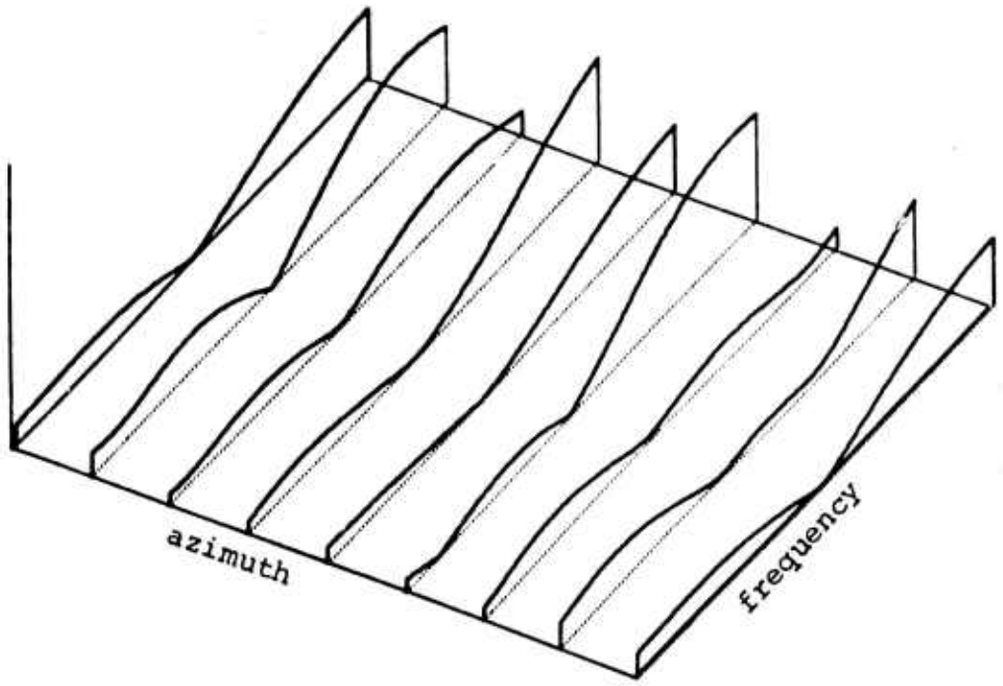

FIG. 31. Two-dimensional array pattern for optimal array processor with 40 weights on data block no. 3.

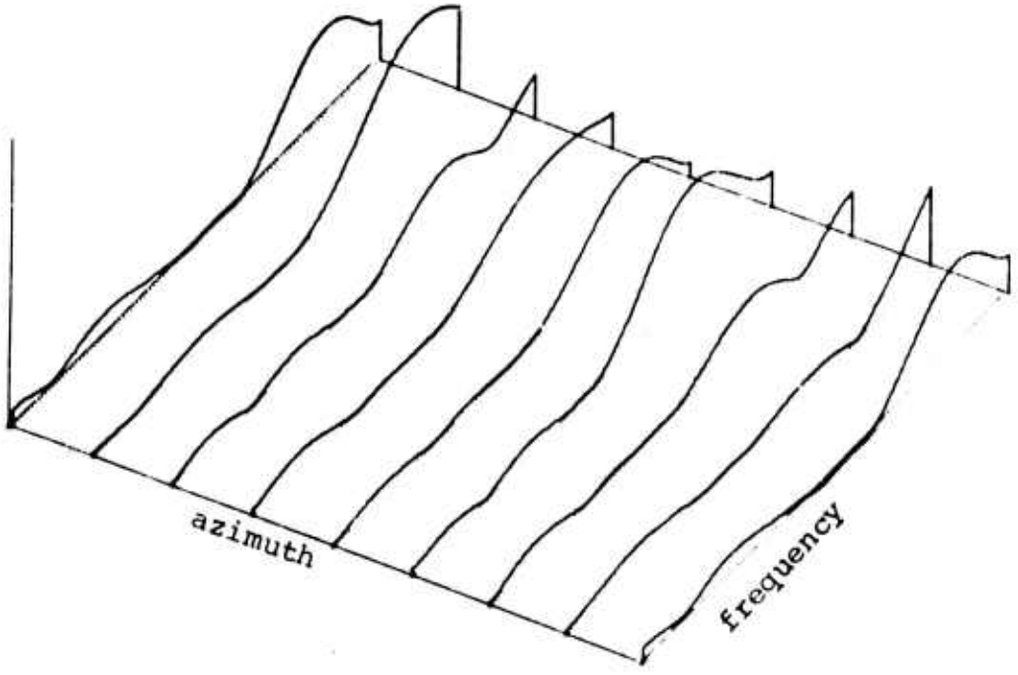

FIG. 32. Two-dimensional array pattern for optimal array processor with 80 weights on data block no. 3.

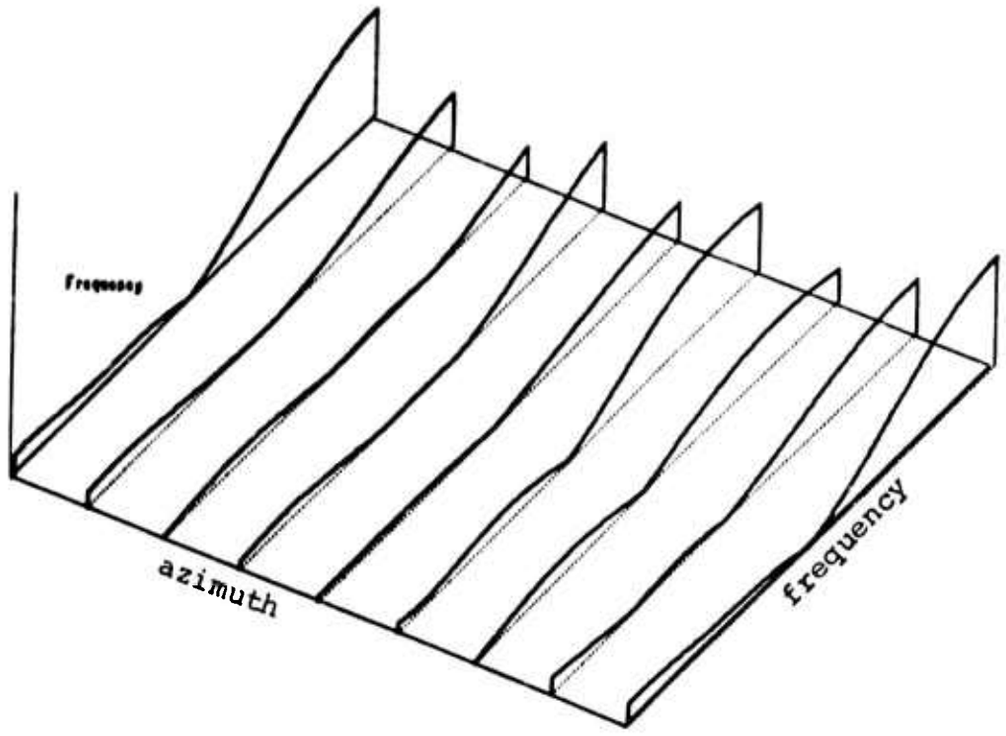

FIG. 33. Two-dimensional array pattern for optimal array processor with 40 weights on data block no. 5.

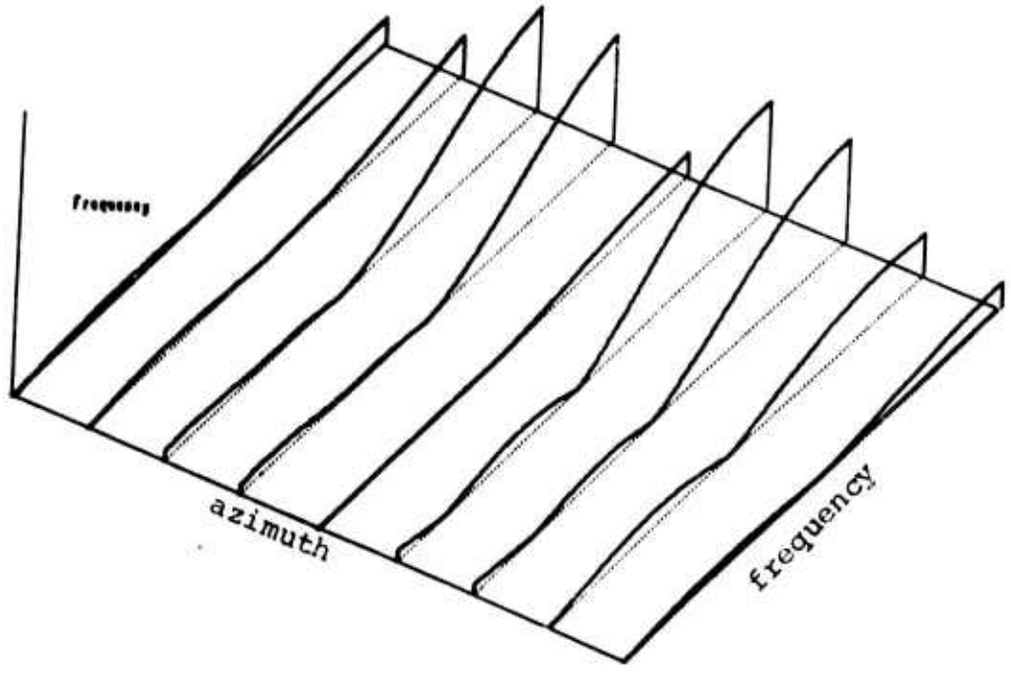

FIG. 34. Two-dimensional array pattern for optimal array processor with 40 weights on data block no. 7.

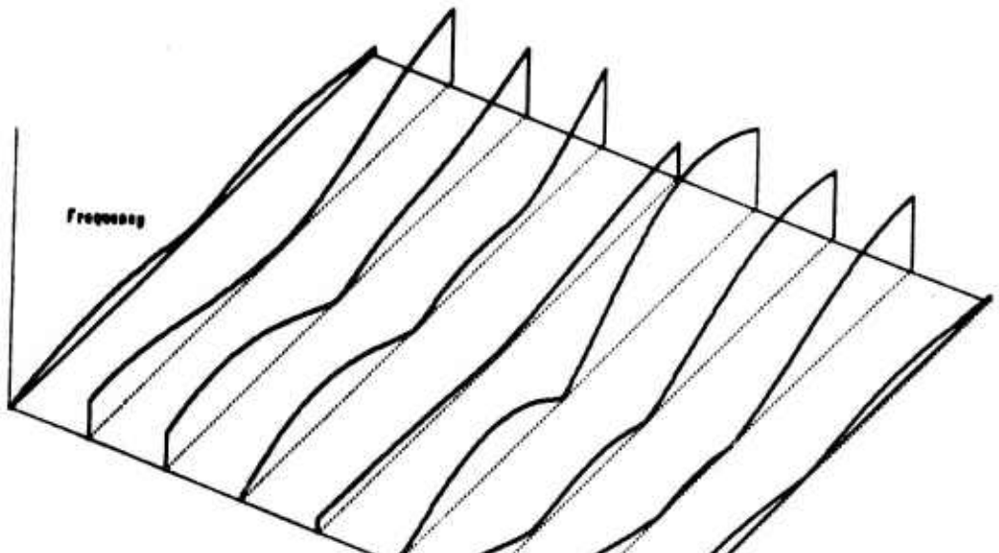

FIG. 35. Two-dimensional array pattern for optimal array processor with 40 weights on data block no. 9.

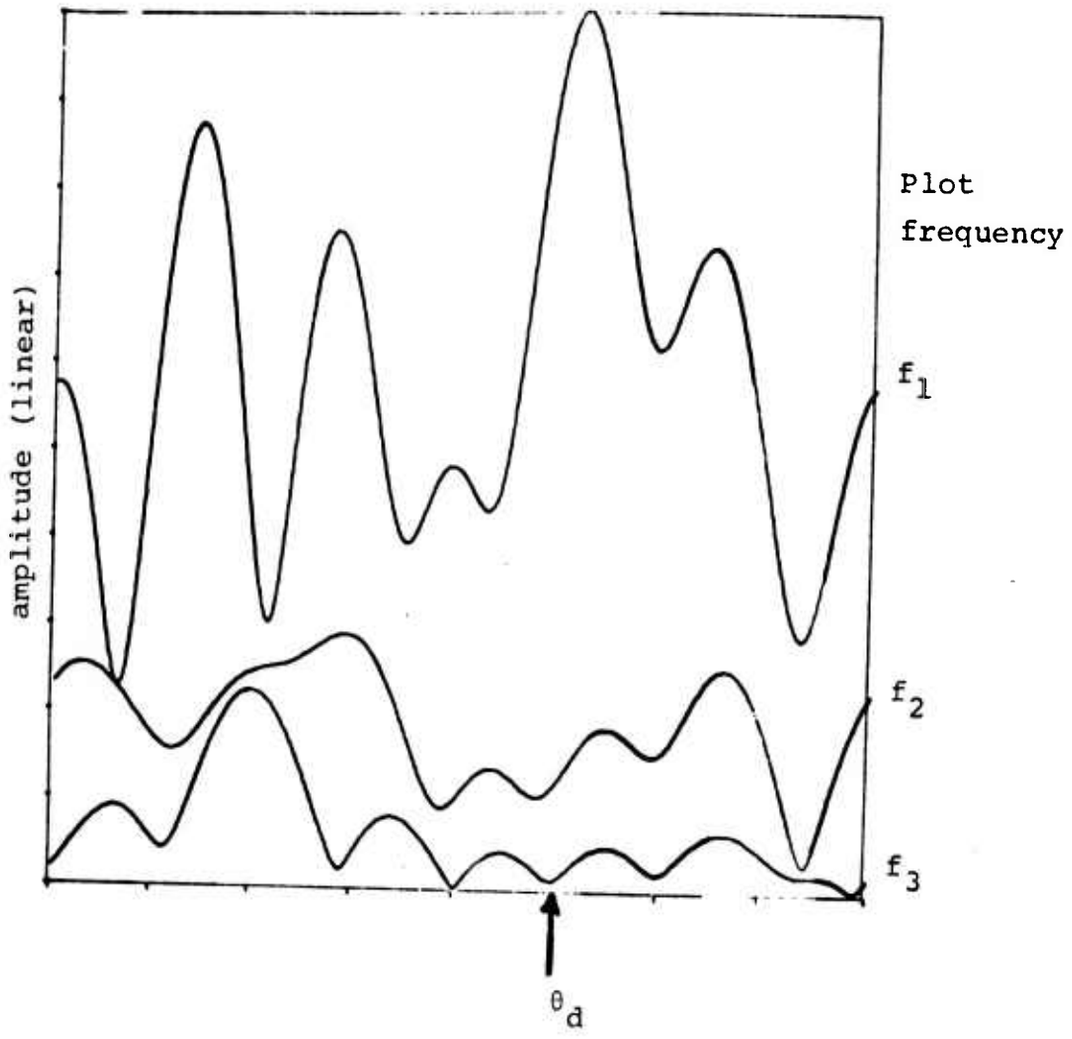

FIG. 36. Single frequency antenna array patterns for optimal filter shown in Fig. 28.

block to block and 2) The received signal-to-noise ratio varies between blocks. An example of the latter factor can be found by comparing the 40 weight optimal filters for blocks 1 and 2. The second block has a processed output SNR which is 13.3 db higher than that for the first data block. Inspection of the elemental SNR's, however, shows that 11.4 db of this change can be attributed to a drop in the received SNR. Variations due to correlation changes are important when considering the potential use of an adaptive processor because they require corresponding changes in the filter coefficients. Received SNR variations are relatively unimportant to an adaptive processor because they reflect simple gain changes and do not require adaptation.

Calculations were made to determine the time rate of change of the correlation statistics. The procedure used was to measure the performance of an optimal filter computed for one particular data block by computing output SNR for other data blocks. In effect, this procedure is equivalent to computing an optimal filter during one data block and then fixing the weights for use in other data blocks. Figure 37 dhows the performance change observed when the optimal 40 weight filter for the first data block was applied to all succeeding blocks. Similar plots for optimal filters computed for blocks 3 and 7 and applied to other data sets are shown in Fig. 38. These plots indicate that the penalty for not adapting to track the optimal filter is the order of 7 to 10 db, depending upon the length of time between the calculation of the optimal filter and the SNR measurement.

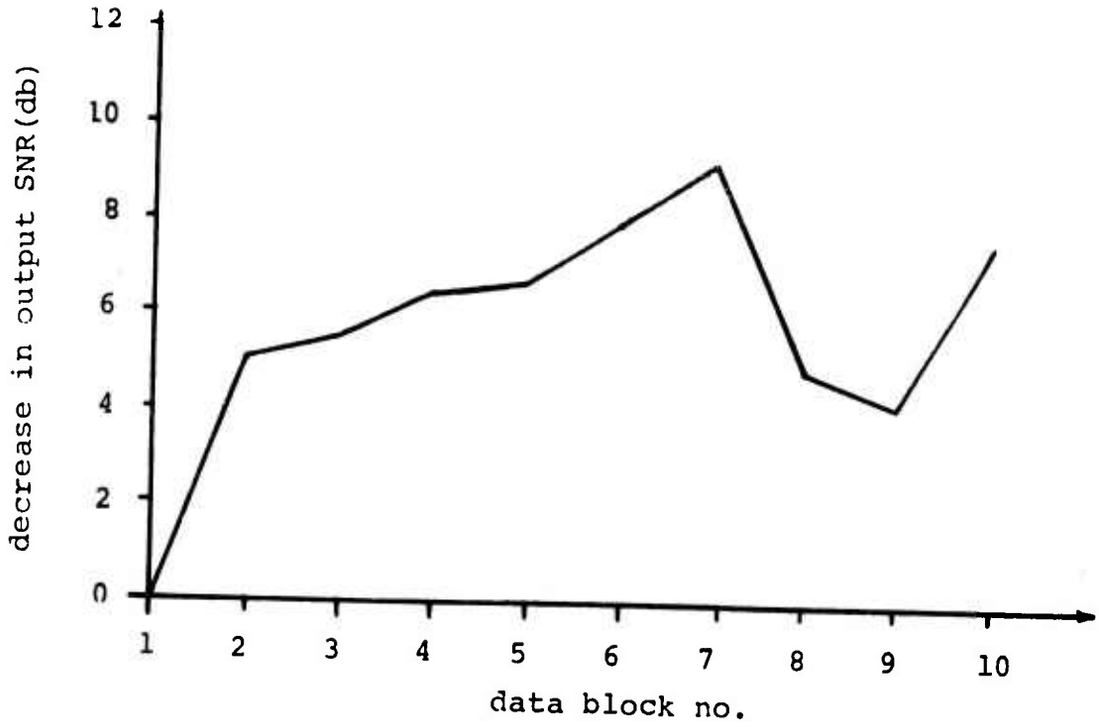

FIG. 37. Performance of block 1 optimal filter on succeeding blocks

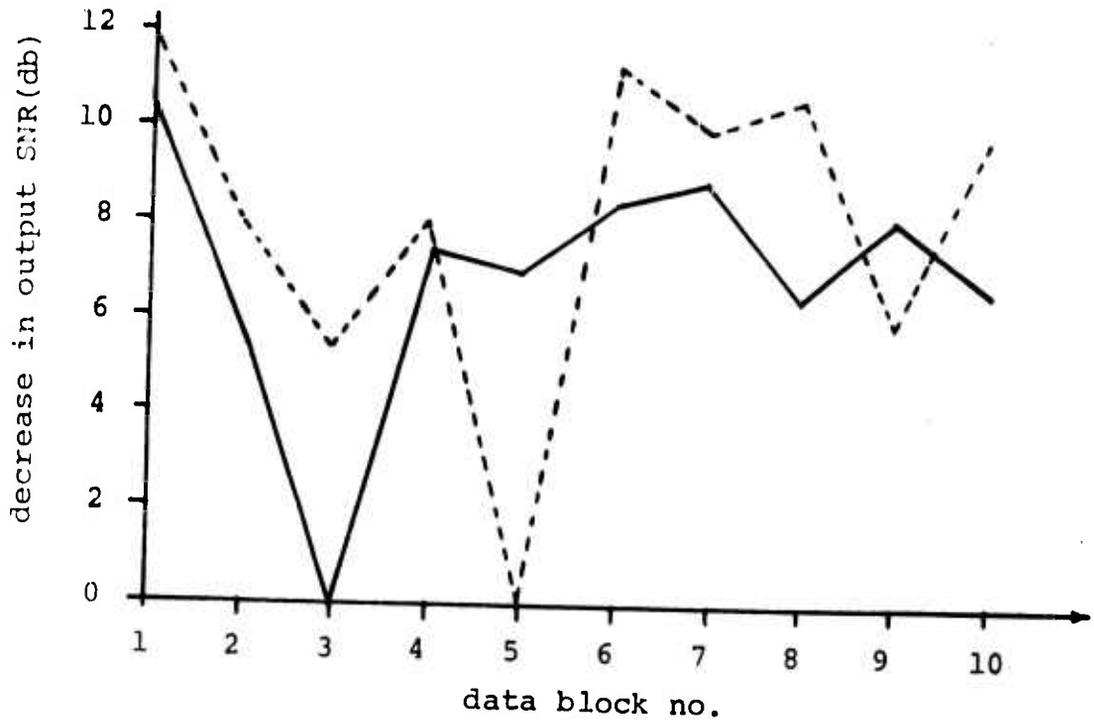

FIG. 38. Performance of block 3 and block 5 optimal filters

D. PERFORMANCE COMPARISONS FOR DESIRED SIGNAL D_2

Inspection of the two dimensional array patterns for the optimal processors given in Figs. 27-36 shows that the major improvement achieved in output SNR is due to the null which is placed on the Bearden transmitter. In order to determine the performance improvement of optimum processing for desired signals which are less isolated in the data displays shown in Figs. 14-19, a second desired signal d_2 was assumed to be present at the Bearden frequency and displaced 1.02 degrees from the Bearden azimuth as shown in Fig. 15. A time delay and amplitude shaded conventional processor was computed for this signal. The resulting antenna pattern is shown in Fig. 26. The pattern for a 40 weight optimal processor computed using signals in the first data block is shown in Fig. 39. Note that the response has a spatial null at the Bearden frequency for all azimuths except that corresponding to the assumed direction of arrival of d_2. The per element SNR for this case was -38.1 db, conventional processing produced an output SNR of -30.9 db and optimal processing resulted in a -25.0 db output SNR.

The rather low resulting antenna gain for the optimal processor is a consequence of the fact that the Bearden signal is widely spread in azimuth. Thus, at the Bearden frequency, the interfering noise is nearly isotropic and conventional processing is near optimal. The five db improvement achieved by the optimal processor is due to spatial irregularities in the Bearden signal.

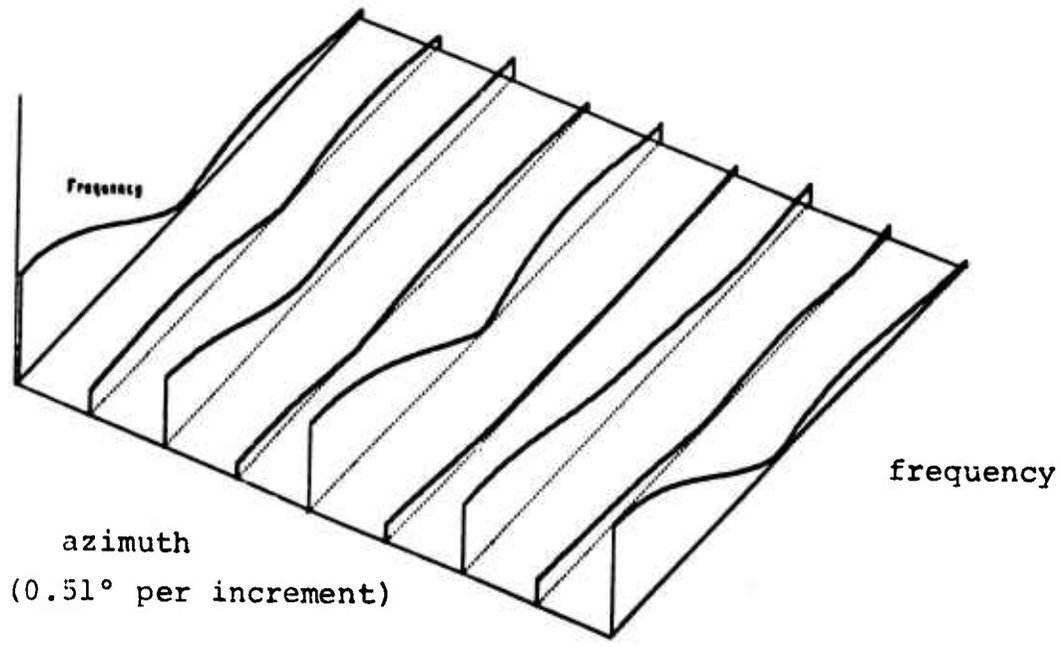

FIG. 39. Optimal filter with 40 weights designed for data block 1 and desired signal d_2.

E. ADAPTIVE ALGORITHM IMPLEMENTATION

The adaptive algorithm given in Eq. (9) was implemented on the recorded data using the out of band signal d_1 as the desired signal. The processor used in these studies contained a total of 40 adapted filter coefficients -- i.e. 5 taps per element. Several initial weight values and adaptation time constants were studied. In all cases, the performance of the adaptive processor showed excellent agreement with theoretical calculations based on the measured correlation statistics of the data.

Figure 40 illustrates the behavior of adaptive filter in the region of the optimal solution. The vertical axis shows the processor output SNR for the optimal set of filter coefficients (-19.42 db) and for 4 adaptive processors implemented using proportionality constants μ = 200, 400, 1000, and 2000 [see Eq. (9)]. The data used for these tests was that recorded in the first data block. In all four adaptation experiments, the filter coefficients were initially set to the optimal values previously computed for this data block. Thus, output SNR of the four processors is equal to the optimum value before adaptation begins. As adaptation progresses, however, the adaptive filters depart from the optimal value by an amount proportional to μ, the adaptive step size.

The suboptimality of the adaptive processors shown in Fig. 40 is a well known consequence of the fact that the weight computation algorithm given in Eq. (9) continually adjusts the

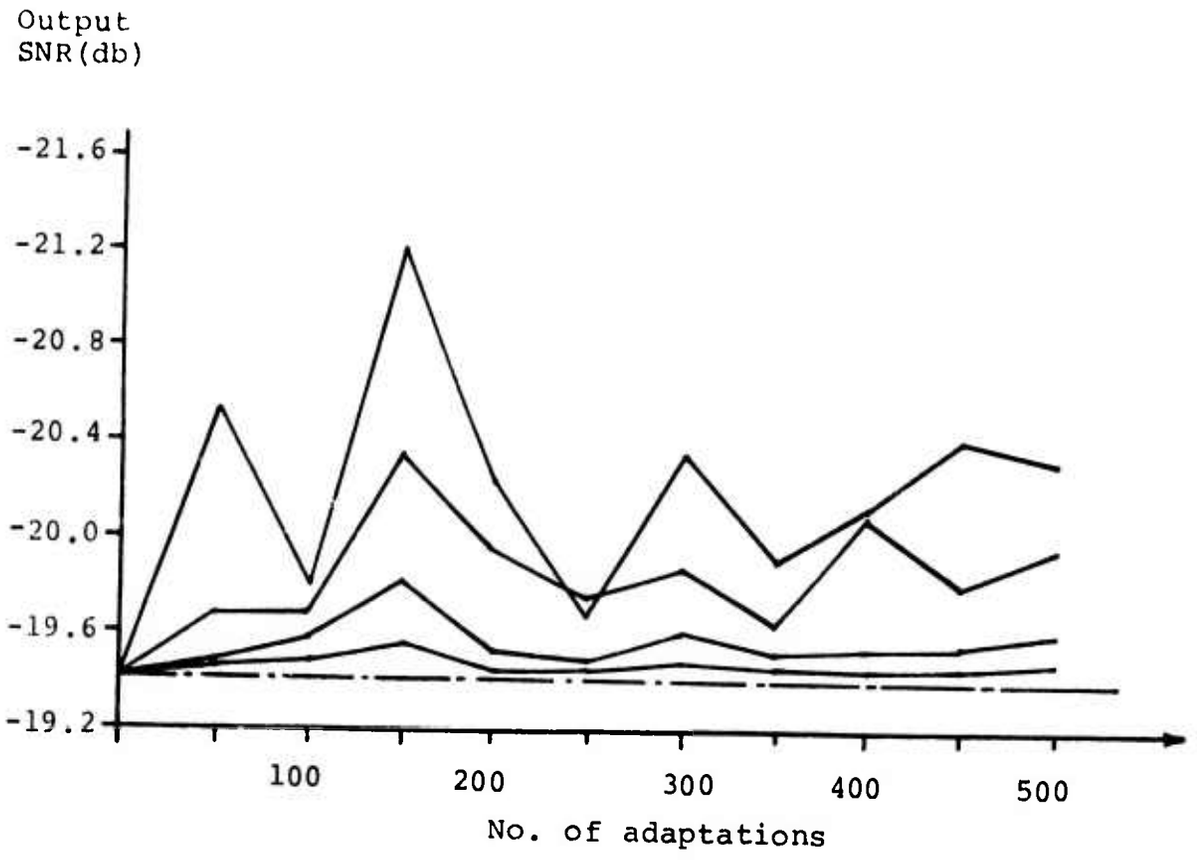

FIG. 40. Adaptive processor output SNR for four values of μ.

filter coefficients. Widrow[22] has termed this behavior misadjustment and has given formulas for calculating the average percentage offset as a function of the proportionality constant μ. It should be noted, however, that even the largest μ value used in these experiments produced a steady-state offset of less than 1 db.

The range of proportionality constants used in these experiments, 200 to 2000, can be related to the upper bound given by Eq. (10) which is repeated below for reference,

$$0 < \mu < 2/ \sum_{i=1}^{KL} E[x_i^2(t_k)] \ . \qquad (10)$$

The bound can also be computed as two over the sum of the diagonal elements in the $\underline{\underline{R}}_{XX}$ matrix. For the first data block, the value is

$$0 < \mu < 5{,}300 \ . \qquad (15)$$

Thus, the values ranged between 0.038 and 0.38 of the upper limit.

A series of adaptive experiments were also carried out to determine the time constant of adaptation, as a function of the proportionality constants. In these experiments, the initial values of the filter coefficients were chosen to be far removed from the optimal values and the relaxation time was measured as the filter adapted toward the optimum solution.

Figures 41-44 illustrate the results of a time constant determination experiment using data block number 4. In each

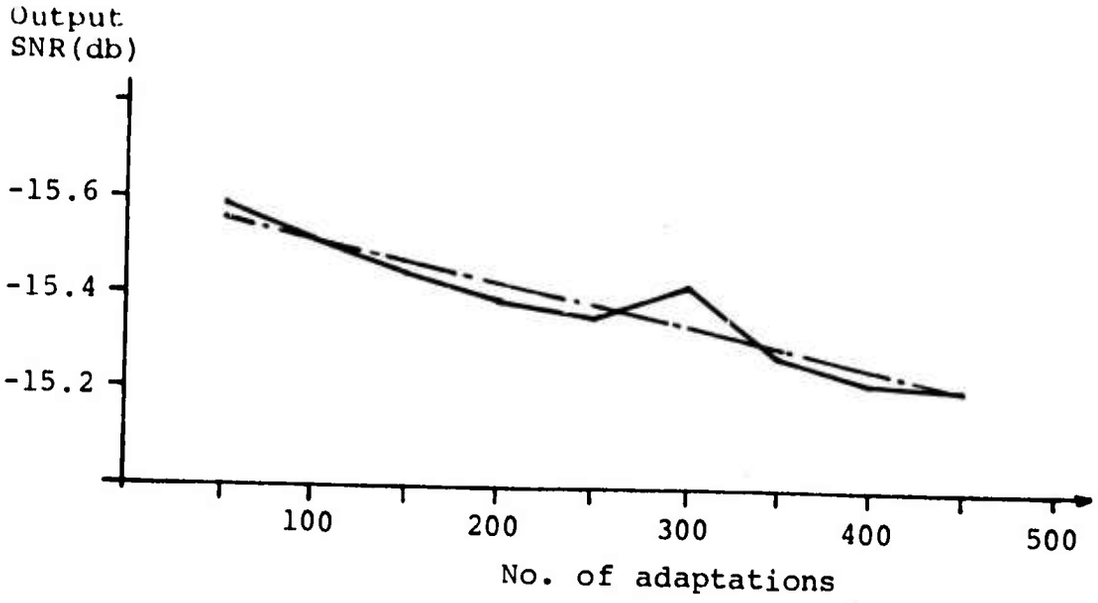

FIG. 41. Adapted output SNR with trend line, $\mu = 200$.

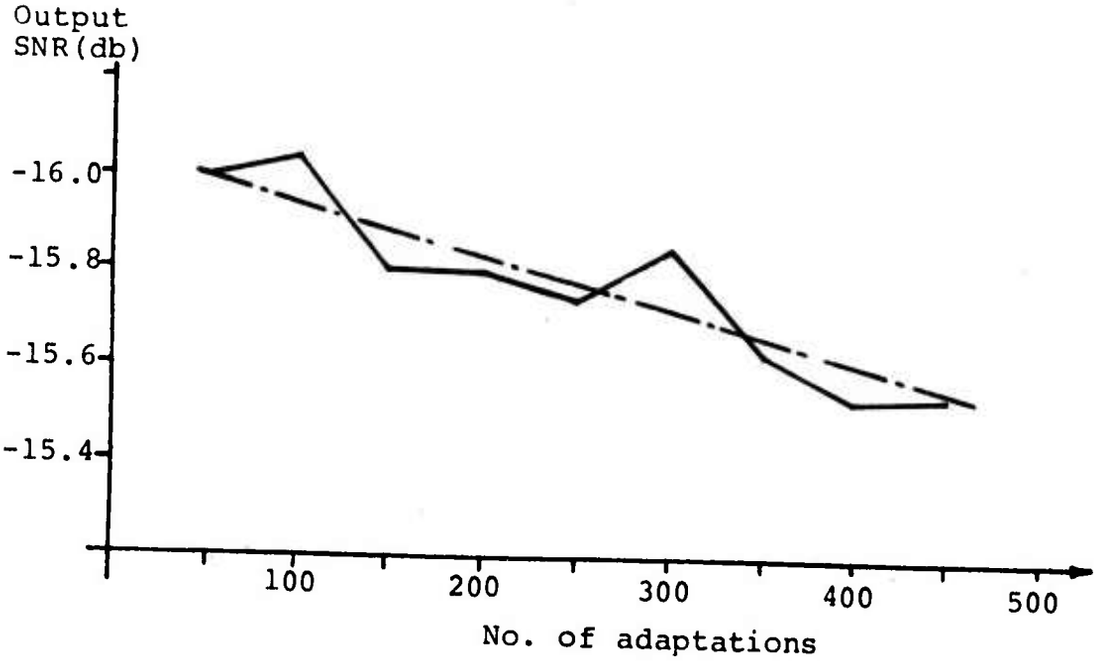

FIG. 42. Adapted output SNR with trend line, $\mu = 400$.

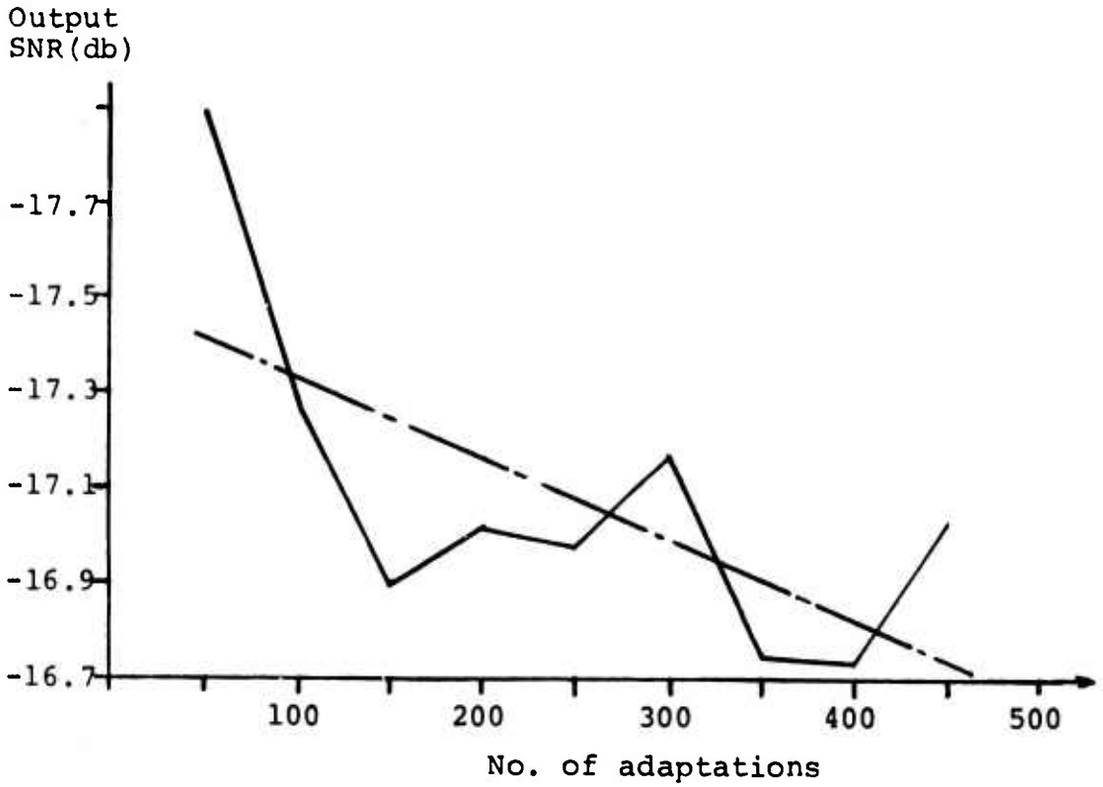

FIG. 43. Adapted output SNR with trend line, μ = 1,000.

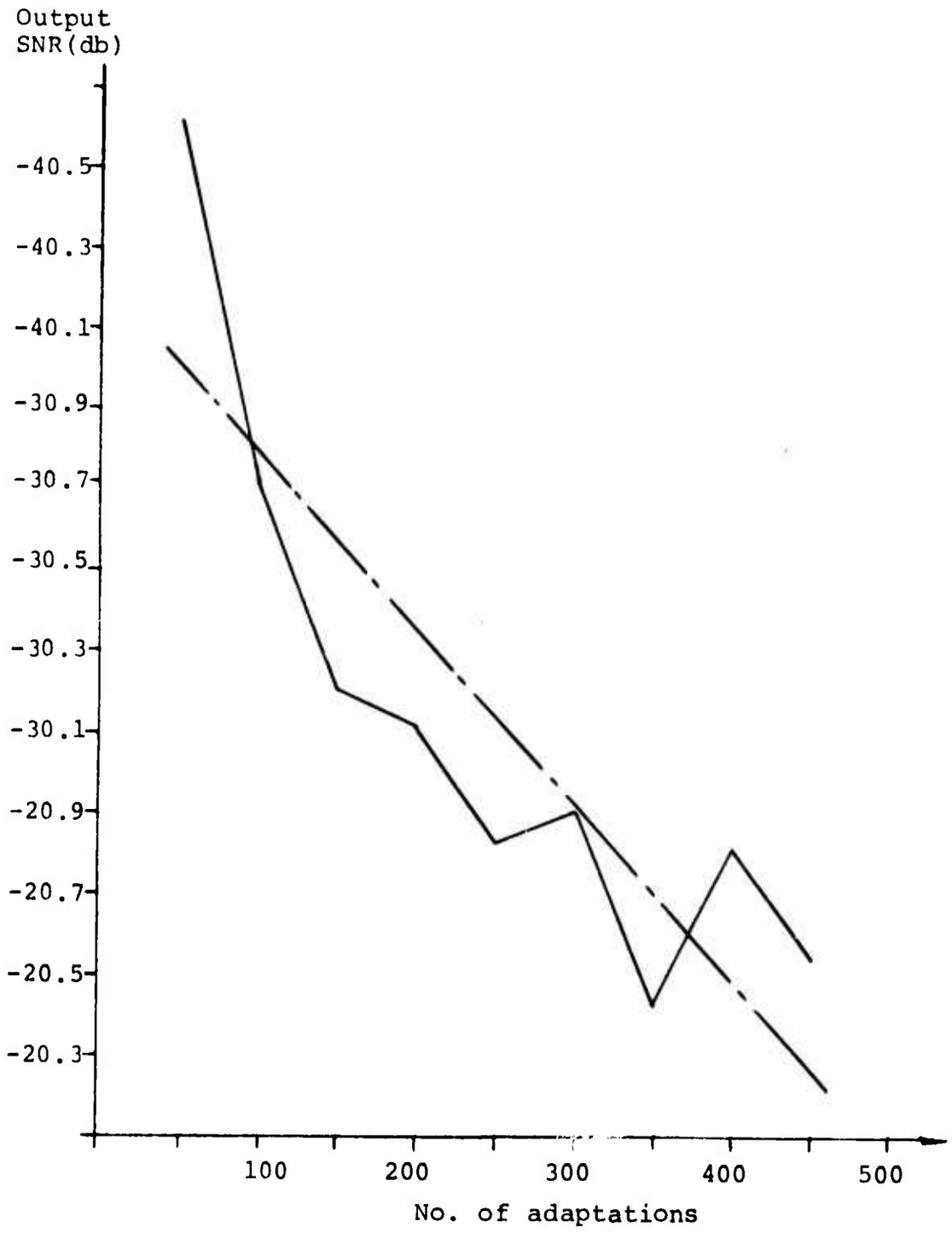

FIG. 44. Adapted output SNR with trend line, μ = 2,000.

case the weight vector was initially set to a random value before adaptation began. These figures show the output SNR as a function of number of adaptations for values of μ of 200, 400, 1000 and 2000. A best-fit linear trend line was also computed and plotted for each experiment. Inspection of these results shows that adaptation time constant decreases with increasing μ, resulting in a faster adaptation rate, and that the adaptive noise -- i.e. variations about the trend line -- increases with increasing μ. Both of these observations agree with theoretical predictions (see Ref's [14] and [22]). Table 5 below summarizes the time constant measurements taken from the trend line on these curves.

TABLE 5

ADAPTIVE TIME CONSTANT MEASUREMENTS

PROPORTIONALITY CONSTANT μ	ADAPTATION RATE	NO. OF ADAPTATIONS TO HALF POWER
200	0.85×10^{-3} db/adapt	3,530
400	1.11×10^{-3}	2,700
1000	1.73×10^{-3}	1,730
2000	4.38×10^{-3}	680

Complete theoretical predictions of adaptive time constants have been carried out[23,24] in terms of the correlation statistics of the data. It can be shown that the adapted mean square error converges as a sum of exponentials in which the exponent rate depends on the eigenvalues of the $\underline{\underline{R}}_{XX}$ correlation matrix and on the value of the proportionality constant. Specifically, it can be shown[24] that the adapted mean square error after k adaptations $\overline{\varepsilon^2}(k)$ is given by

$$\overline{\varepsilon^2}(k) = \overline{\varepsilon^2_{ss}} + \sum_{i=1}^{KL} c_i r_i^{2k} \qquad (16)$$

where,

$\overline{\varepsilon^2_{ss}}$ = steady-state adapted mean-square error

c_i = constant depending upon initial set of coefficients (prior to adaptation)

$r_i = (1 - \mu\lambda_i)$

$\lambda_i = i^{th}$ eigenvalue of $\underline{\underline{R}}_{XX}$.

Because of the constraints on μ, each r_i has a magnitude value less than unity. Thus, the second term in (16), which is the transient term, tends to zero as $k \to \infty$. It should be noted that the value of $\overline{\varepsilon^2_{ss}}$ depends upon μ and is somewhat higher than the optimum value as shown experimentally in Fig. 41.

Although the convergence rate of a sum of exponentials cannot be accurately approximated by one exponential rate, it can be bounded in terms of the largest and smallest exponent. The fastest and slowest possible convergence rates are given by

$$\varepsilon^2(k) \geq \varepsilon^2_{ss} + c_{max}\, r^{2k}_{max} \qquad (17)$$

$$\varepsilon^2(k) \leq \varepsilon^2_{ss} + c_{min}\, r^{2k}_{min} \qquad (18)$$

where r_{max} and r_{min} are the maximum and minimum values of r_i, respectively. These values were computed for the fourth data block in terms of the eigenvalues of the $\underline{\underline{R}}_{XX}$ matrix given

in Table 6.

TABLE 6

EIGENVALUES OF R_{XX} MATRIX FOR 4^{th} DATA BLOCK

NO.	EIGENVALUE	NO.	EIGENVALUE
1	7.22798E-05	21	6.77182E-05
2	3.13664E-05	22	2.98098E-05
3	6.61898E-06	23	6.05305E-06
4	4.41183E-06	24	4.21684E-06
5	1.31422E-06	25	1.04394E-06
6	5.73037E-07	26	5.03522E-07
7	4.72674E-07	27	3.99563E-07
8	3.69323E-07	28	3.39554E-07
9	2.57834E-07	29	2.17305E-07
10	1.89351E-07	30	1.63232E-07
11	1.54275E-07	31	1.30565E-07
12	1.07782E-07	32	8.50601E-08
13	7.24330E-08	33	6.19560E-08
14	4.42107E-08	34	4.02069E-08
15	3.68840E-08	35	3.05655E-08
16	2.83914E-08	36	2.73219E-08
17	2.11313E-08	37	1.82156E-08
18	1.65635E-08	38	1.56636E-08
19	1.21556E-08	39	8.17442E-09
20	7.77124E-09	40	5.54834E-09

Assuming that the output SNR convergence rate is similar to that given for the mean-square error in (16), the adaptation rates can be bounded using the maximum and minimum eigenvalues in Table 6. That is,

$$r_{max} = 1 - \mu \times 7.23 \times 10^{-5} \qquad (19)$$

$$r_{min} = 1 - \mu \times 5.55 \times 10^{-5} \qquad (20)$$

Table 7 shows the results of these calculations which indicate that the observed time constants are well within the theoretical bounds.

TABLE 7

THEORETICAL BOUNDS ON ADAPTATION RATES FOR 4^{th} DATA BLOCK

PROPORTIONALITY CONSTANT μ	MAXIMUM THEO. RATE	MINIMUM THEO. RATE
200	0.126 db/adapt	0.97×10^{-5} db/adapt
400	0.161	1.93×10^{-5}
1000	0.653	4.78×10^{-5}
2000	1.360	9.65×10^{-5}

VI. CONCLUSIONS

The research results described in this report were obtained by processing digital recordings of wide aperture HF array data taken at the WARF facility in Los Banos, California. These recordings were taken early in 1970 over a one-hop, forward scatter ionospheric path using a transmitter located in Bearden, Arkansas. The data were originally collected for an experiment concerned with measuring the ultimate spatial resolution of a large HF array. In effect, the purpose of the experiment was to determine the degree to which ionospheric irregularities limit the spatial coherence of one-hop reflected signals. For this reason the signals were recorded under extremely high signal-to-noise ratio conditions. The operating frequency was carefully selected to avoid interference and, because ionospheric doppler shifts are seldom more than a few Hertz, a very narrow receiver bandwidth (31.25 Hz) was used.

Receiving parameters such as these are not typical of most HF systems which utilize bandwidths as large as 100 KHz and are often interference limited. However, the data were recorded at eight spatially separated elements and thus could be used to examine the potential advantages of adaptive beamforming procedures. The conclusions drawn from these measurements were encouraging but must necessarily be restricted to narrow-band systems operating in the presence of a single, spatially distributed, strong interfering CW signal.

The research results summarized in section V above have demonstrated that potentially large processing gains may accrue to a narrow band HF antenna array system which employs adaptive beamforming techniques to eliminate a single, CW interfering signal. Adaptive processing methods similar to those used in sonar and seismic systems have direct application to such HF systems. No problems unique to the HF environment were found to influence the adaptive processing. The performance of the HF adaptive beamforming system was accurately predictable using theoretical results obtained in the acoustical signal processing area.

This research also demonstrated that continuous adaptive beamforming is desirable. It was shown that "freezing" the adaptive process for as little as 60 seconds can cause a degradation of 8 to 10 db in output signal-to-noise ratio. Time constant investigations indicated that as few as 680 adaptions are required to achieve a 3 db improvement in output SNR for an 8 element array with 40 adaptive weights. The algorithm employed to obtain these results requires one multiply and add for each weight adapted. Thus, a total of 27,200 such operations are required for each 3 db improvement. Modern low cost digital hardware can easily perform one multiply and add in two μsec. The time constant of adaptation would then become 54.4 milliseconds, a rate sufficiently fast to track ionospheric variations.

In addition, this research program also suggested and investigated a technique for implementing stable adaptive digital

feedback filters. No other methods are presently available for feedback filters. Although only preliminary results have been obtained, they are encouraging and may lead to the development of an adaptive processing system for use in arrays with a large number of elements and/or simultaneous beams.

VII. SUGGESTIONS FOR FUTURE RESEARCH

The research results and conclusions described in this report have demonstrated that adaptive beamforming methods have great potential in HF antenna arrays. Unfortunately, these results are based upon a data sample which is not representative of the system parameters used in most HF applications. To this end, further research should be conducted to examine the potential of adaptive methods in an environment which better approximates that of actual systems. The specific recommendations are as follows:

1. To record and process data observed simultaneously at array elements using receiver bandwidths greater than 1 KHz.
2. To investigate the performance of adaptive beamforming methods in multiple, high amplitude interference environments such as that generated by teletype transmitters.
3. To measure the capability of an adaptive processor to track time-varying interference -- i.e. a noise source with time-varying frequency spectrum and/or direction of arrival.
4. To determine the effectiveness of adaptive processing in the presence of signal-generated clutter and/or multipath. Previous work has been based on the assumption that the time waveform of the interference is uncorrelated with that of the desired signal.
5. To develop adaptive algorithms better suited to those problems specific to HF systems -- e.g. multiple beam

processors, range/doppler adaptation, and direction finding methods.

6. To investigate the hardware requirements for the implementation of real time adaptive processors. This study should include an investigation of the relative merits of an all digital processor vs. a hybrid analog/digital system.
7. To further explore and develop procedures for utilizing feedback in adaptive filters. This work should include array studies as well as one-dimensional filters.

APPENDIX

THE DESIGN OF ADAPTIVE TAPPED-DELAY LINE PROCESSORS WHICH EMPLOY FEEDBACK

Non-recursive adaptive tapped-delay line processors of the type shown in Fig. 22 do not employ feedback signal paths. As a result, the impulse response of such filters is necessarily limited to the total length of the delay line. In order to obtain fine frequency resolution with this processor, it may be necessary to use an inordinate number of taps in the line. Since the convergence rate of adaptive processors decrease as the number of taps increases[22], a multiplicity of taps may impose prohibitively long convergence times on the adaptive processor; particularly in the case of array processing where N lines are required for an N element array.

An alternative tapped-delay-line processor, which does employ feedback, is shown in Fig. 45. This processor is commonly referred to as a recursive digital filter. Because of the presence of feedback, an infinite length impulse response can be obtained using a finite number of filter coefficients. Alternatively, a recursive filter can provide an equivalently fine frequency resolution with fewer filter coefficients than for a non-recursive design.

One problem which occurs with recursive filter design is that of obtaining a stable impulse response. It is well known[25]

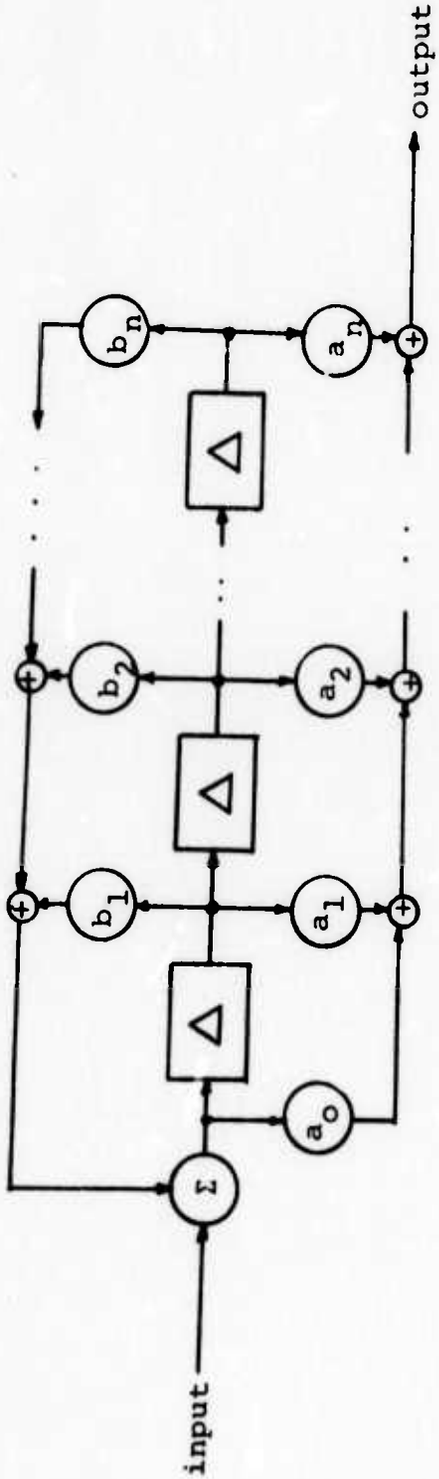

FIG. 45. Tapped-delay line with feedback

that when the poles of the feedback polynomial lie outside the unit circle*, the resulting filter is unstable. Since the feedback coefficients determine the location of these poles in a non-linear manner, it is not an easy task to reflect the stability requirement in terms of the coefficient values. For this reason, simple adaptive feedback processors have not yet been proposed.

The approach taken in this research was to design a minimum-phase non-recursive digital filter and then to use this filter to set the feedback coefficients in a recursive design. Minimum phase filters are constrained to have all zeros in the stable region and thus the resulting recursive design necessarily has all poles in the stable region and is therefore stable. Simple adaptive procedures <u>are</u> available for the design of minimum phase filters and have been widely developed in the field of inverse or deconvolution filtering.

A. DECONVOLUTION AND INVERSE FILTERING

A filter $\{g_k\}$ is defined as the <u>inverse</u> of a second filter $\{h_k\}$ if it "undoes" the effect of $\{h_k\}$, that is, for any input sequence $\{W_k\}$

$$[\{W_k\} * \{h_k\}] * \{g_k\} = \{W_k\} .$$

Note that $\{g_k\}$ is often referred to as a <u>deconvolution</u> filter

---

*The z-transform used herein is defined as

$$X(z) = \sum_k x_k z^k$$

using a positive power of z convention. The region of causal stability is $|z| > 1$.

for $\{h_k\}$. Taking z-transforms of both sides with

$$G(z) = z\{g_k\} \quad \text{and} \quad H(z) = z\{h_k\}$$

this means

$$H(z)G(z) = 1.$$

$$G(z) = 1./H(z) \tag{A1}$$

Such a requirement appears simple, but has several inherent problems. Most serious is the problem of stability. If the filter transform $H(z)$ were to have a zero inside the unit circle, that is, if it were non-minimum phase, the required $G(z)$ would have a pole inside the unit circle. The resulting $\{g_k\}$ would be causal but unstable. Secondly, a finite duration impulse response $\{h_k\}$ would invariably require an infinite duration $\{g_k\}$ as its inverse. This indicates that $\{g_k\}$ could not always be realized by a tapped delay line or non-recursive filter. For ease of implementation such a non-recursive or all zero, realization is desirable. Thus, subjected to such constraints, there may exist no ideal inverse filter $\{g_k\}$.

To avoid such problems it becomes necessary to loosen the definition given by Eq. (A1). Instead, to be an inverse, it is only necessary that $\{g_k\}$ do the best possible job of inverting $\{h_k\}$. The performance measure to optimize is the mean-square error; the solution that minimizes the mean-square error is the Wiener filter. In its non-recursive form it is defined by this familiar system of normal equations

$$\underline{G}^{(N)} = R_{xx}^{-1} \underline{P}_{xd} \qquad \text{(A2)}$$

where

$G^{(N)T} = [g_0 g_1 g_2 \cdots g_{N-1}]$, the N filter coefficients $\{g_k\}$,

$P_{xd}^T = [E(d_k x_{k-j})] \quad 0 \leq j \leq N-1$, cross correlation

of the filter input $\{x_k\}$ and the desired output $\{d_k\}$, and

$$R_{xx} = [E(x_{k-1} x_{k-j})] \quad 0 \leq i, \; j \leq N-1$$

the matrix of input $\{x_k\}$ autocorrelation. For the special case of inverting a filter $\{h_k\}$, where $\{d_k\} = \{W_k\}$,

$$P_{xd}^T = [h_0 \; 0 \; 0 \; \ldots \; 0]$$

and

$$R_{xx} = [E(h_{k-i} h_{k-j})] \quad 0 \leq i, \; j \leq N-1$$

B. TOEPLITZ MATRICES

When dealing with stationary random processes, the coefficient matrix of the system of normal equations R_{xx} has a pleasing property: it is Toeplitz, so that all elements along any diagonal are equal, and it is symmetric. It is therefore defined by the elements of its first row,

$$[r_{xx}(0) \; r_{xx}(1) \; \ldots \; r_{xx}(N-1)]$$

where $r_{xx}(j) = E(x_k x_{k-j})$. Levinson[26] in 1947 outlined a simple algorithm for solving a system of linear equations having a Toeplitz coefficient matrix. The algorithm requires only the first row of coefficients, thus reducing the required storage space from N^2 to N, over conventional Gaussian matrix solutions techniques. Likewise, the number of operations reduces by a factor of roughly N.

An additional advantage is that Levinson's algorithm uses a recursive approach; it solves a system of N equations in N unknowns using the solution to a subsystem of N-1 equations in N-1 unknowns. By starting with the trivial case N-1

$$r_{xx}(0)g_0 = P_0$$

the algorithm can recurse through all values of N. Note that the mean-square error performance can be calculated at each step of the recursion. When the error is small enough, the recursion process will stop.

C. STABILITY OF INVERSE FILTERS

It is interesting to note that there are no restrictions on the original filter when using Eq. (A2) to find the inverse filter. Recall that the first definition given for inverse

$$G(z) = 1./H(z)$$

required that $H(z) = z\{h_k\}$ have no zeros inside the unit circle.

Here, however, since $\{g_k\}$ is derived non-recursively and has only N coefficients, its time response must be stable for any $\{h_k\}$. It might be asked, what good reason, if this stability is artificial, due only to the finite duration of the impulse response; as N grows indefinitely will instability result? It can be shown that $\{g_k\}$ will indeed be stable if unrestricted in length, irrespective of $\{h_k\}$. Furthermore, as N grows $\{g_k\}$ becomes a better inverse of $\{h_k\}$ in the mean-square error sense, and if $H(z)$ is minimum phase,

$$\lim_{N\to\infty} G^{(N)}(z) = 1/H(z) ,$$

which is the intuitive definition set forth originally.

If $H(z)$ is minimum phase with a simple zero

$$H(z) = 1 - z/a \quad |a| > 1$$

This result indicates that

$$\lim_{N\to\infty} G^{(N)}(z) = \frac{1}{H(z)} = \frac{1}{1-z/a}$$

or for finite N

$$G^{(N)}(z) \approx \frac{1}{1-z/a}$$

Thus the N-1 zeros of the non-recursive inverse $\{g_k\}$ are distributed as to approximate a pole in the mean-square error sense. Read and Burrus[27] showed that a simple pole can be approximated by N zeros distributed uniformly around a circle

of radius a with the zero at $z = a$ removed. This approximation was derived simply from the truncated impulse response of a filter having a simple pole,

$$\frac{1}{1-z/a} \simeq 1 + \frac{z}{a} + \left(\frac{z}{a}\right)^2 + \cdots + \left(\frac{z}{a}\right)^{N-1} = \frac{1 - \left(\frac{z}{a}\right)^N}{1 - \left(\frac{z}{a}\right)}$$

Such an approximation, however, will not have minimum mean-square error. The filter $G^{(N)}(z)$ derived non-recursively as above has its zeros slightly perturbed from the circle $z = a$. For example, consider the case of a pole at $z = 2$ and $N = 6$ shown in Table A1.

TABLE A1. INVERSE APPROXIMATIONS

TRUNCATION		INVERSE OF (1 - (z/2))	
IMPULSE RESPONSE	ZERO LOCATIONS	IMPULSE RESPONSE	ZERO LOCATIONS
1.00000	-2.00	.99982	-2.1719
.50000	$2.00e^{j120}$	.49954	$2.1444e^{j121.7}$
.25000	$2.00e^{-j120}$	.24904	$2.1444e^{-j121.7}$
.12500	$2.00e^{j60}$	.12305	$2.0666e^{j62.3}$
.03125	$2.00e^{-j60}$	.05860	$2.0666e^{-j62.3}$
		.02344	

Since $G^{(N)}(z)$ approximates $1/H(z)$ in the mean-square error sense, it follows that $1/G^{(N)}(z)$ must similarly approximate $H(z)$. This leads perhaps to the most important property

of the inverse filter proved by Szegö[28]. For a polynomial

$$G^{(N)}(z) = Z\{g_k\}$$

the roots must always lie outside the unit circle in the complex z plane, if $\{g_k\}$ is the minimum mean-square error inverse of any filter $\{h_k\}$. This means that the poles of a filter defined as

$$\hat{H}^{(N)}(z) = 1./G^{(N)}(z)$$

must be outside of the unit circle. With the poles outside, the new filter $\hat{H}^{(N)}(z)$ must have a stable causal time response.

D. INVERSE FILTERS IN RECURSIVE FILTER DESIGN

The non-recursive filter is most popular for data processing applications. The greatest advantage is its ease of design; while it is extremely difficult to optimize a recursive filter in all but the most structured problems, the non-recursive filter is uniquely defined by a set of linear equations. Also, it has guaranteed stability. Since the non-recursive filter by definition has no feedback, its transfer function can have no poles, only zeros in the plane, and thus must be stable. Furthermore, by allowing the filter's delay line to lengthen, its impulse response will approach that of the optimal causal filter, and its mean-square error will monotonically converge to the optimal performance. Thus, the optimal causal filter which is recursive may be approximated to any degree of accuracy by the optimal non-recursive filter, given enough delay elements.

A serious disadvantage of the non-recursive filter configuration is its poor bandpass capabilities. For estimating a narrow-band signal in noise, a good filter must be selective with a sharply defined passband. With no poles in the non-recursive filter's transfer function, a narrow passband can only be approximated by placement of a finite number of zeros. A recursive filter with a single pole pair, on the other hand, will in general have a better bandpass characteristic than a low order non-recursive filter. A desirable filter would possess the selectivity of a recursive filter, while retaining the design advantages of the non-recursive filter.

The transfer function of a recursive filter takes the form

$$H(z) = \frac{A(z)}{B(z)}$$

where $A(z)$ and $B(z)$ are polynomials in positive powers of z. Such a filter will be unstable if any of its poles, that is, zeros of $B(z)$, fall inside the unit circle in the z plane. However, if both numerator and denominator were inverted non-recursively with $C^{(N)}(z)$ the inverse of $B(z)$, and $D^{(N)}(z)$ the inverse of $A(z)$, the ratio

$$\tilde{H}^{(N)}(z) = \frac{C^{(N)}(z)}{D^{(N)}(z)}$$

would necessarily be stable, since $D(z)$ has its zeros outside the unit circle according to Szegö's theorem. Therefore, to design a recursive filter by this technique, it is only

necessary to find the expression

$$H(z) = \frac{A(z)}{B(z)}$$

such that $H(z)$ approximates an optimal filter $H_0(z)$ and such that

$$\tilde{H}^{(N)}(t) = \frac{C^{(N)}(z)}{D^{(N)}(z)}$$

approximates $H(z)$ sufficiently well. Note that if $H(z)$ were both stable and minimum phase, so that

$$\lim_{N\to\infty} C^{(N)}(z) = 1/B(z) \quad \text{and} \quad \lim_{N\to\infty} D^{(N)}(z) = 1/A(z)$$

then it follows

$$\lim_{N\to\infty} H^{(N)}(z) = \frac{1/B(z)}{1/A(z)} = \frac{A(z)}{B(z)} = H(z) \ .$$

E. DESIGN APPROACHES AND EXAMPLES

Three different design approaches were taken. The first two used the fact that the unconstrained optimal Wiener filter takes the form

$$H_{opt}(z) = \frac{\Phi_{ss}(z)}{\Phi_{xx}(z)}$$

for the estimation problem, with the signal power spectrum

$$\Phi_{ss}(z) = \sum_{k=-\infty}^{\infty} \phi_{ss}(k)\ z^k$$

and the input power spectrum

$$\Phi_{xx}(z) = \sum_{k=-\infty}^{\infty} \phi_{xx}(k)\ z^k \ .$$

Each infinite summation is truncated and then used to form an approximation to the optimal filter

$$H_I(z) = \frac{\sum_{k=-M}^{M} \phi_{ss}(k) z^k}{\sum_{k=-M}^{M} \phi_{xx}(k) z^k} = \frac{\sum_{k=0}^{2M} \phi_{ss}(k-M) z^k}{\sum_{k=0}^{2M} \phi_{xx}(k-M) z^k} = \frac{A(z)}{B(z)} \ .$$

Finally, both $A(z)$ and $B(z)$ are inverted by $D^{(N)}(z)$ and $C^{(N)}(z)$ respectively as explained earlier to form the stable filter

$$H_I^{(N)}(z) = \frac{C^{(N)}(z)}{D^{(N)}(z)} \qquad \text{(A3)}$$

This is called the <u>double-sided autocorrelation inversion</u> filter. The second approach was similar, except that the truncation took only positive powers of z, giving

$$H_{II}(z) = \frac{\sum_{k=0}^{M} \phi_{ss}(k) z^k}{\sum_{k=0}^{M} \phi_{xx}(k) z^k} = \frac{A(z)}{B(z)} \qquad \text{(A4)}$$

This led to the <u>single-sided autocorrelation inversion</u> filter.

The third approach is considerably different. Let

$$\Phi_{ss}(z) = H_s(z)H_s(\tfrac{1}{z})$$

$$\Phi_{xx}(z) = H_x(z)H_x(\tfrac{1}{z})$$

with

$$H_s(z) = \frac{R(z)}{S(s)}$$

Both filters $H_s(z)$ and $H_x(z)$ are minimum phase and stable. Then the optimal causal filter takes the form

$$H_{optc}(z) = \frac{H_s(z)}{H_x(z)} \quad \frac{Q(z)}{R(z)}$$

where the additional polynomial $Q(z)$ accounts for any new zero locations defined by the causality constraint. Next let an approximation to this expression be

$$\tilde{H}(z) = \frac{H_s(z)}{H_x(z)}$$

With $C^{(N)}(z)$ inverting $H_x(z)$ and $D^{(N)}(z)$ inverting $H_s(z)$, the <u>inversion processor</u> is then given by

$$H_{III}(z) = \frac{C^{(N)}(z)}{D^{(N)}(z)} \qquad \text{(A5)}$$

All three filters were tested using a specific problem involving a narrowband signal embedded in broadband noise. The overall signal to noise ratio was -13db. The power spectra can be seen in Figs. 46 and 47. In addition to the three filter

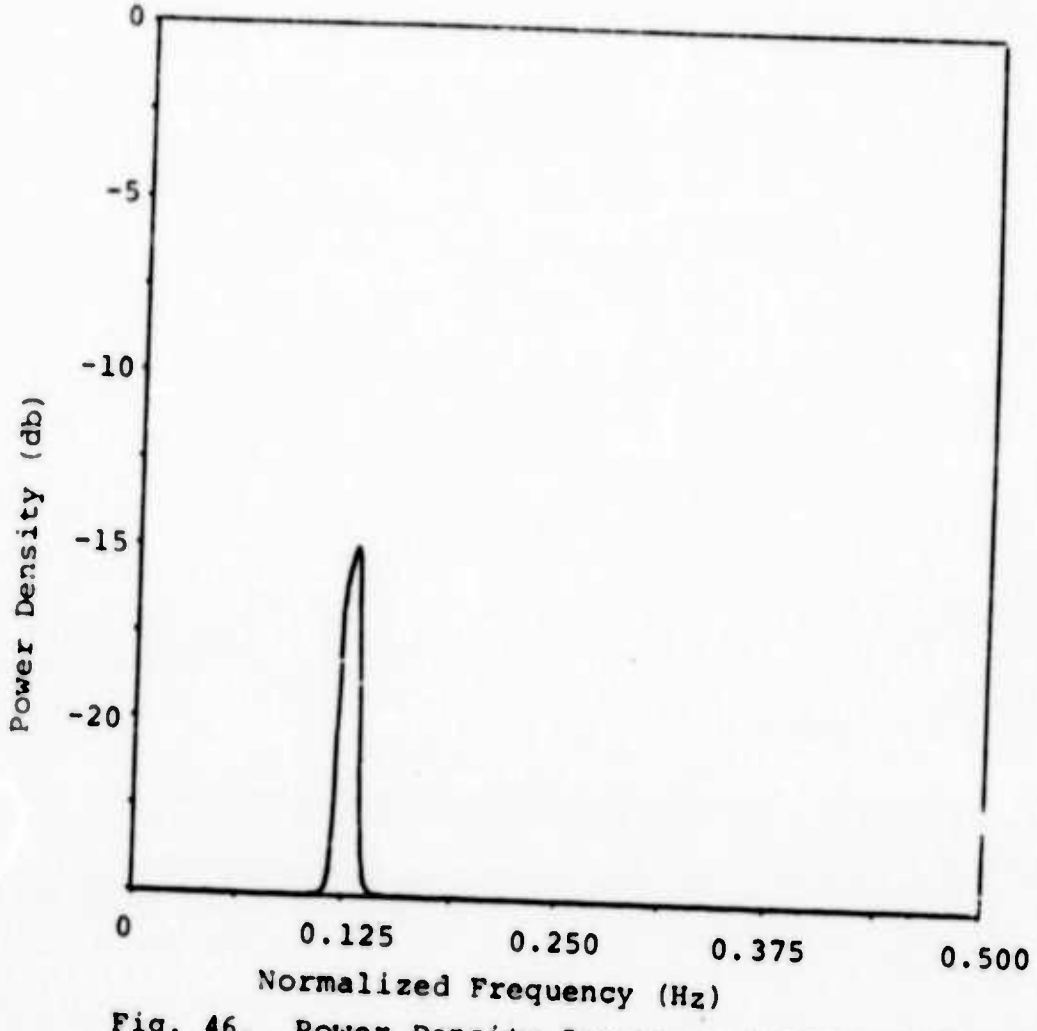

Fig. 46. Power Density Spectrum of Desired Signal

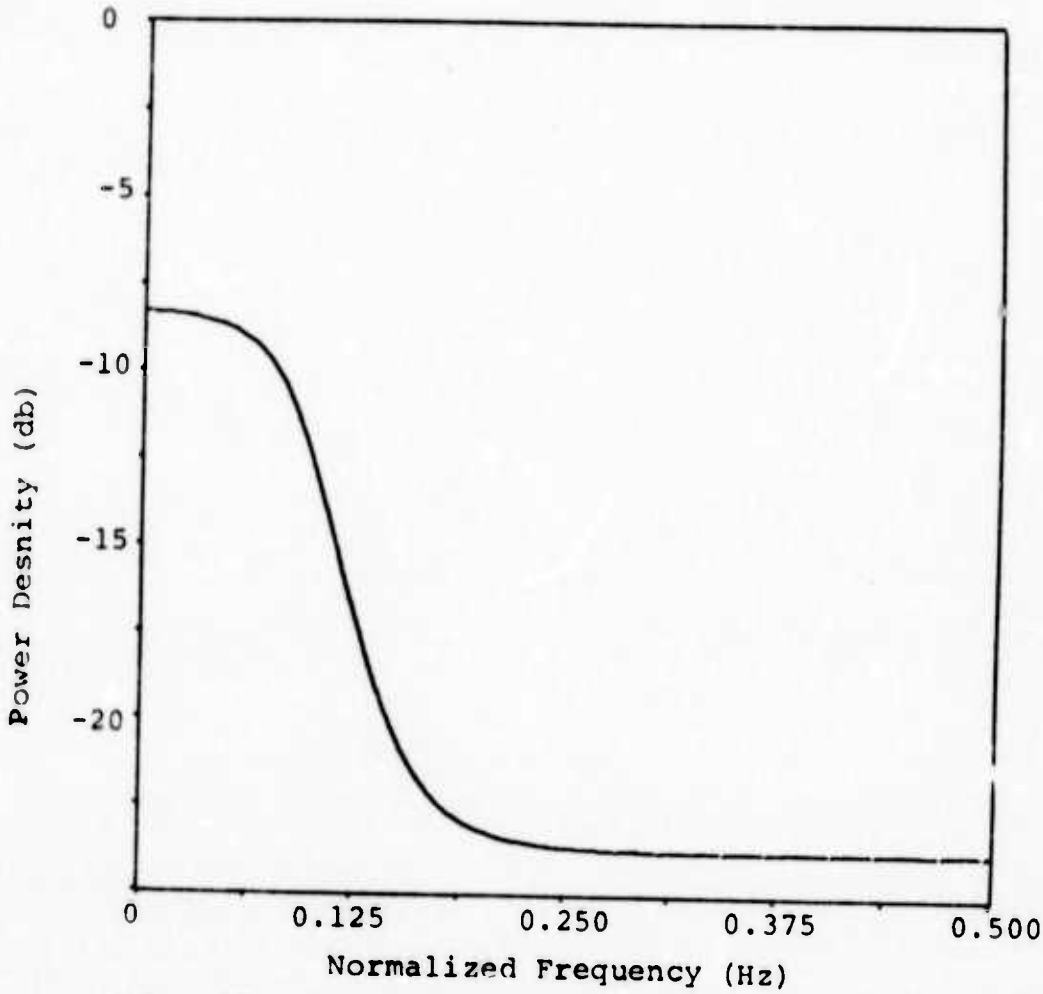

Fig. 47. Power density Spectrum of Undesired Noise

designs described above, three Wiener filters were designed: the unconstrained Wiener filter, the causal Wiener filter, and the non-recursive Wiener filter. The logarithmic magnitude responses of each filter is shown in Figs. 48-53. Note that each of the five recursive filters is far superior in its bandpass selectivity to the single non-recursive filter.

The mean-square error evaluation indicated that the newly derived filters were inferior with the error defined as

$$e_k^2 = (S_k - Y_k)^2$$

$$Y_k = \text{filter output}$$

To evaluate the performance independent of time delay between actual signal value and the estimated value, the error was redefined as

$$e_k^2 = (S_{k-B} - Y_k)^2$$

and B was allowed to very. The universal minimum for each filter was then found. Table A2 summarizes these results.

Table A2. MEAN-SQUARE ERROR CALCULATIONS

	TYPE OF FILTER		B = 0 MSE	VARIABLE B MSE	OUTPUT SNR
1)	WIENER	UNCONSTRAINED	.511	.511	-1.803 DB
2)		CAUSAL	.683	.611	-4.384 DB
3)		NON-RECURSIVE	.750	.734	
4)	DOUBLE-SIDED AUTOCORRELATION Eq. (A3)		.984	.585	
5)	SINGLE-SIDED AUTOCORRELATION Eq. (A4)		.812	.591	
6)	INVERSION PROCESSION Eq. (A5)		.923	.632	0.614 DB

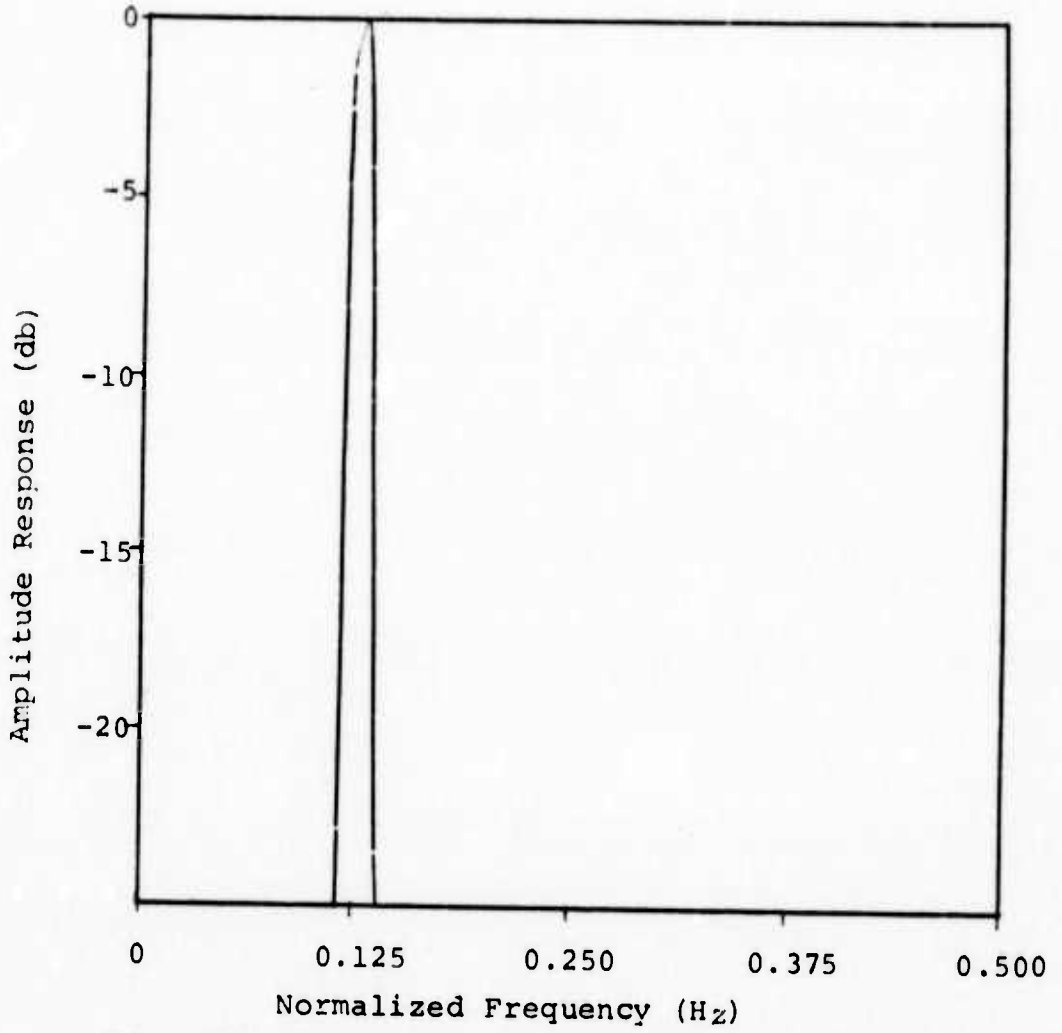

Fig. 48. Amplitude response for optimal non-causal filter.

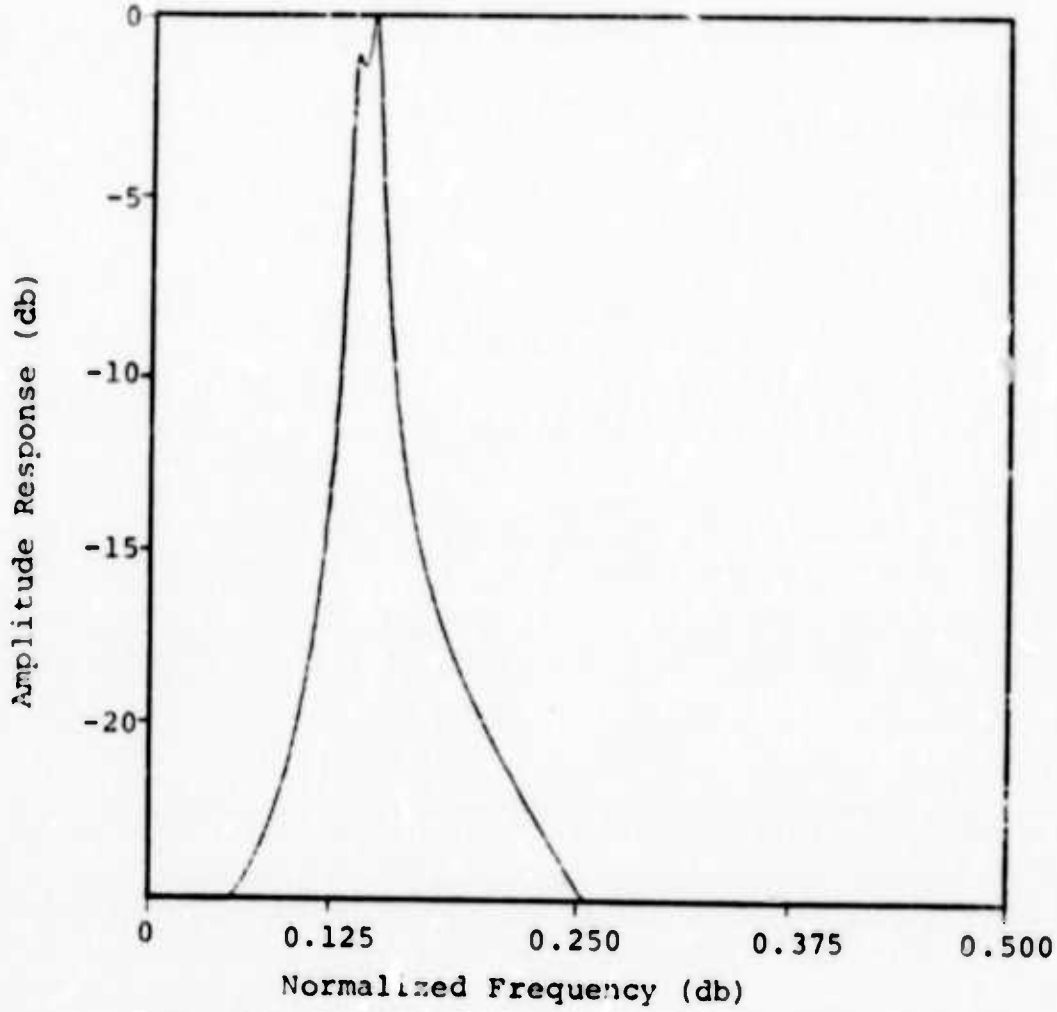

Fig. 49. Amplitude response for optimal causal filter.

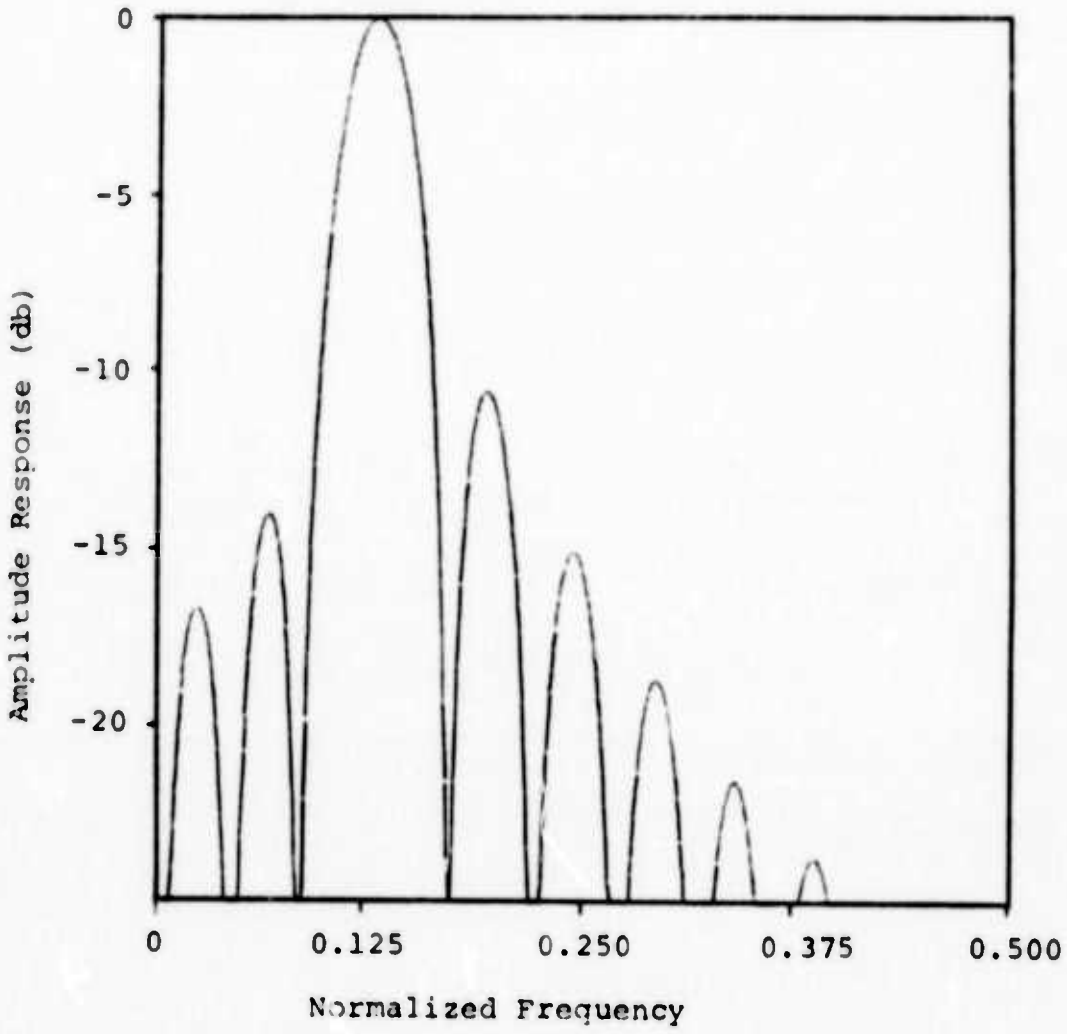

Fig. 50. Amplitude response for twenty-weight optimal non-recursive filter

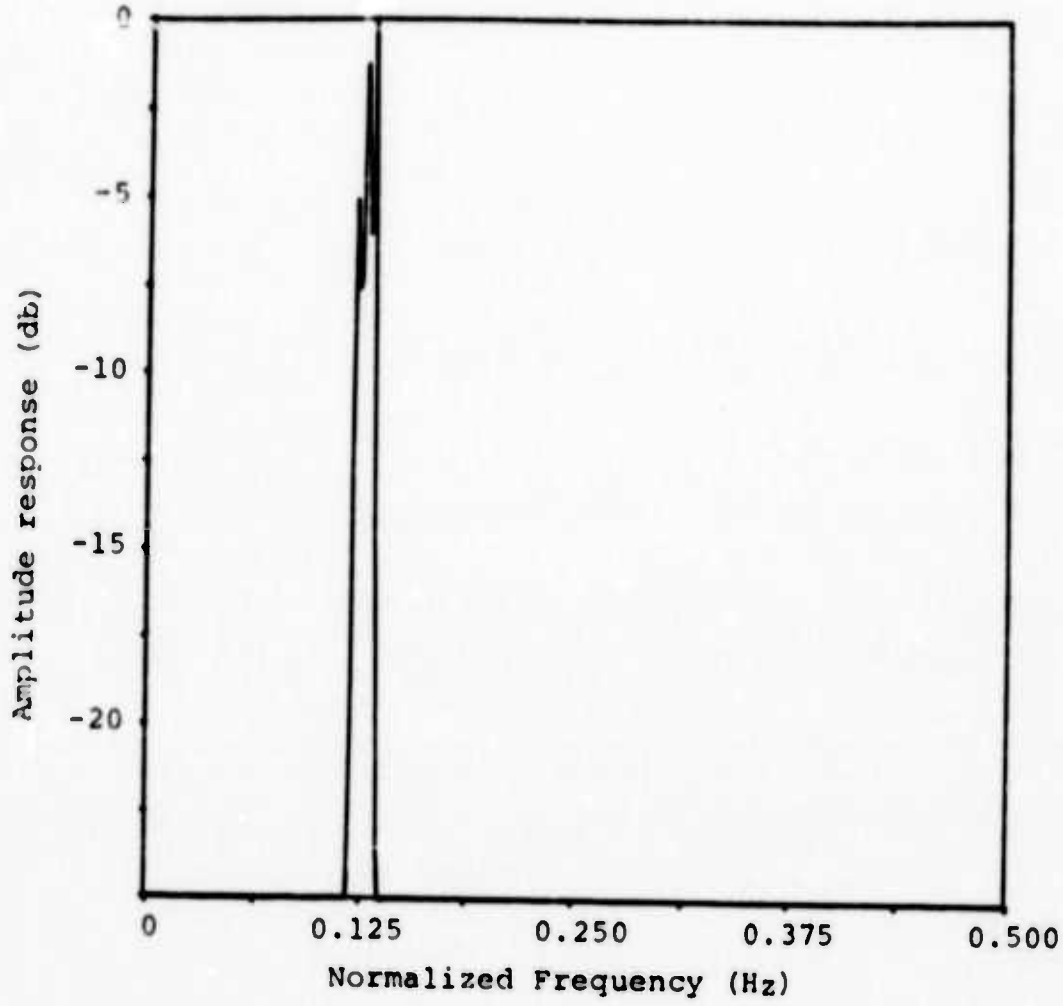

Fig. 51. Amplitude response for suboptimal processor $H_I(Z)$ given in Eq. (A3).

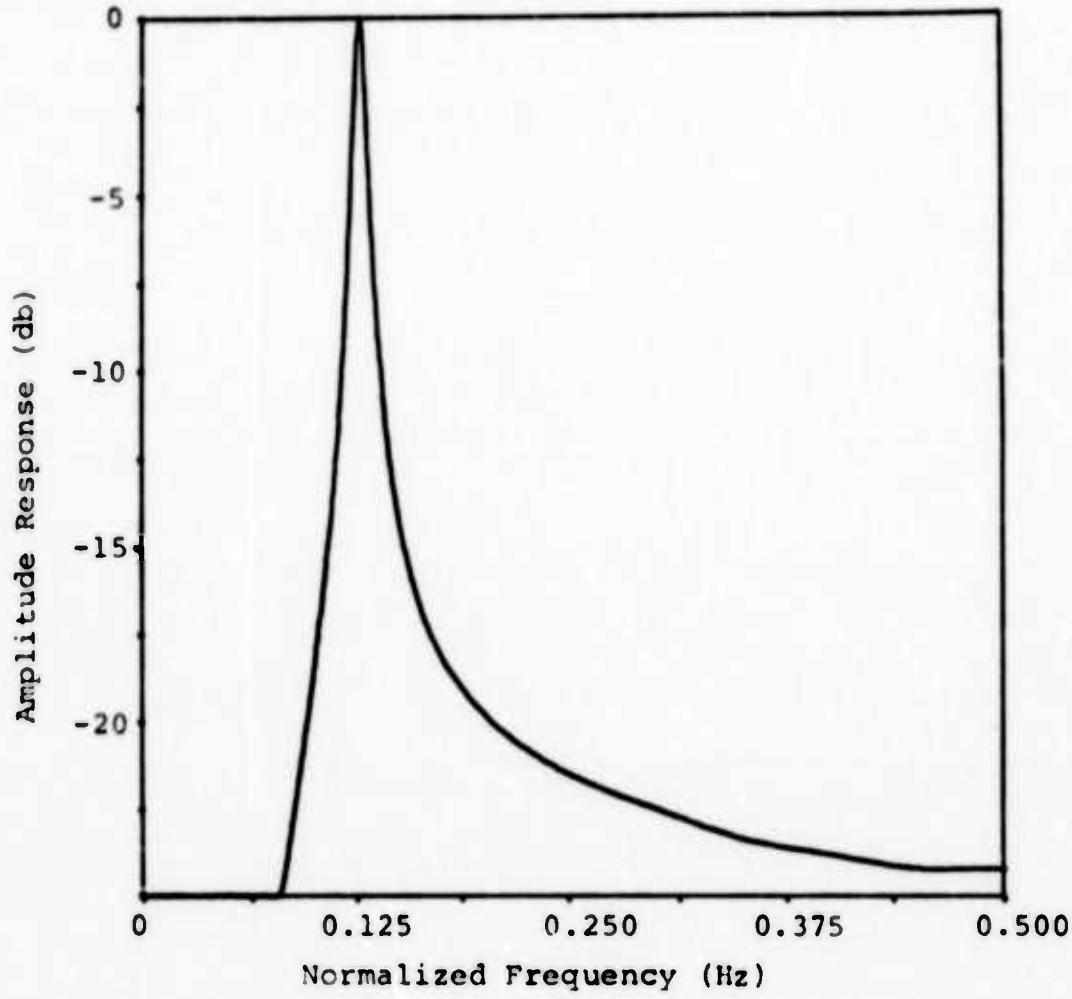

Fig. 52. Amplitude response for suboptimal recursive processor $H_{II}(Z)$ given in Eq. (A4).

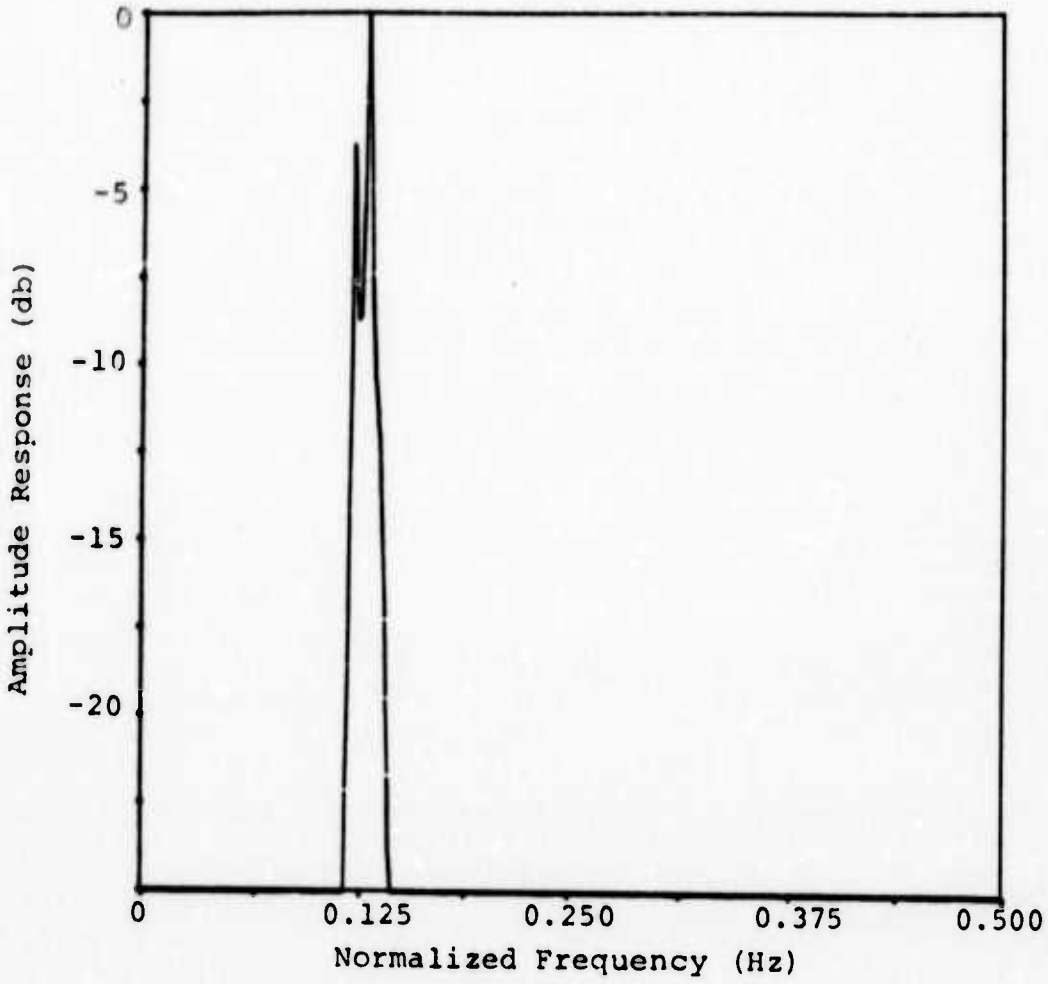

Fig. 53. Amplitude response for suboptimal recursive processor $H_{III}(Z)$ given in Eq. (A5)

For narrowband signals in broadband noise, the recursive filters derived using the properties of inverse filtering may perform quite well, if delay between the signal estimate and the actual signal value is not important. Indeed, in many applications even delays of several seconds may not be significant. The technique used in the derivation of these filters is a new way of imposing stability on a recursive filter where before instability was a problem. It could probably have greatest impact in an extension of the work set forth here, the problem of adaptive recursive filtering.

F. DISCUSSION AND CONCLUSIONS

Encouraging results have been obtained indicating that minimum phase filters can be used successfully in the design of recursive Wiener filters. Three specific design procedures were suggested and investigated. Each design is amenable to the implementation of adaptive methods. Further research into this problem is continuing to determine the applicability to array processing.

REFERENCES

1. Sweeney, L. E. Jr., "Spatial Properties of Ionospheric Radio Propagation as Determined With Half-Degree Azimuthal Resolution," Stanford Electronics Laboratory Report No. TR-155, Stanford University, Stanford, Calif., June, 1970.

2. Griffiths, L. J., "Final Report: Adaptive Antenna Processing Literature Survey," Department of Electrical Engineering Report No. 13789, University of Colorado, Boulder, Colo., Jan., 1972.

3. Mermoz, H., "Adaptive Filtering and Optimum Utilization of an Antenna," Bureau of Ships Translation No. 93, Washington, D. C., October 4, 1965.

4. Shor, S., "Adaptive Technique to Discriminate Against Coherent Noise in a Narrow Band System," J. Acoust. Soc. Amer., Vol. 39, No. 1, pp. 74-78, January, 1966.

5. Stocklin, P. L., "Space-time Sampling and Likelihood Ratio Processing in Acoustic Pressure Fields," Journ. Brit. IRE, Vol. 26, No. 1, pp. 79-91, July, 1963.

6. Vanderkulk, N., "Optimum Processing for Acoustic Arrays," J. Brit. IRE, p. 286, October, 1963.

7. Anderson, V. C. and P. Rudnick, "Rejection of a Coherent Arrival at an Array," J. Acoustic. Soc. Amer., Vol. 45, No. 2, pp. 406-410, February, 1969.

8. Bryn, F., "Optimum Signal Processing of Three-Dimensional Arrays Operating on Gaussian Signals and Noise," J. Acoust. Soc. Am., Vol. 34, No. 3, pp. 283-297, March, 1962.

9. Burg, J. P., "Three-Dimensional Filtering with an Array of Seismometers," Geophysics, Vol. 29, No. 5, pp. 693-713, October, 1964.

10. Kelley, E. J., Jr., and M. J. Levin, "Signal Parameter Estimation for Seismometer Arrays," Tech. Rept. 333, Lincoln Lab., MIT, Lexington, Mass., Jan. 8, 1964.

11. Widrow, B. W., P. E. Mantey, L. J. Griffiths, and B. B. Goode, "Adaptive Antenna Systems," Proc. IEEE, Vol. 55, No. 12, pp. 2143-2159, December, 1967.

12. Chang, J. and F. Tuteur, "A New Class of Adaptive Array Processors," J. Acoust. Soc. Amer., Vol. 49, No. 3, pp. 639-649, March, 1971.

13. Compton, R. T., Jr., "Adaptive Arrays on Power Equalization with Proportional Control," Report 3234-1, Electro-Science Lab., Dept. of Elec. Engineering, The Ohio State University, December, 1971.

14. Griffiths, L. J., "A Simple Adaptive Algorithm for Real-Time Processing in Antenna Arrays," Proc. IEEE, Vol. 57, No. 10, pp. 1696-1704, October, 1969.

15. Capon, J., R. J. Greenfield, and R. J. Kolker, "Multi-dimensional Maximum-Likelihood Processing of a Large Aperture Seismic Array," Proc. IEEE, Vol. 55, No. 2, pp. 192-217, February, 1967.

16. Robinson, E. A., and S. Treitel, "Principles of Digital Wiener Filtering," Geophys - Prosp., Vol. 15, No. 3, 1967.

17. Claerbout, J., "A Summary, by Illustrations, of Least-Squares Filters with Constraints," IEEE Trans. Info. Thy., Vol. IT-14, pp. 269-272, March, 1968.

18. Treitel, S. and E. A. Robinson, "Seismic Wave Propagation in Layered Media in Terms of Communication Theory," Geophys., Vol. 31, No. 1, January, 1966.

19. Sweeney, L. E., Jr., "Digital Beam Formation," letter to DARPA/STO Attn: Mr. A. Van Every, 1400 Wilson Boulevard, Arlington, Virginia, 27 June 1972.

20. Staff, "Wide-Aperture High-Frequency Radio Research Facility," Ionospheric Dynamics Group, Radioscience Laboratory, Stanford University, California, 1969.

21. Robinson, E. A., "Statistical Communication and Detection," Hafner Publishing Company, New York, 1967.

22. Widrow, B., "Adaptive Filters I: Fundamentals," Rept. SEL-66-126 (TR No. 6764-6), Stanford Electronics Laboratories, Stanford, Calif., December 1966.

23. Daniell, T. P., "Adaptive Estimation with Mutually Correlated Training Samples, Ph.D. dissertation, Stanford University, Stanford, Calif., September, 1968.

24. Senne, K., "Adaptive Linear Discrete-Time Estimation," Ph.D. dissertation, Stanford University, Stanford, Calif., June, 1968.

25. Gold, B. and Rader, C., "Digital Processing of Signals," McGraw-Hill Book Company, New York, 1969.

26. Levinson, N., "An Heuristic Exposition of Wiener's Mathematical Theory of Prediction and Filtering," J. Math Phys., Vol. 26, pp. 110-119, 1947.

27. Read, R. R. and C. S. Burrus, "Use of the Geometry of Partial Sums in Digital Filter Analysis," IEEE Trans. on Audio and Electroacoustics, Vol. Au-20, No. 3.

28. Szego, G., Orthogonal Polynomials, Vol. 23, American Mathematical Society Colloquium Publications, Ch. 11, 1939.